



másterFUEGO

Assessing the effects of fuel treatments on fire spread and behavior in Strategic Management Points using a fluid dynamics model.

Master Thesis

Olga Puebla Vendrell



Version 4.0

October 31st, 2018

*This work has been
developed with Dr.Chad
Hoffman from Colorado
State University and Dr.
Domingo Molina from
University of Lleida.*

Index

Abstract	9
1. Introduction.....	10
2. Objectives.....	12
3. Material and methods	13
3.1 General framework.....	13
3.2 Study area.....	14
3.3 Fuel treatments in Strategic Management Points	21
3.4 Fire simulation modeling	23
3.4.1 Selection of the simulator	23
3.4.2 Input file	26
3.4.3 Modeling scenarios	35
3.4.4 Simulation set-up.....	36
4. Results	50
Crown fire activity.....	53
Rate of Spread	56
Rate of Spread	56
Wind speed profiles	58
5. Discussion and conclusions	69
6. Acknowledgements.....	71
7. References.....	72
8. Annexes.....	74
Annex I	74
Annex II	75

Annex III	76
Annex IV	95
Annex V	96
Annex VI	97
Annex VII	98

Figure Index

Figure 1: General framework.....	13
Figure 2: Location of the study area.	15
Figure 3: Topography and aspect of the study zone.....	16
Figure 4: Walter-Lieth diagram of the weather station of Bon Repòs. Where Tm: mean monthly temperature (°C); Pm: mean monthly precipitation (mm).....	18
Figure 5: Area burned in the region of Pallars Jussà since 1.986 until 2017.....	19
Figure 6: Wildfire history of Pallars Jussà.....	20
Figure 7: Graphics of the treatments applied in the study zone. Analysis of the number of trees and the diametric class. A) thinning 30% of the Basal Area (Q1). B) thinning 50% of the Basal Area (Q2).	22
Figure 8: First Figure is an ideal mesh. Second one is allowed as long as there are an integral number of fine cells abutting each coarse cell. Third one: Allowed but with a questionable value. Fourth one: Not allowed. Source: FDS User Guide	28
Figure 9: Diagram summarizing the procedure to set-up the input file.	34
Figure 10: Modeling scenarios.....	35
Figure 11: Boundary areas created for Q1(A) and Q2(B).	36
Figure 12: Conversion of coordinates into WFDS format. Source: Own elaboration.....	37
Figure 13: Surrounding domain created around the study plot.....	37
Figure 14: Overall domain of the simulation. A) Domain filled up with study plots. B) Domain filled up with randomly rotated study plots.	38
Figure 15: Smokeview visualization of the topography obtained.	40
Figure 16: Errors found trying to get the correct topography.....	40
Figure 17: Study area with the meshes created. The Figure above, represents a test of the forest we were creating. It is possible to see that the topography has been extracted correctly and all the trees with their coordinates and data too.	42
Figure 18: Bitwise SSH visualization.	47
Figure 19: Topography simulations scenario (A) and Flat terrain simulations scenario (B).	49
Figure 20: Visualization of fire spread in Topography simulations.....	51

Figure 21: Canopy consumption results.....	53
Figure 22: Total canopy fuel amount pre and post fire.	54
Figure 23: Smokeview visualization of the Crown Fire Activity in Q1 and Q2, before and after the treatments, with initial high wind speed conditions.....	55
Figure 24: Mean Rate of Spread results.	57
Figure 25: Mean streamwise wind velocity profile.....	58
Figure 26: Mean streamwise wind velocity with high and low wind speed conditions respectively.....	59
Figure 27: Mean crosswind velocity.....	60
Figure 28: Mean vertical velocity.	61
Figure 29: Turbulent Kinetic Energy.	62
Figure 30: Smokeview visualization of streamwise velocities of pre Q1 and post Q1 with low wind speed conditions at 8 meters high.....	63
Figure 31: Smokeview visualization of streamwise velocities of pre Q1 and post Q1 with high wind speed conditions at 8 meters high.	63
Figure 32: Smokeview visualization of streamwise velocities of pre Q1 and post Q1 with high wind speed conditions at 15 meters high.....	64
Figure 33: Smokeview visualization of streamwise velocities of pre Q1 and post Q1 with high wind speed conditions at 8 meters high and with active fire.	64
Figure 34: Smokeview visualization of streamwise velocities of pre Q2 and post Q2 with low wind speed conditions at 8 meters high.....	65
Figure 35: Smokeview visualization of streamwise velocities of pre Q2 and post Q2 with high wind speed conditions at 8 meters high.	65
Figure 36: Smokeview visualization of streamwise velocities of pre Q2 and post Q2 with high wind speed conditions at 15 meters high.....	66
Figure 37: Smokeview visualization of streamwise velocities of pre Q2 and post Q2 with high wind speed conditions at 8 meters high and with active fire.	66
Figure 38: Smokeview visualization of streamwise velocities at Q1 and Q2 after treatments with high wind speed conditions at 8 meters high.....	67
Figure 39 Smokeview visualization of streamwise velocities of Q1 and Q2 after treatments with high wind speed conditions at 8 meters high and with active fire.....	67
Figure 40: Smokeview visualization of streamwise velocities at Q1 and Q2 after treatments with low wind speed conditions at 8 meters high.	68

Figure 41: Smokeview visualization of streamwise velocities of Q1 and Q2 after treatments with low wind speed conditions at 8 meters high and with active fire.68

Tables Index

Table 1: Summary of the annual and monthly temperature of the weather Station of Comiols. Where T: absolute maximum temperature (°C); T': mean maximum monthly temperature (°C); t: absolute minimum monthly temperature (°C); t': mean minimum monthly temperature (°C); Tm: mean monthly temperature (°C).	17
Table 2: Mean monthly precipitation of the weather station of Comiols. Where Pm is the mean monthly precipitation (mm).	17
Table 3: Wildfire history of Pallars Jussà.	19
Table 4: Treatments applied in the study area.	21
Table 5: Meshes generator table.	41
Table 6: Rates of Spread obtained from Topography simulations.	50
Table 7: Flat terrain simulations results	52
Table 8: Differences of the results obtained before and after the treatments.....	52
Table 9: Rate of Spread outputs.	56
Table 10: Other values obtained from ROS.....	57

Abstract

In the last decades, forest fires have become the main hazard for the Mediterranean landscapes. In order to know the fire spread and behavior of fire on different landscapes, several fire models have been developed, the most common FARSITE and FlamMap. Moreover, in Catalonia, "Strategic Management Points" (SMPs) have been created with the aim to maximize the efficiency of fuel treatments and facilitate the suppression services and to limit the spread of the fire. In this study case, a physics-based, fluid dynamics simulator (Wildland-Urban interface Fire Dynamics simulator, WFDS) was used to test two different fuel treatments (thinning 30% and 50% of the basal area (BA)) on a specific SMP and with two different initial wind speed conditions (3.3 m/s and 7 m/s). The crown fire activity (CFA), the rate of spread (ROS) and the different wind profiles obtained were analyzed depending on the treatment applied and the initial wind speed conditions. Our results confirm that the CFA decreases after both treatments and specially after thinning 50% of the BA. It is also confirmed that the ROS decreases after treatments with initial high wind speed conditions whereas it increases with initial low wind speed conditions. Finally, all wind speed profiles obtained after treatments show higher wind speeds on all three directions (streamwise, crosswind and vertical) and higher values of turbulent kinetic energy. These simulations indicate that thinning 30% of the BA is the treatment that reduces the most the crown fire activity and that both treatments show a similar reduction of the ROS. All wind speed profiles show higher values after treatments as well as higher turbulent kinetic energy, especially after thinning 50%.

Keywords: *fire simulation modeling, strategic management points, fire behavior, fire spread, WFDS.*

1. Introduction

Nowadays, forest fire is the main perturbation of most of the Mediterranean landscapes. Forest management of 21st century and the actual context of climate change should consider more than ever forest fires. To orient forest management and develop management models to integrate fire as a crucial factor, it is needed a specific analysis of its recurrence, intensity and spatial pattern of affection (Castellnou *et.al*, 2009). So we need and we have progressed in our management models as well as in our fire simulators. A good example of it, is the creation of the Strategic Management Points (SMPs) (Alcubierre, *et.al*, 2011).

A model fire serves as a reference and describes the maximal potential of a fire to become a large wildfire in a particular landscape unit. (Costa, *et.al*, 2011). These model fires identify different unit areas depending on those characteristics that describe the expected spread of a large wildfire. This type of planning allow to identify Strategic Management Points (SMPs).

Fire simulators cannot be considered as exact predictors of what is going to happen but as a tool. A tool that may not be useful for suppression performances but an excellent one for planning and prevention. Simulators can foresee critical areas, expected fire behaviors and movements. As long as there is a good data source, there will be a good prediction and analysis. An important part to take into account when simulating, is the interaction of the wind either with the landscape and the fire.

FARSITE (Finney, 1994) and FlamMap (Finney, 1999) are internationally known simulators. However, these simulators use WindNinja (Forthofer, 2013) to calculate winds. This program is good at calculating wind directions but it also has a huge lack due to there is no interaction with fire and winds are entered in 2-D. This lack is fixed on the Wildland-Urban Interface Fire Dynamics Simulator (WFDS)(NIST, 2007).

WFDS is a fire behavior model developed by the National Institute of Standards and Technology (NIST) and the US Forest Service Pacific Northwest Research Station. WFDS employs computational fluid dynamics (CFD) methods to solve the spatial and temporal evolution of fire using a three dimensional numerical grid. This approach allows for representation of fuels and prediction of fire behavior through time in three dimensions. A

more detailed description of the physical and mathematical formulations in WFDS can be found in Mell et al., (2007, 2009). (Ziegler et al., 2017)

2. Objectives

This project aims to assess different fuel treatments and their effects on fire behavior and spread as well as their efficiency to allow firefighters to contain eventual wildland fires in worse conditions in a Strategic Management Point in Catalonia.

It also aims to work and get to know WFDS.

The main objectives of this study are:

- To assess the effect of fuel treatments on the crown fire activity (CFA).
- To assess the effect of fuel treatments on the rate of spread (ROS).
- To evaluate the effect of fuel treatments on the wind speed profiles.
- To assess the fuel treatments' efficiency.

3. Material and methods

3.1 General framework

A diagram to summarize and clarify the overall study project and its procedure was done (Figure 1).

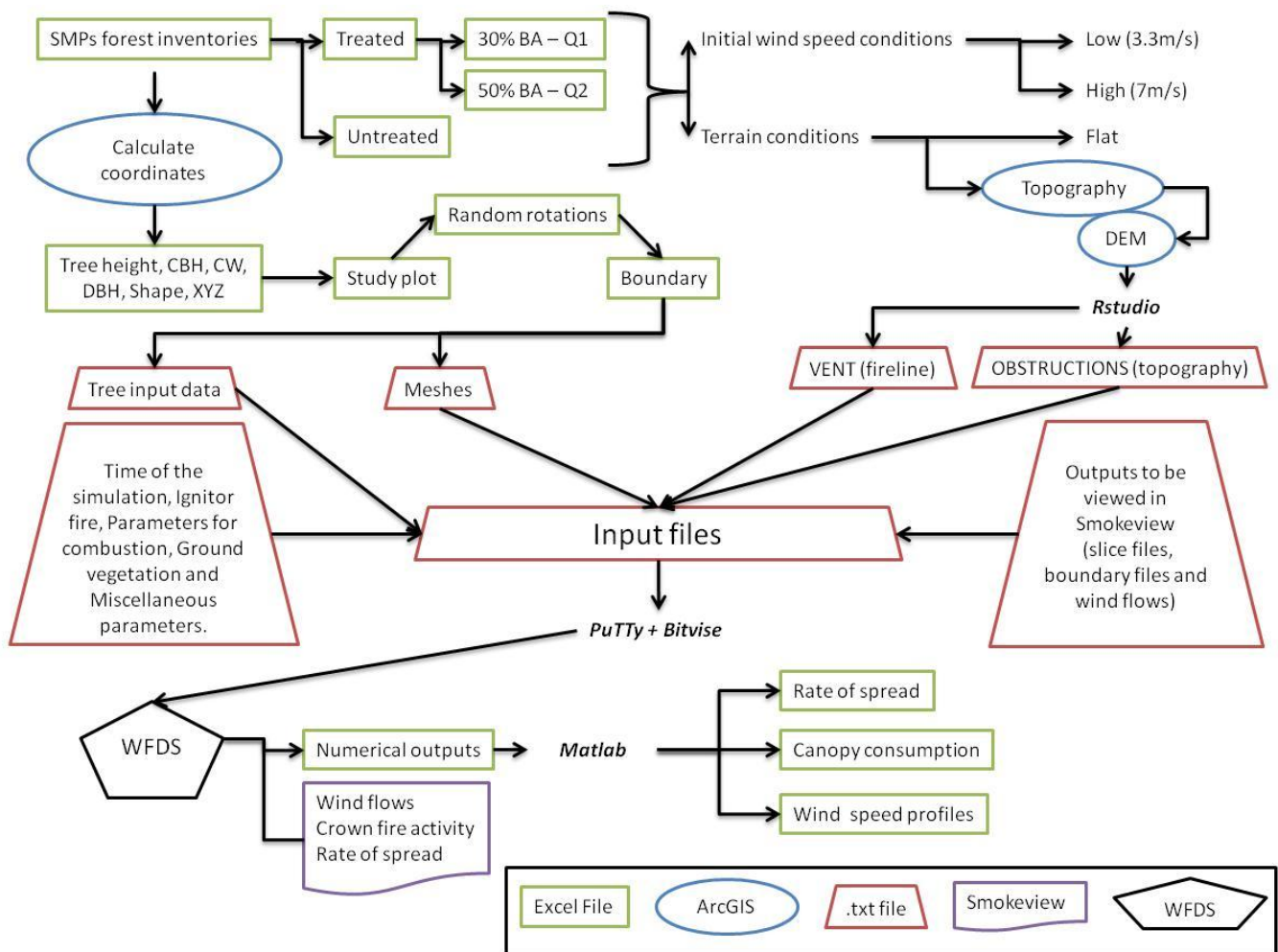


Figure 1: General framework.

3.2 Study area

WFDS works with 3D grids. In order to create that 3D forest, it was necessary a spatially explicit forest inventory data to write an input file with the exact coordinates of everything that was wanted in the grid.

The CTFC (Centre Tecnologic Forestal de Catalunya) sent us 4 forest inventories with this data. These inventories were taken in the northern part of Catalonia, in the region of Pallars Jussà, town council of Gavet de la Conca and in the forest property called Bon Repòs.

The data obtained, was from 4 different plots (Q5, Q6, Q8 and Q9). These plots were grouped depending the treatment applied.

- Plot Q5 and Q8 --> Plot Q1 --> thinning 30% of the basal area.
- Plot Q6 and Q9 --> Plot Q2 --> thinning 50% of the basal area.

So, from now on, the plots we will talk about are the grouped ones, Q1 and Q2.

The data that CTFC provided to us and was the reason why we selected this area to work on was:

- Georeferenced trees.
- Tree height, diameter, crown bulk height and crown width of each tree.
- Forest inventory before and after treatments.

Location

Our study area is located north-west of Catalonia, in the catalan pre-Pyrenees. There we find the region called Pallars Jussà, where the city council of Gavet de la Conca is part of it. The forest property where the study has been carried out is called Bon repòs and is part of Gavet de la Conca (Figure 2).

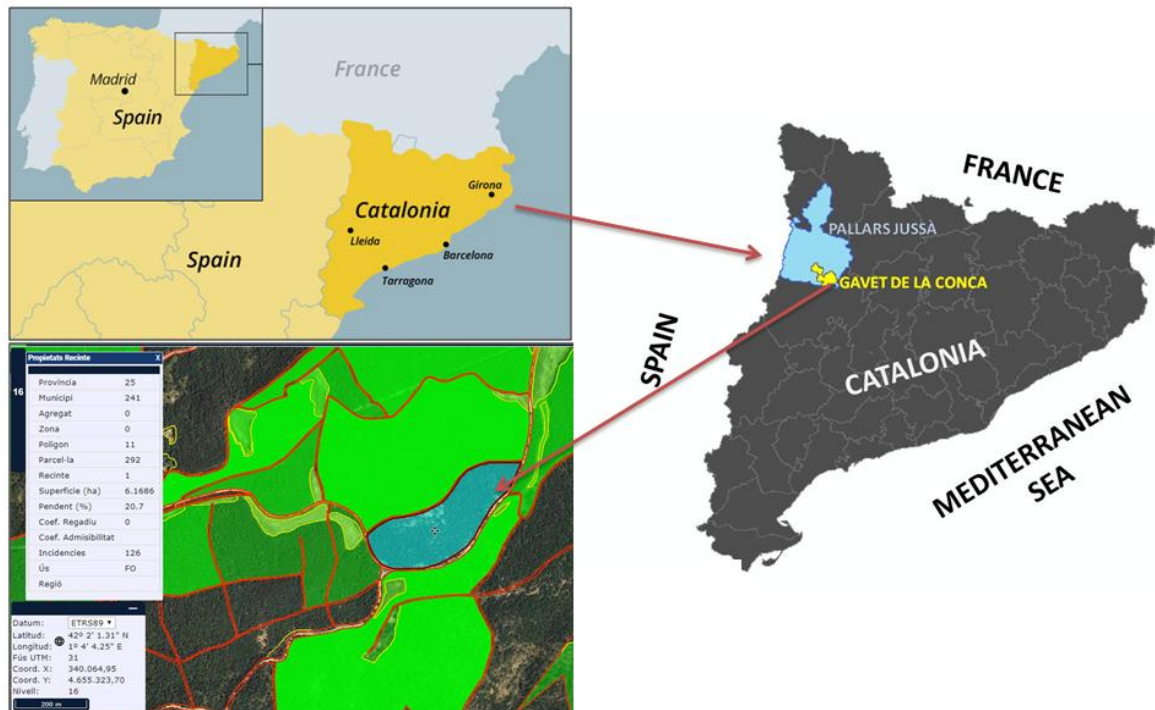


Figure 2: Location of the study area.

Topography

The study zone is located in the south-eastern part of the region Pallars Jussà. It covers the mountain range called Cucut and the north part of the mountain range called Comiols. The main topographic characteristics of this mountain range are a minimum slope of 0.3% and a maximum of 123%. Regarding the elevation, the lowest point is at 800 meters above the sea level and the highest at 1.225 meters (Figure 3). The dominant aspect of the study zone is southwest. (Figure 3).

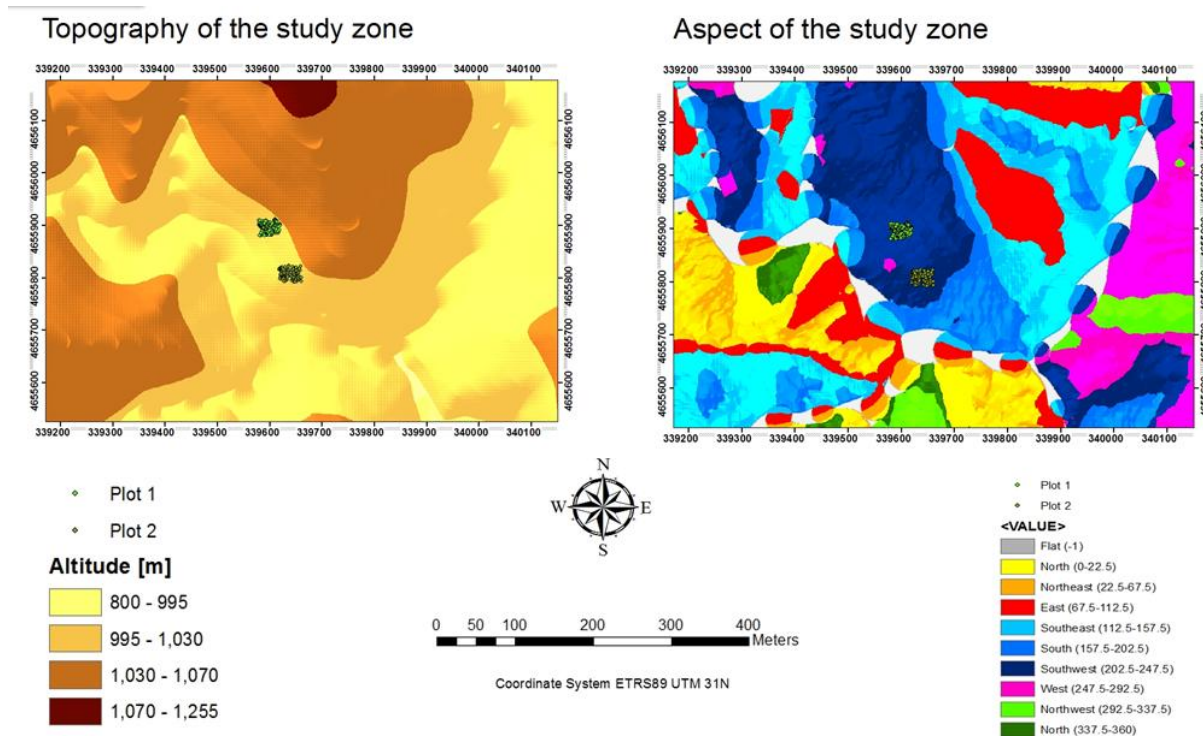


Figure 3: Topography and aspect of the study zone.

Vegetation

As described in a previous forest inventory made by Gerald Pujantell, 2005, the main species of the tree layer are *Quercus cerrioides*, *Pinus sylvestris*, *Pinus nigra ssp. salzmannii* and *Quercus ilex ssp. ballota*. Pines and oaks form mixed forests in the shady spots, whereas in the sunny spots, the oaks are mixed with *Quercus ilex ssp. ballota*. Other species found are *Sorbus aucuparia*, *Sorbus aria*, *Acer opalus*, *Acer campestre* and *Pinus pinaster*. The more abundant species in the shrub layer are *Erica scoparia* and *Buxus sempervirens*. Other shrubs found are *Juniperus communis*, *Rosa sp.*, *Genista scoparius*, *Crataegus monogyna* and *Calluna vulgaris*. The herb layer is relatively abundant and is represented by *Hepatica nobilis*, *Brachypodium phoenicoides*, *Carex halleriana*, *Arctostaphylos uva-ursi* and *Aphyllantes monspeliensis*. The oak that is found in the study plots is called *Quercus humilis* hybridized with *Quercus faginea* which is called *Quercus cerrioides*.

Weather

The weather station called Comiols is the most representative one of the study zone due to it is located inside the forest property of Bon Repòs. It is located at 1.049 meters above the sea level. The data provided are a 30-years-serie from 1.968 to 1.998.

The summarize of the monthly and annual temperature is in Table 1:

Table 1: Summary of the annual and monthly temperature of the weather Station of Comiols. Where T: absolute maximum temperature (°C); T': mean maximum monthly temperature (°C); t: absolute minimum monthly temperature (°C); t': mean minimum monthly temperature (°C); Tm: mean monthly temperature (°C).

	January	February	March	April	May	June	July	August	September	October	November	December	Mean
T	13.0	13.5	19.7	22.0	27.9	32.9	37.6	34.3	29.5	26.3	21.0	15.3	24.4
T'	4.7	5.6	8.9	11.2	17.3	23.5	29.9	29.3	23.9	17.3	10.7	5.7	15.7
t	-6.1	-6.6	-5.8	-4.6	-2.1	-0.2	4.7	4.6	0.1	-1.9	-4.8	-5.9	-2.4
t'	-2.6	-2.9	-1.9	-0.9	3.4	8.3	12.9	12.9	8.7	3.4	-0.7	-2.0	3.2
Tm	1.1	3.3	6.6	9.9	14.7	18.0	20.4	21.3	17.6	11.0	5.1	1.1	10.8

The summarize of the monthly and annual rain is in Table 2:

Table 2: Mean monthly precipitation of the weather station of Comiols. Where Pm is the mean monthly precipitation (mm).

	Pm
January	32.8
February	34.9
March	58.8
April	61.0
May	99.5
June	60.9
July	23.9
August	70.3
September	94.5
October	73.1
November	61.2
December	53.5
Total	730.4

From the Walter-Lieth diagram (Figure 4) it is possible to interpret the following statements:

- Negative mean minimum temperatures and so frosts during January, February, March, April, November and December.
- Likelihood of frosts during May, June and October due to an absolute negative minimum temperature.

- During July there is a dry period where the mean monthly precipitation is lower than the mean monthly temperature.

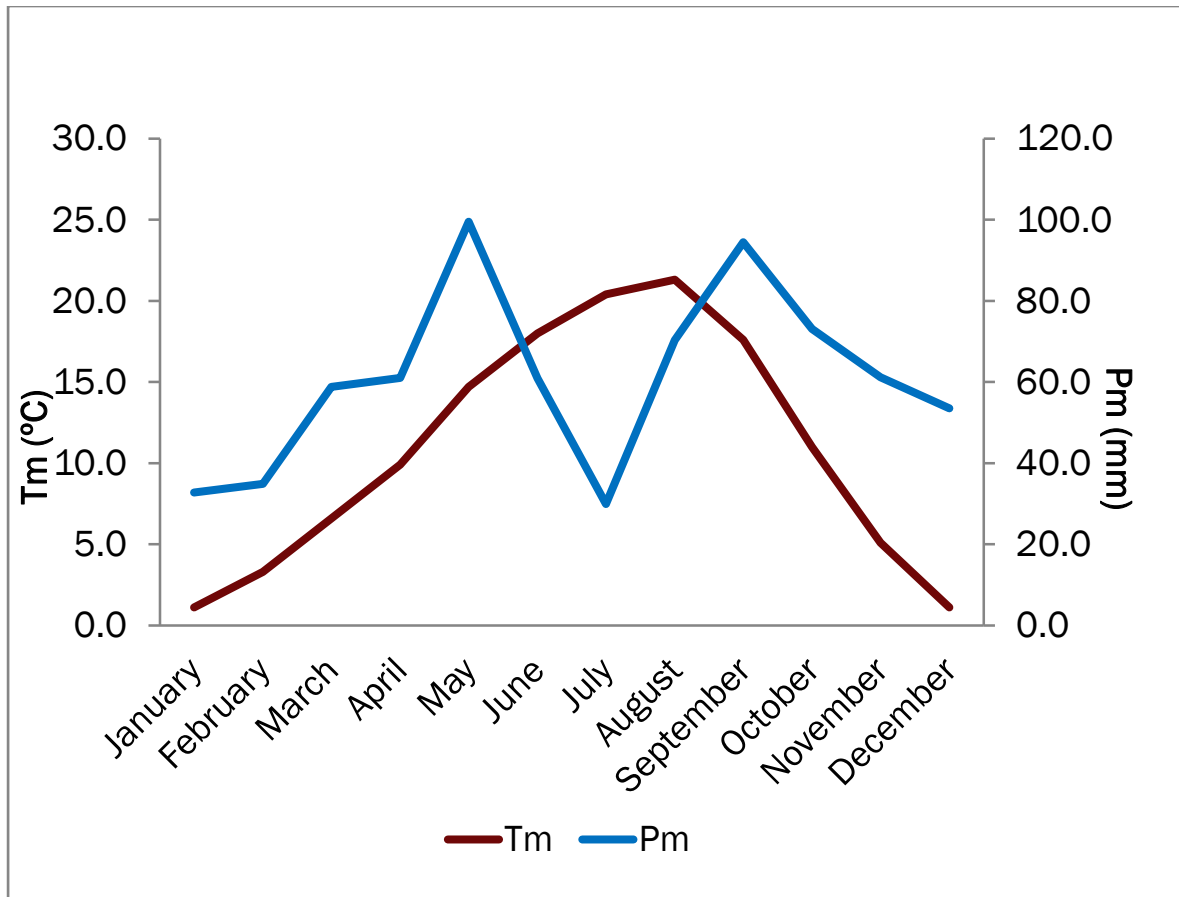


Figure 4: Walter-Lieth diagram of the weather station of Bon Repòs. Where Tm: mean monthly temperature (°C); Pm: mean monthly precipitation (mm).

Wildfire history

In this section, the number of wildfires occurred in the region of Pallars Subirà are analyzed. The data has been obtained from the Catalan Government webpage (gencat.cat) and the available data goes from 1954 to 2017. In Table 3: Wildfire history of Pallars Jussà. we can observe the number of hectares burned from 1954 to 2014 each year a fire has occurred.

Table 3: Wildfire history of Pallars Jussà.

Wildfire history of Pallars Jussà	
Year	Fire size [ha]
1954 - 1986	4865.6
1998	50
1999	19.4
2002	28.8
2005	9.8
2008	15.8
2011	6.9
2012	285.9

In Figure 5, it is possible to visualize the area burned since 1986 until 2014. With this graphic we can also see the fire frequency over years that there has been in the region of Pallars Jussà.

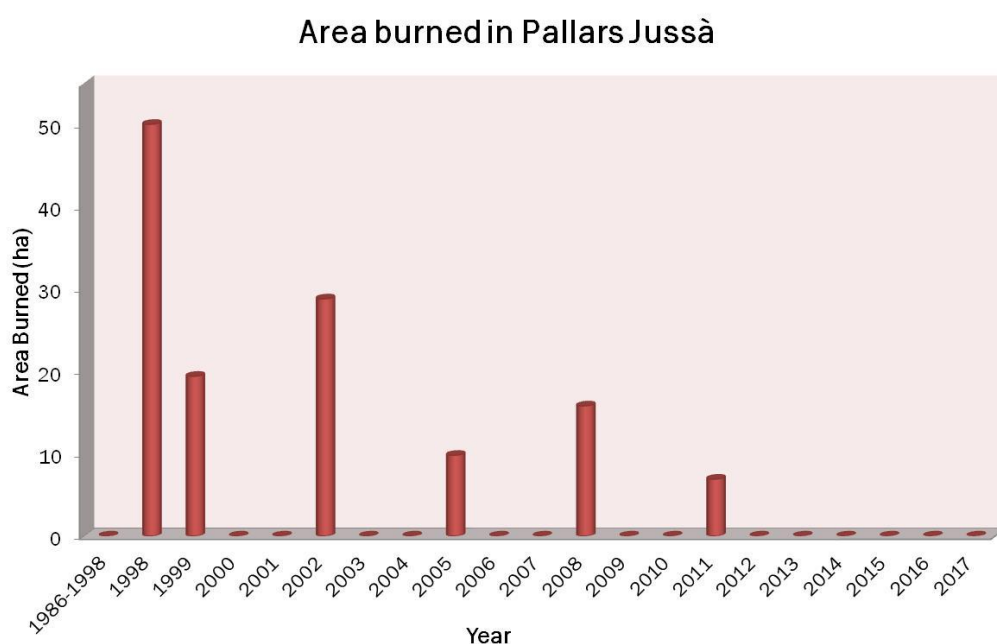


Figure 5: Area burned in the region of Pallars Jussà since 1.986 until 2017.

In Figure 6 it is possible to see the distribution of fires over the region of Pallars Jussà and their sizes. The biggest fire occurred in the region was in 1.978 with an extension of 2.200 hectares.

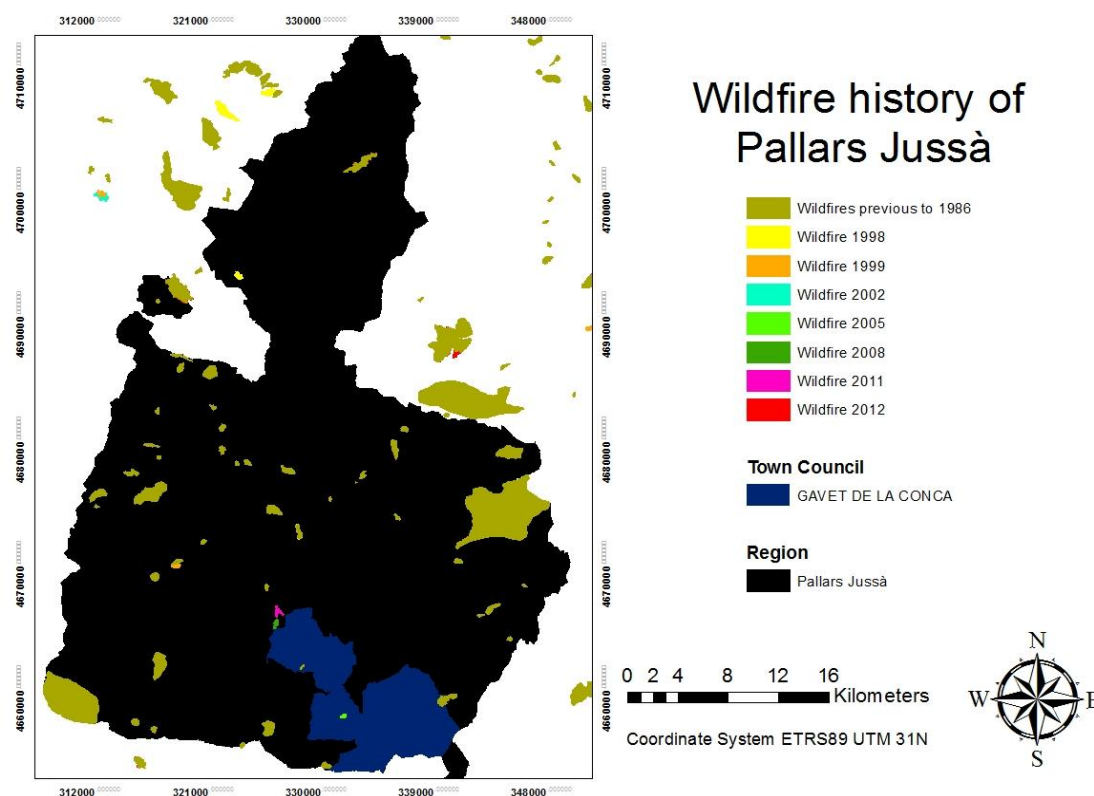


Figure 6: Wildfire history of Pallars Jussà.

All the maps showed in the description of the study area can be found in Annex I.

3.3 Fuel treatments in Strategic Management Points

The study area is located in a Strategic Management Point. So previous to explain the treatments applied, the Fire Type, Model Fire and Strategic Management Point Concepts are explained:

When analyzing historical fires it becomes obvious that under the same topography and weather conditions, fire spreads following similar spread schemes. These similar patterns define the Fire Types Concept. The specification of a region through the Fire Types Concept with adjustments to particular landscape features is translated into the concept of Model Fires. A model fire serves as a reference and describes the maximal potential of a fire to become a large wildfire in a particular landscape unit. It provides information and criteria for discussing and placing measures that need to be implemented to provide support to fire management and suppression operations. The model fires concept allows to understand the main characteristics that describe the expected movement of a large wildfire in a particular areas, pointing out it spread scheme. This advance in planning allows to identify the Strategic Management Points (SMPs), which are locations throughout a region where the modification of fuel and/or preparation of infrastructures enable the suppression service to carry out safe operations to attack and limit the range of a large wildfire. (Costa, et al. 2011).

The treatments applied on our study area are shown in Table 4. And a graphic where it is possible to see the variation of the number of the trees and the diametric classes can be seen in Figure 7.

Table 4: Treatments applied in the study area.

Plots	Treatment
Q1	Low thinning 30% of the BA
Q2	Low thinning 50% of the BA

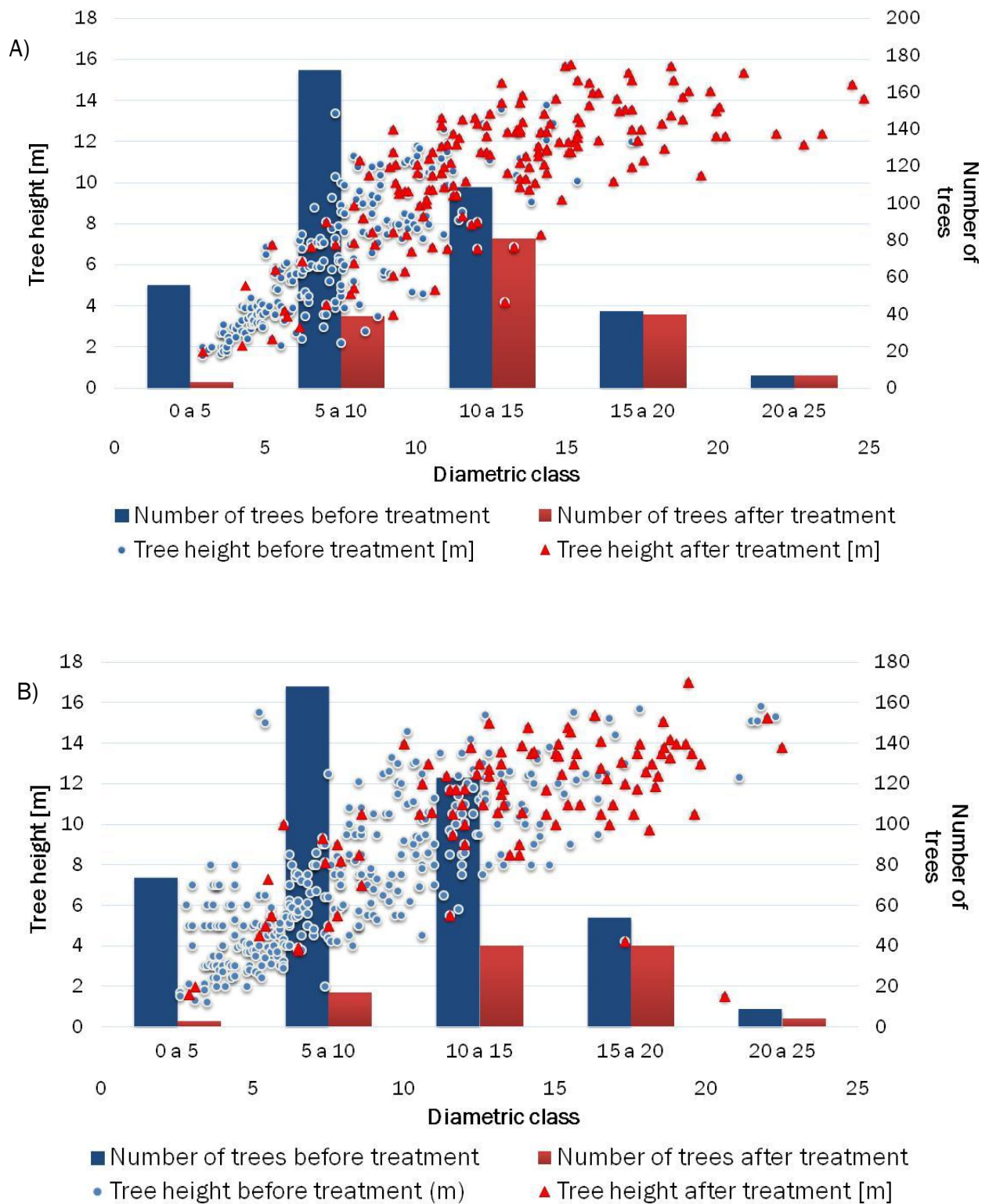


Figure 7: Graphics of the treatments applied in the study zone. Analysis of the number of trees and the diametric class. A) thinning 30% of the Basal Area (Q1). B) thinning 50% of the Basal Area (Q2).

3.4 Fire simulation modeling

3.4.1 Selection of the simulator

In order to meet the described objectives of this project, it was possible to work with different fire behavior simulators such as FARSITE or WFDS.

Bova et al., 2015, described simulations of fire spread created using a level set Eulerian approach (as implemented in the wildland-urban interface fire dynamics simulator, WFDS) and a marker method (as implemented in FARSITE).

In describing the motion of a fire front, an observer can focus on the changes that take place at given points in space as the front passes (Eulerian frame of reference) or on what happens while following the points comprising the moving front (Lagrangian frame of reference).

The FARSITE model computes the movement of separate Lagrangian points, also called markers. An Eulerian alternative to the marker approach is the 'level set' method of tracking an interface, where the Lagrangian perspective is exchanged with the Eulerian via a relatively simple mathematical transformation (Sethian, 1992). An advantage of this method is that the behavior of merging front arises naturally from the underlying mathematics and thus does not require the special handling that is needed when a marker method is used (Rehm and McDermott, 2009).

After the simulations, it was found that for simple scenarios such as flat terrain and uniform fuel type, both models, FARSITE and WFDS give virtually identical results. Although there are noticeable differences between the results of both models in more complex cases, such as a variable terrain and fuels.. (Bova et al., 2015).

However, there are several additional advantages on using WFDS rather than FARSITE.

In FARSITE there is much room for improvement in fire growth simulation. Aside from incorporating more sophisticated fire behavior models, other dimensions of fire behavior and effects can be included. For example, smoke production, holdover of fire activity in different fuel complexes after precipitation, live fuel moisture variation, use of harmonic mean spread rates for spatial fuel mixtures, and gridded weather and wind inputs would allow a more comprehensive simulation of fire growth and behavior (Finney, 2004).

WFDS solves numerically a form of the Navier-Stokes equations appropriate for thermally-driven flows with an emphasis on smoke and heat transport from fires. Moreover, its results can be visualized in 3D with Smokeview (G.P.Forney, 2013).

Some features of WFDS are:

- Large Eddy Simulations (LES) is the default mode of operation.
- Uses a single-step, mixing-controlled chemical reaction which uses three lumped species such as air, fuel and products.
- Radiative heat transfer is included in the model via the solution of the radiation transport equation for a gray gas and in some limited cases using a wide band model. Liquid droplets can absorb and scatter thermal radiations.
- It approximates the governing equations on a rectilinear mesh.
- It is possible to prescribe more than one rectangular mesh with different resolutions.
- It is possible to run WFDS calculations on more than one computer using MPI.
- All solid surfaces are assigned thermal boundary conditions, plus information about the burning behavior of the material.
- Possibility to change fuels' characteristics.
- Calculation of dry weights and variation of fuel moisture.
- 3D wind flows , interaction with fire and forest structures.

In conclusion, it was decided to work with WFDS due to all the additional advantages of all its features.

WFDS

The Wildland-Urban Interface Fire Dynamics Simulator (WFDS) model (NIST, 2007) is a recent extension of the Fire Dynamics Simulator (FDS)(NIST, 2000), a computational fluid dynamics (CFD) fire model designed for structural fire applications. FDS was extended to accommodate vegetative fuels, such as foliage, as well as complex terrain and ambient wind flows. WFDS is a physical numerical fire behavior model in which CFD methods are used to solve three-dimensional, time-dependent equations governing fluid motion, combustion, and heat transfer.

A low-Mach number approximation (Rehm and Baum, 1978) of the governing equations for mass, momentum, and energy is used; a large eddy simulation (LES) approach for turbulence modeling (Smagorisky 1963) provides a time-dependent, coarse-grained numerical solution to those equations. A direct solver for the pressure Poisson equation significantly speeds up calculations compared to iterative methods.

3.4.2 Input file

In this section, the input file needed to run the simulations is explained. The input files used for this study can be found in Annex V and Annex VI.

INPUT DATA

The operation of WFDS is based on a single ASCII text file containing parameters organized into namelist groups. The input file provides WFDS with all the necessary information to describe the scenario.

In this section, the contents of this ASCII text file are described.

Each of these namelist group begins with the aperstand character "&", followed by the name of the namelist group. Then a coma-delimited list of the input parameters and finally a forward slash "/".

HEAD

To ensure that FDS reads the entire input file it is necessary to add "&HEAD" at the start of the file and "&TAIL/" at the end of the input file. This completes the file from head to tail.

The namelist group HEAD contains two parameters:

```
&HEAD CHID='postq1extreme'
      TITLE='postq1extreme' /
```

These are used to tag the output files. They can be different but in order to make things easier it is recommended to use the same tag. No periods or spaces are allowed.

TIME

TIME is the name of a group of parameters that define the time duration of the simulation and the initial time step used to advance the solution of the discretized equations.

```
&TIME TWFIN=1700 /
```

If it is wanted the time line to start at a number other than zero, it is possible to use: T_BEGIN to specify the time.

COMPUTATIONAL MESHES

All WFDS calculations must be performed within a domain that is made up of rectilinear volumes called meshes. Each mesh is divided into rectangular cells, the number of which depends on the desired resolution of the flow dynamics.

```
&MESH ID='MESH1', IJK=50,100,100,XB=0,100,0,200,0,200/
&MESH ID='MESH2', IJK=200,10,200,XB=100,300,0,10,0,200/
&MESH ID='MESH3', IJK=200,10,200,XB=100,300,10,20,0,200/
&MESH ID='MESH4', IJK=200,10,200,XB=100,300,20,30,0,200/
&MESH ID='MESH5', IJK=200,10,200,XB=100,300,30,40,0,200/
etc.
```

The coordinate system is in meters on the X,Y and Z.

IJK is the parameter that defines the cells in which the mesh is subdivided.

XB is the parameter that defines the coordinates of the mesh, the volume.

It is possible to transform the cells using "&TRNX","&TRNY" or "&TRNZ". It has not been used in this study.

Because an important part of the calculation uses a Poisson solver based on Fast Fourier Transforms, in the y and z directions, the second and third dimensions of the mesh should each be form:

$$2^l 3^m 5^n$$

Where l, m and n are intergers.

Important information about meshes:

- More than one computational mesh are usually connected although it is not necessary.
- It is necessary that there is a MESH line for each mesh and they should be entered from finest to coarsest.
- Meshes can overlap or not touch at all.

- It is possible to assign more than one mesh to a single process and it is possible to assign more than one process to a single processor.
- It is very important to avoid putting mesh boundaries where critical action is expected, especially fire.

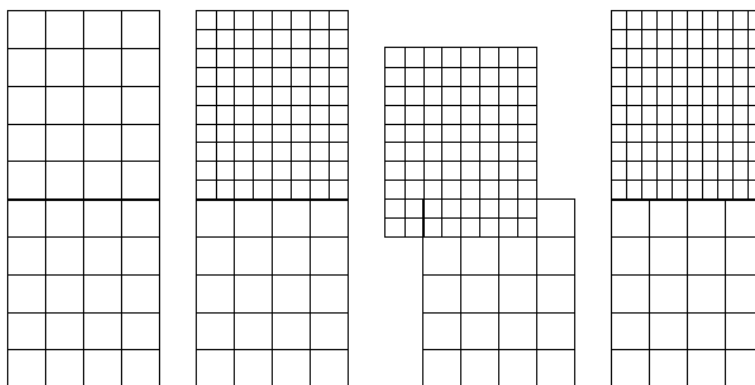


Figure 8: First Figure is an ideal mesh. Second one is allowed as long as there are an integral number of fine cells abutting each coarse cell. Third one: Allowed but with a questionable value. Fourth one: Not allowed. Source: FDS User Guide

Mesh resolution depends on what it is wanted to accomplish. What is recommended is to build a WFDS input file using a relatively coarse mesh and then gradually refine it until it isn't possible to see appreciable differences in the results.

In this study, coarse meshes were built for the study areas where we didn't want to study the results obtained, and fine meshes were built for those areas where we wanted to analyze the results obtained.

MISCELLANEOUS PARAMETERS

MISC is the namelist group of global miscellaneous input parameters. It contains parameters that do not logically fit into any other category.

Only one MISC line should be entered in the data file. In this study case:

```
&MISC
RADIATION=.TRUE.,BAROCLINIC=.TRUE.,TERRAIN_CASE=.TRUE.,WIND_ONLY=.FALSE. /
```


BUILDING THE MODEL

A considerable amount of work in setting up a calculation lies in specifying the geometry of the space to be modeled and applying boundary conditions to the solid surfaces.

Geometry is described in terms of:

- Rectangular Obstructions that can heat up, burn, conduct heat, etc.
- Vents, from which air or fuel can be injected into or drawn from the flow domain.

A boundary condition needs to be assigned to each obstruction and vent describing its thermal properties. For example, a fire is one type of boundary condition.

The bounding surfaces have the SURF namelist group. This one defines the structure of all solid surfaces or openings within or bounding the flow domain.

The default boundary condition for all solid surfaces is that of a smooth inert wall with temperature fixed and is referred as "INERT". If additional boundary conditions are desired, they have to be listed one boundary condition at a time.

On each obstacle and vent line the character string "SURF_ID=" indicates the ID of the SURF line containing the boundary condition parameters. For example:

```
&VENT XB=0,100,0,100,0,0,SURF_ID='GROUND VEG1' /
```

- Ground VEG1 For Timber Litter fuel class based on Scott & Burgan TL3

```
&SURF ID = 'GROUND VEG1'
VEGETATION = .TRUE.
VEG_DRAG_COEFFICIENT = 0.25
VEG_MOISTURE = 0.10
VEG_SV= 5028
VEG_CHAR_FRACTION = 0.265
VEG_LOAD = 1.21
VEG_HEIGHT = 0.09
VEG_DENSITY= 510
FIRELINE_MLR_MAX = 0.3
RGB = 122,117,48 /
```

Then the characteristics of the new vent have to be specified. These values are already defined for all the Scott & Burgan fuel models. Some are constants and some can be modified.

To create the obstructions it is necessary to know that the entire geometry of the model is made up entirely of rectangular solids, each one introduced on a single line in the input file.

The basics of the Obstructions (OBST) namelist group are:

Each OBST line contains the coordinates of a rectangular solid within the flow domain.

The boundary conditions for the obstruction can be specified with the parameter "SURF_ID".

If the obstruction has different properties for its top, sides and bottom, use "SURF_ID", three character strings specifying the boundary condition for top, sides and bottom. For example:

```
&SURF_IF='FIRE', HRRPUA=1000.0/
```

```
&OBST XB=2.3,4.5,1.3,4.8,0.0,9.2, SURF_ID='FIRE' 'INERT' 'INERT'
```

This example puts the fire on top of the obstruction.

For full functionality, the obstruction should be specified to be at least one mesh cell thick.

Example of the obstruction created in this study to build the topography:

-Elevation

```
&OBST XB=550,551,0,1,0,50, SURF_ID='surface' /
&OBST XB=550,551,2,3,0,50, SURF_ID='surface' /
&OBST XB=550,551,2,3,0,50, SURF_ID='surface' /
&OBST XB=550,551,4,5,0,51, SURF_ID='surface' /
&OBST XB=550,551,4,5,0,51, SURF_ID='surface' /
&OBST XB=550,551,6,7,0,51, SURF_ID='surface' /
&OBST XB=550,551,6,7,0,51, SURF_ID='surface' /
&OBST XB=550,551,8,9,0,52, SURF_ID='surface' /
&OBST XB=550,551,8,9,0,52, SURF_ID='surface' /
&OBST XB=550,551,10,11,0,52, SURF_ID='surface' /
&OBST XB=550,551,10,11,0,52, SURF_ID='surface' /
&OBST XB=550,551,12,13,0,53, SURF_ID='surface' /
&OBST XB=550,551,12,13,0,53, SURF_ID='surface' /
etc.
```

Whereas the OBST group is used to specify obstruction conditions within the computational domain, the VENT group is used to prescribe planes adjacent to obstructions or external walls.

The VENTS are chosen in a similar manner to the obstructions with the sextuplet XB denoting a plane abutting a solid surface.

A fire, for example, is usually created by first generating a solid obstruction via OBST line, and then specifying a VENT somewhere on one of the faces of the solid with a SURF_ID with the characteristics of the thermal and combustion properties of the fuel.

An easy way to specify an entire external wall is to replace XB with MB (mesh boundary), a character string whose value is one of the following: XMAX, XMIN, YMAX, YMIN, ZMAX, ZMIN. Like an obstruction, the boundary condition index of a vent is specified with SURF_ID, indicating which of the listed SURF line to apply.

For example, to specify the wind flow, in this study it has been written:

```
- Domain-Boundary conditions
&VENT MB = XMIN, SURF_ID = 'INFLOW' /
&VENT MB = XMAX, SURF_ID = 'OPEN' /
&VENT MB = YMIN, SURF_ID = 'MIRROR' /
&VENT MB = YMAX, SURF_ID = 'MIRROR' /
&VENT MB = ZMAX, SURF_ID = 'MIRROR' /
```

This example defines the wind flow in our study area. Imagine a rectangle where the X coordinate is the shortest side of it, Y the longest one and Z the elevation. Now consider this rectangle as a box. The minimum X side of the box is open, so there is an "INFLOW", the maximum X side is open as well, so we create a wind flow. Then the Y sides and Z sides work like a mirror to avoid the wind acting like in a closed space.

TIME-DEPENDENT FUNCTIONS AND FIRELINE

At the start of any calculation, the temperature is ambient everywhere, the flow velocity is zero everywhere and nothing is burning. When the calculation starts, temperatures, velocities, burning rates...are ramped-up from their starting values because nothing can happen instantaneously. By default, everything is ramped-up to their prescribed values un approximately 1 second. However, it is possible to control the rate at which things turn on or turn off. To do this, set RAMP_Q equal to a character string designating the ramp function to use for that particular surface type, then somewhere in the input file generate lines of the form:

```
&RAMP ID='RAMPNAME1', T= 0.0, F=0.0 /
```

```
&RAMP ID='RAMPNAME1', T= 5.0, F=0.5 /
```

```
&RAMP ID='RAMPNAME1', T= 10.0, F=0.7 /
```

Where, T is the time, and F indicates the fraction of the heat release rate, velocity, mass fraction, etc...to apply.

Note that each set of RAMP lines must have a unique ID and that the lines must be listed with monotonically increasing T.

So, when it is desired to create a ignition fireline, it is possible to specify it directly. To do this, it is necessary to first add a SURF line with a specified heat release rate per unit area, HRRPUA, and a time history parameter: RAMP_Q. Then, it is needed to specify XYZ on either a VENT or the same SURF line. The fire is directed to start at the point XYZ. For example:

```
&SURF ID='IGN FIRE', HRRPUA=500.0, RAMP_Q='RAMPFIRE' /
&RAMP ID='RAMPFIRE', T= 0.0, F=0.0 /
&RAMP ID='RAMPFIRE', T= 1.0, F=1.0 /
&RAMP ID='RAMPFIRE', T=30.0, F=1.0 /
&RAMP ID='RAMPFIRE', T=31.0, F=0.0 /
&VENT XB=150,155,40,160,0,0, SURF_ID='IGN FIRE' /
```

These lines specify that the fire line has been created in the coordinates that indicate XB. The RAMP_Q is used to turn the burning on and off to simulate the consumption of fuel as the fire spreads.

OTHER PARAMETERS

Other parameters specified in the Input files of this study are:

```
&SPEC ID='WATER VAPOR' /
```

This parameter accounts for water vapor from drying vegetation.

```
&REAC ID='WOOD'
FYI='Ritchie, et al., 5th IAFSS, C_3.4 H_6.2 O_2.5'
SOOT_YIELD = 0.002
O           = 2.5
C           = 3.4
H           = 6.2
HEAT_OF_COMBUSTION = 17700 /
```

This namelist group specify the parameters for combustion of fuel gases from pyrolysis of the solid fuels.

OUTPUT DATA

WFDS has various types of output files that store computed data. Some of the files are binary format and intended to be read and rendered by Smokeview (G.P.Forney, 2013). Some of the files are just comma-delimited text files. It is important to take into account that you must explicitly declare in the input file most of the WFDS output data.

To visualize the flow pattern better, it is possible to create planar slices of data, either in the gas or solid phases by using the SLCF (slice file) or BNDF (boundary file) namelist group. Both of these outputs formats permit to animate these quantities in time.

The namelist group DUMP contains parameters that control the rate at which output files are written, and various other global parameters associated with output files.

In this study case it has been chosen to work with slice files.

SLICE FILES

The SLCF namelist group parameters allows to record various gas phase quantities at more than a single point. A "slice" refers to a subset of the whole domain, it can be a line, plane or volume, depending on the values of XB.

It is possible to specify, for example, $PBY=5.3$ instead of XB if it is desired that the entire plane $y=5.3$ slicing through the domain be saved. PBX and PBZ control planes perpendicular to the x and z axes, respectively.

```
&SLCF PBY=100, QUANTITY='U-VELOCITY' /
&SLCF PBY=100, QUANTITY='V-VELOCITY' /
&SLCF PBY=100, QUANTITY='W-VELOCITY' /
```

With 1-D and 2-D slice files, it is possible to control the frequency of the output with DT_SLCF on the DUMP line. If the slice is a 3-D volume, then its output frequency is controlled by the parameter DT_SL3D . But no 3-D slices had been used in this study case.

It is also possible to create slice files parallel to the surface by writing for example: $AGL_SLICE=1$.

```
&SLCF XB=0,550,0,200,1,1, AGL_SLICE=1, QUANTITY='U-VELOCITY' /
&SLCF XB=0,550,0,200,2,2, AGL_SLICE=2, QUANTITY='U-VELOCITY' /
&SLCF XB=0,550,0,200,3,3, AGL_SLICE=3, QUANTITY='U-VELOCITY' /
&SLCF XB=0,550,0,200,4,4, AGL_SLICE=4, QUANTITY='U-VELOCITY' /
&SLCF XB=0,550,0,200,5,5, AGL_SLICE=5, QUANTITY='U-VELOCITY' /
```

These lines describe the creation of slice files parallel to the surface at 1 meter high, 2 meters high, etc.

BOUNDARY FILES

The BNDF (boundary file) namelist group parameters allow to record surface quantities at all solid obstructions. As with the SLCF group, each quantity is prescribed with a separate BNDF line. No physical coordinates need to be specified, however, just QUANTITY.

For example, in this study case, it has been written:

```
&BNDF QUANTITY = 'WALL THICKNESS' /
```

By comparing the wall thickness at start and finish it is possible to have an idea of how much surface fuel was consumed.

A diagram to summarize the procedure to set up the input file is shown below:

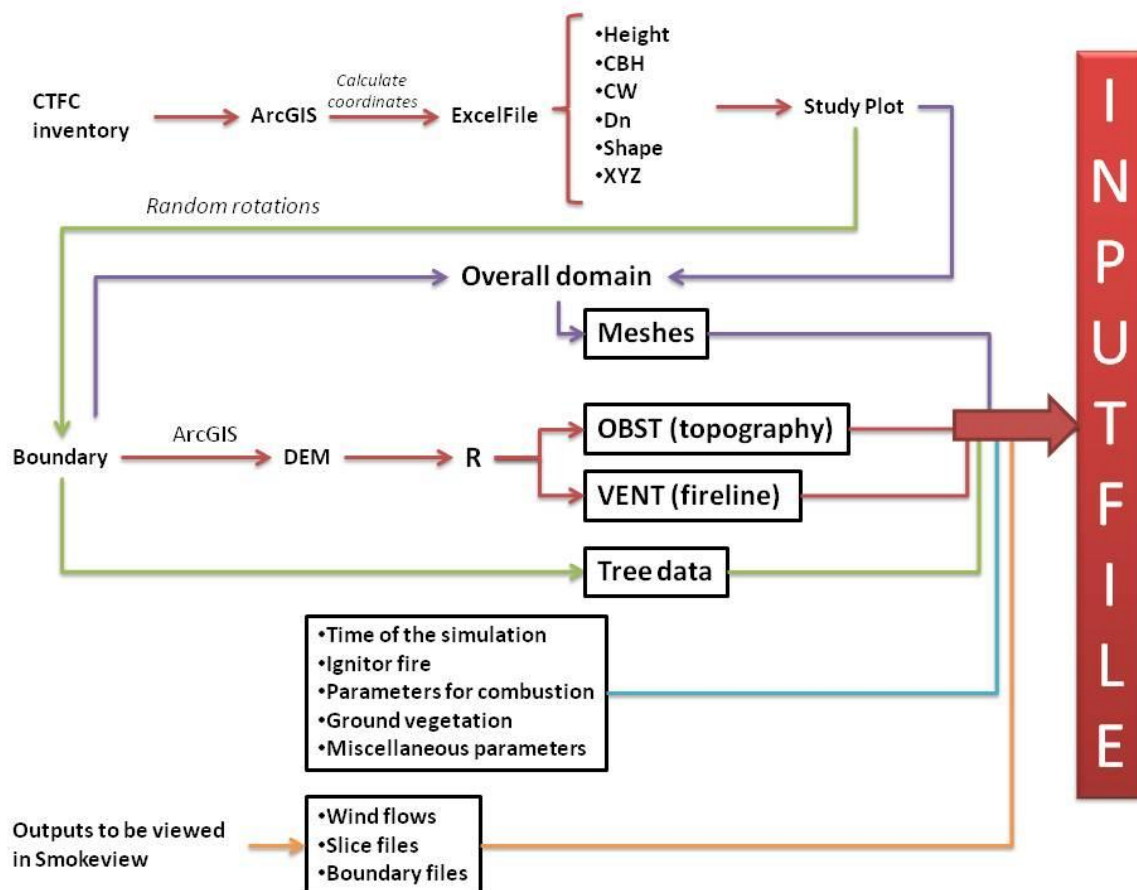


Figure 9: Diagram summarizing the procedure to set-up the input file.

3.4.3 Modeling scenarios

The different modeling scenarios can be seen in Figure 10. Depending on the treatment, status, initial wind speed conditions and type of terrain, sixteen simulations were carried out.

Also in Figure 10, it is possible to see the main 8 combinations that were simulated for both types of terrain: flat terrain and terrain with topography.

Plots	Treatment	Status		Wind speed conditions		Terrain	
Q1	Thinning 30% of BA	Pre treatments	Post treatment	3.3m/s (10.8 km/h)	7 m/s (25.2 km/h)	Topography	Flat
Q2	Thinning 50% of BA	Pre treatments	Post treatment	3.3m/s (10.8 km/h)	7 m/s (25.2 km/h)	Topography	Flat
				Low	High		

- Q1 pre low
- Q1 post low
- Q1 pre high
- Q1 post high
- Q2 pre low
- Q2 post low
- Q2 pre high
- Q2 post high

Figure 10: Modeling scenarios.

3.4.4 Simulation set-up

After knowing the methodology of WFDS, the setting-up of the simulations started. The first step was to get all the ETRS89 coordinates of all trees of the forest inventories.

The 4 plots were circular with a radius of 15 meters. We knew the angle and the distance from the center, so using trigonometry we could calculate the ETRS89 coordinates (calculations can be found in Annex II). Using ArcGIS (Esri, 2012), all trees were located on the topography scenario (Figure 11). The vegetation represented was made up with oaks in the tree layer and a fuel model SH1 of the Scott and Burgan fuel models for the shrub layer.

The next step was to group the different plots, as explained before, obtaining two final plots, Q1 and Q2, of 60x40 meters each. An Excel file with the following data for all trees in the plots was created: tree height, crown base height, crown width, diameter of the trunk, crown shape (in this study case it was defined as cylinders) and ETRS89 coordinates (X, Y and Z). These Excel files can be found in Annex III.

Once obtained the study plots, it was necessary to create a boundary layer big enough to get real conditions inside the study plot. In order to do that, we needed five different parts inside the overall domain:

- A wind entry field at $x=\min$.
- An exiting wind field along $x=\max$.
- A wind field development zone from $x=\min$ to the study plot.
- An area of interest (the study plot).
- The outflow zone from the study plot to $x=\max$.

After doing that, the final result was an overall domain of 550 meters on the x, 200 meters on the y and 200 meters on the z axes. The boundary area and its topography can be seen in Figure 11.

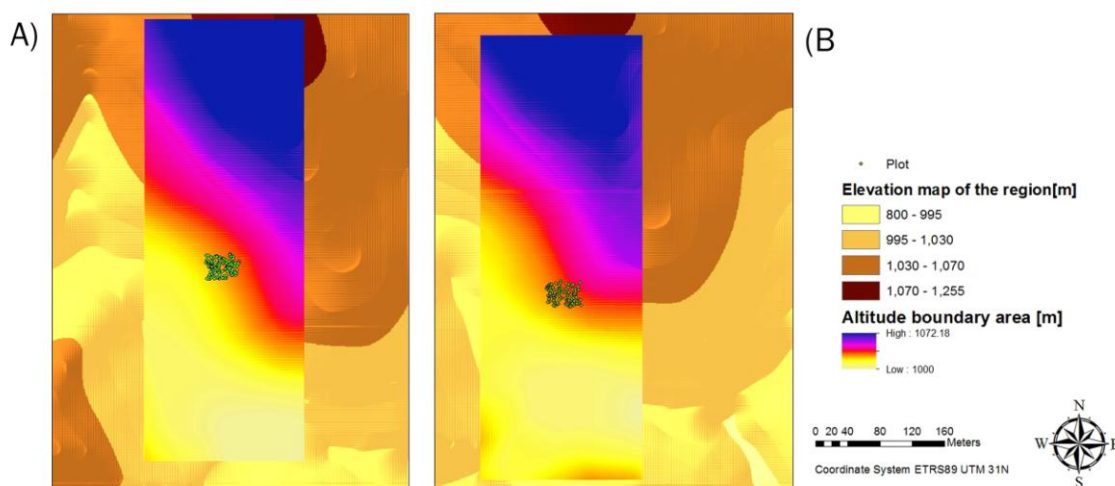


Figure 11: Boundary areas created for Q1(A) and Q2(B).

From ArcGIS, we obtained the coordinates of the boundary area vertex and converted them into a WFDS format as showed in Figure 12:

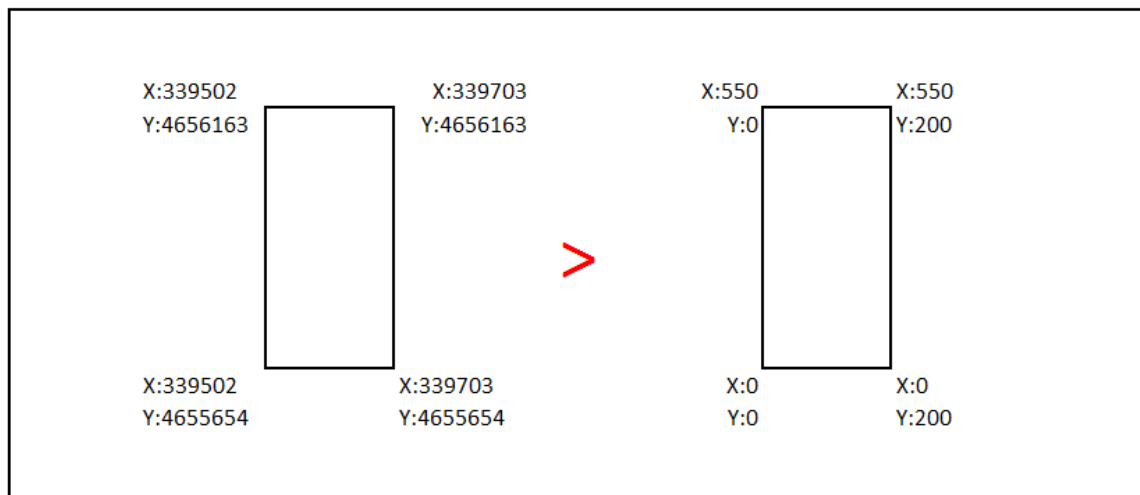


Figure 12: Conversion of coordinates into WFDS format. Source: Own elaboration.

The same procedure was done with the coordinates of all trees by subtracting the lower-left vertex coordinates to the tree coordinates. To obtain the Z value of the trees in a WFDS format, the minimum altitude of the boundary area was subtracted to the altitude obtained from the elevation layer of the overall region of Pallars Jussà in ArcGIS.

The surrounding domain created, was first filled by repeating the study plot around it (Figure 13). As seen in Figure 14a, the result wasn't neither a realistic nor a representative forest. In order to obtain that, the domain was filled up by randomly rotating the study plot around the domain, obtaining a much more realistic forest as seen in Figure 14b.

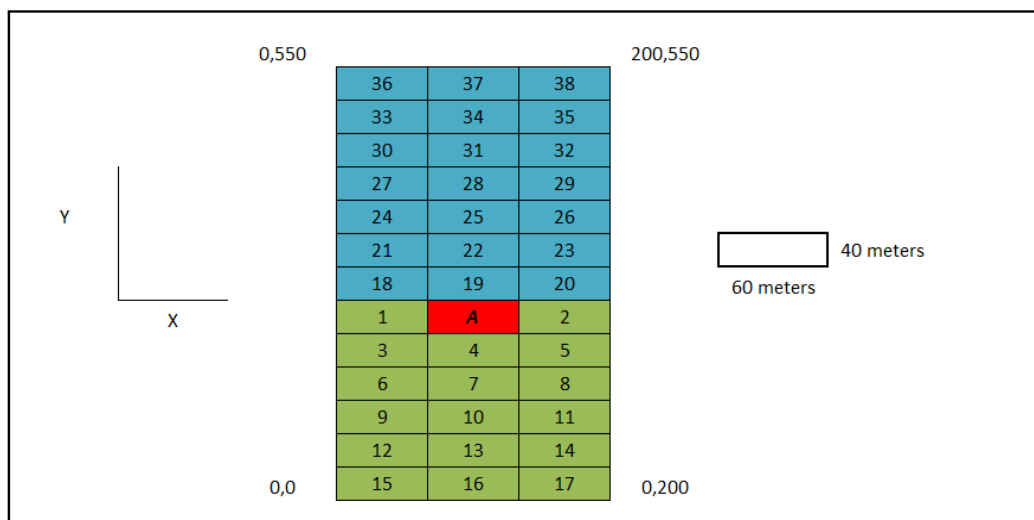


Figure 13: Surrounding domain created around the study plot.

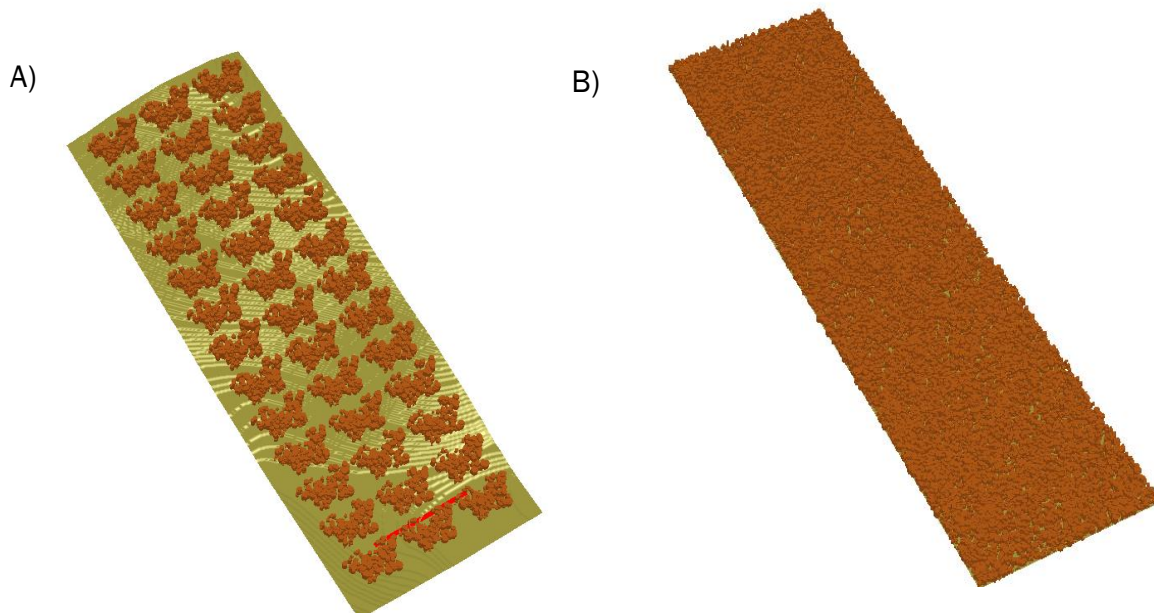


Figure 14: Overall domain of the simulation. A) Domain filled up with study plots. B) Domain filled up with randomly rotated study plots.

After obtaining all trees coordinates, the Excel file with all the tree characteristics was completed and we generated the following data. By writing this data in the input file, WFDS could build all the trees.

```
&TREE XYZ=252,96,0,PART_ID="TREE",FUEL_GEOM="CYLINDER",CROWN_WIDTH=3.025
,CROWN_BASE_HEIGHT=8,TREE_HEIGHT=11.2,OUTPUT_TREE=.TRUE.,LABEL="TREE1"/
&TREE XYZ=251,94,0,PART_ID="TREE",FUEL_GEOM="CYLINDER",CROWN_WIDTH=2.675
,CROWN_BASE_HEIGHT=3.8,TREE_HEIGHT=9,OUTPUT_TREE=.TRUE.,LABEL="TREE2"/
&TREE XYZ=250,95,0,PART_ID="TREE",FUEL_GEOM="CYLINDER",CROWN_WIDTH=2.35
,CROWN_BASE_HEIGHT=5.3,TREE_HEIGHT=12.2,OUTPUT_TREE=.TRUE.,LABEL="TREE3"/
&TREE XYZ=248,96,0,PART_ID="TREE",FUEL_GEOM="CYLINDER",CROWN_WIDTH=6.05
,CROWN_BASE_HEIGHT=6.4,TREE_HEIGHT=12.4,OUTPUT_TREE=.TRUE.,LABEL="TREE4"/
&TREE XYZ=246,95,0,PART_ID="TREE",FUEL_GEOM="CYLINDER",CROWN_WIDTH=3.125
,CROWN_BASE_HEIGHT=4.5,TREE_HEIGHT=7,OUTPUT_TREE=.TRUE.,LABEL="TREE5"/
&TREE XYZ=250,97,0,PART_ID="TREE",FUEL_GEOM="CYLINDER",CROWN_WIDTH=2.2
,CROWN_BASE_HEIGHT=3,TREE_HEIGHT=5.9,OUTPUT_TREE=.TRUE.,LABEL="TREE6"/
&TREE XYZ=244,95,0,PART_ID="TREE",FUEL_GEOM="CYLINDER",CROWN_WIDTH=0.9
,CROWN_BASE_HEIGHT=1.2,TREE_HEIGHT=2.7,OUTPUT_TREE=.TRUE.,LABEL="TREE7"/
&TREE XYZ=242,96,0,PART_ID="TREE",FUEL_GEOM="CYLINDER",CROWN_WIDTH=3.5
,CROWN_BASE_HEIGHT=7.7,TREE_HEIGHT=11,OUTPUT_TREE=.TRUE.,LABEL="TREE8"/
&TREE XYZ=243,96,0,PART_ID="TREE",FUEL_GEOM="CYLINDER",CROWN_WIDTH=1
,CROWN_BASE_HEIGHT=1.1,TREE_HEIGHT=2,OUTPUT_TREE=.TRUE.,LABEL="TREE9"/
&TREE XYZ=241,96,0,PART_ID="TREE",FUEL_GEOM="CYLINDER",CROWN_WIDTH=3.375
,CROWN_BASE_HEIGHT=6.3,TREE_HEIGHT=13.6,OUTPUT_TREE=.TRUE.,LABEL="TREE10"/
&TREE XYZ=242,97,0,PART_ID="TREE",FUEL_GEOM="CYLINDER",CROWN_WIDTH=1.875
,CROWN_BASE_HEIGHT=6.8,TREE_HEIGHT=11.1,OUTPUT_TREE=.TRUE.,LABEL="TREE11"/
&TREE XYZ=241,97,0,PART_ID="TREE",FUEL_GEOM="CYLINDER",CROWN_WIDTH=1.75
,CROWN_BASE_HEIGHT=2.2,TREE_HEIGHT=3.1,OUTPUT_TREE=.TRUE.,LABEL="TREE12"/
&TREE XYZ=241,97,0,PART_ID="TREE",FUEL_GEOM="CYLINDER",CROWN_WIDTH=3.225
,CROWN_BASE_HEIGHT=4.2,TREE_HEIGHT=8.5,OUTPUT_TREE=.TRUE.,LABEL="TREE13"/
&TREE XYZ=242,94,0,PART_ID="TREE",FUEL_GEOM="CYLINDER",CROWN_WIDTH=3.025
,CROWN_BASE_HEIGHT=7.1,TREE_HEIGHT=11.5,OUTPUT_TREE=.TRUE.,LABEL="TREE14"/
etc.
```

To create the topography in WFDS, we first created the Digital Elevation Model (DEM) of the boundary area in ArcGIS. That raster was converted into .tif format by using "copy raster" in ArcGIS. After that, the copied raster file was opened in Rstudio (Rstudio, 2015) to convert the Digital Elevation Model into obstructions in WFDS. To do that, an script similar to the next one was entered in the program:

```
memory.limit(size=15500)
options(scipen=999)
setwd('C:/Users/Olga/Documents/WFDS/Q1')
warning(lapply(c('rgl','raster'), require, character.only = TRUE))

DEM <- raster("q1rastcopy.tif")
DEM.df <- round(as.data.frame(DEM,xy=T),0)
names(DEM.df)[3] <- 'Elev'

DEM.df$SurfID <- 'surface'
DEM.df$x <- DEM.df$x - min(DEM.df$x)
DEM.df$y <- DEM.df$y - min(DEM.df$y)
DEM.df$Elev <- DEM.df$Elev - min(DEM.df$Elev)

DEM.df$text <- paste('&OBST
XB=',DEM.df$x,',',DEM.df$x,',',DEM.df$y,',',DEM.df$y,',',min(round(DEM.df$Elev,0)),
',',round(DEM.df$Elev,0),', SURF_ID=',',DEM.df$SurfID,'"/',sep='')

write.table(DEM.df$text,paste('Elevation.csv',sep=''),row.names=F)
```

With this script, R studio found the raster in the directory indicated, and created an excel file with the OBST namelist group parameters that, once in the input file, created the topography in WFDS as shown in Figure 15. The data generated in the Excel file is shown below:

-Elevation

```
&OBST XB=0,1,508,509,0,47, SURF_ID='surface' /
&OBST XB=1,2,508,509,0,47, SURF_ID='surface' /
&OBST XB=2,3,508,509,0,47, SURF_ID='surface' /
&OBST XB=3,4,508,509,0,48, SURF_ID='surface' /
&OBST XB=4,5,508,509,0,48, SURF_ID='surface' /
&OBST XB=5,6,508,509,0,48, SURF_ID='surface' /
&OBST XB=6,7,508,509,0,48, SURF_ID='surface' /
&OBST XB=7,8,508,509,0,49, SURF_ID='surface' /
&OBST XB=8,9,508,509,0,49, SURF_ID='surface' /
&OBST XB=9,10,508,509,0,49, SURF_ID='surface' /
&OBST XB=10,11,508,509,0,49, SURF_ID='surface' /
&OBST XB=11,12,508,509,0,50, SURF_ID='surface' /
&OBST XB=12,13,508,509,0,50, SURF_ID='surface' /
etc.
```

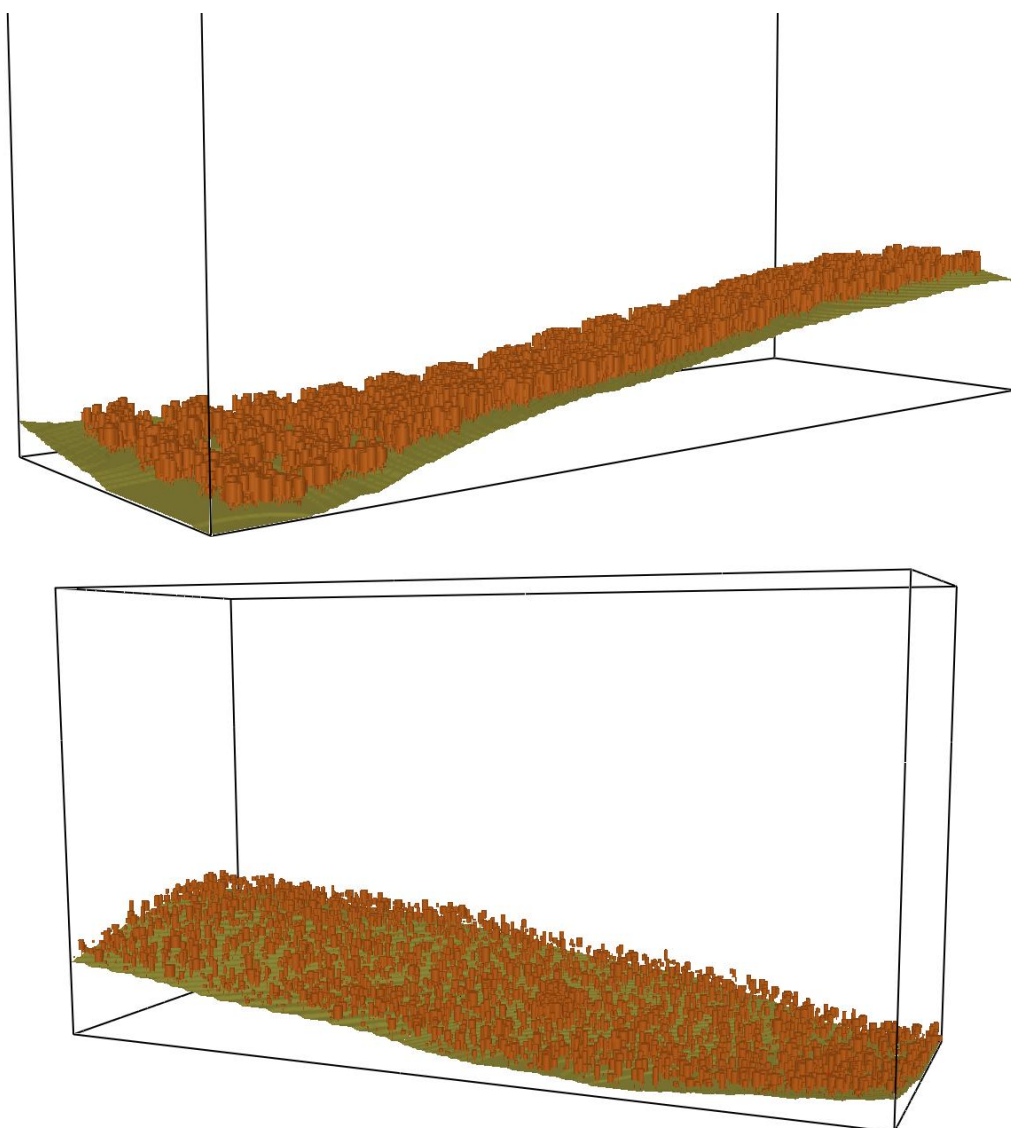


Figure 15: Smokeview visualization of the topography obtained.

Building the topography in WFDS was one of the most difficult parts to learn. Some of the errors found while trying to obtain it are shown below:

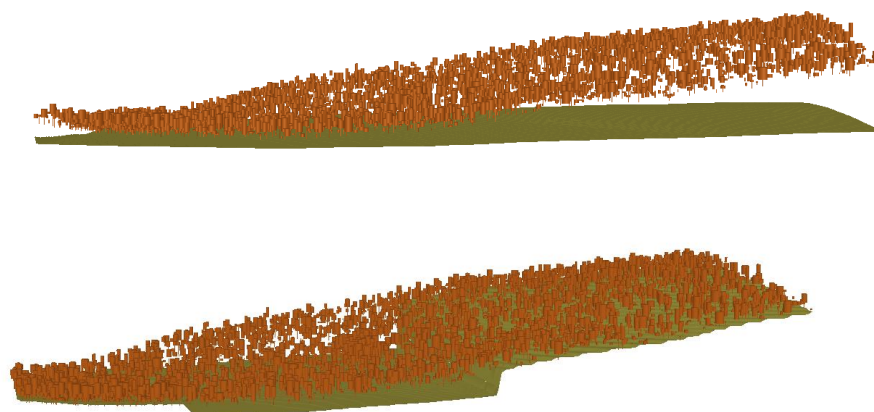


Figure 16: Errors found trying to get the correct topography.

Once obtained the topography and all trees built in the model, the next step was to create the meshes. As explained before, meshes are domains made up of rectilinear volumes where all FDS calculations perform. The resolutions of these domains define the resolution of the simulations on each zone. In order to avoid long simulations and large output files, it is not recommended to build high resolutions meshes for the overall domain. That could take months of simulations.

So, as expected, the high resolution meshes were located in the area of the study plot, where we wanted to obtain our results, whereas the coarse meshes and so low resolutions meshes, were located in the boundary area created such as the wind entry field and the exiting wind field.

To define the meshes, the following table has to be completed (Table 5):

Table 5: Meshes generator table.

	xcells	ycells	zcells		xmin	xmax	ymin	ymax	zmin	zmax	xres	yres	zres	cells	comments	#meshes
&MESH ID='MESH1', IJK=	50	100	100	XB=	0	100	0	200	0	200	2	2	2	500000.0	pre-core	1
&MESH ID='MESH2', IJK=	200	10	200	XB=	100	300	0	10	0	200	1	1	1	400000.0	core area	2
&MESH ID='MESH3', IJK=	200	10	200	XB=	100	300	10	20	0	200	1	1	1	400000.0	core area	3
&MESH ID='MESH4', IJK=	200	10	200	XB=	100	300	20	30	0	200	1	1	1	400000.0	core area	4
&MESH ID='MESH5', IJK=	200	10	200	XB=	100	300	30	40	0	200	1	1	1	400000.0	core area	5
&MESH ID='MESH6', IJK=	200	10	200	XB=	100	300	40	50	0	200	1	1	1	400000.0	core area	6
&MESH ID='MESH7', IJK=	200	10	200	XB=	100	300	50	60	0	200	1	1	1	400000.0	core area	7
&MESH ID='MESH8', IJK=	200	10	200	XB=	100	300	60	70	0	200	1	1	1	400000.0	core area	8
&MESH ID='MESH9', IJK=	200	10	200	XB=	100	300	70	80	0	200	1	1	1	400000.0	core area	9
&MESH ID='MESH10', IJK=	200	10	200	XB=	100	300	80	90	0	200	1	1	1	400000.0	core area	10
&MESH ID='MESH11', IJK=	200	10	200	XB=	100	300	90	100	0	200	1	1	1	400000.0	core area	11
&MESH ID='MESH12', IJK=	200	10	200	XB=	100	300	100	110	0	200	1	1	1	400000.0	core area	12
&MESH ID='MESH13', IJK=	200	10	200	XB=	100	300	110	120	0	200	1	1	1	400000.0	core area	13
&MESH ID='MESH14', IJK=	200	10	200	XB=	100	300	120	130	0	200	1	1	1	400000.0	core area	14
&MESH ID='MESH15', IJK=	200	10	200	XB=	100	300	130	140	0	200	1	1	1	400000.0	core area	15
&MESH ID='MESH16', IJK=	200	10	200	XB=	100	300	140	150	0	200	1	1	1	400000.0	core area	16
&MESH ID='MESH17', IJK=	200	10	200	XB=	100	300	150	160	0	200	1	1	1	400000.0	core area	17
&MESH ID='MESH18', IJK=	200	10	200	XB=	100	300	160	170	0	200	1	1	1	400000.0	core area	18
&MESH ID='MESH19', IJK=	200	10	200	XB=	100	300	170	180	0	200	1	1	1	400000.0	core area	19
&MESH ID='MESH20', IJK=	200	10	200	XB=	100	300	180	190	0	200	1	1	1	400000.0	core area	20
&MESH ID='MESH21', IJK=	200	10	200	XB=	100	300	190	200	0	200	1	1	1	400000.0	core area	21
&MESH ID='MESH22', IJK=	125	50	100	XB=	300	550	0	100	0	200	2	2	2	625000.0	back	22
&MESH ID='MESH23', IJK=	125	50	100	XB=	300	550	100	200	0	200	2	2	2	625000.0	back	23
&MESH ID='MESH24', IJK=	100	100	50	XB=	-200	0	0	200	0	100	2	2	2	500000.0	initial zone	24
&MESH ID='MESH25', IJK=	100	100	50	XB=	-200	0	0	200	100	200	2	2	2	500000.0	initial zone	25

By completing this table, we obtain the following data to write in the input file in order to obtain the meshes in WFDS:

```
&MESH ID='MESH1', IJK=50,100,100,XB=0,100,0,200,0,200/
&MESH ID='MESH2', IJK=200,10,200,XB=100,300,0,10,0,200/
&MESH ID='MESH3', IJK=200,10,200,XB=100,300,10,20,0,200/
&MESH ID='MESH4', IJK=200,10,200,XB=100,300,20,30,0,200/
&MESH ID='MESH5', IJK=200,10,200,XB=100,300,30,40,0,200/
&MESH ID='MESH6', IJK=200,10,200,XB=100,300,40,50,0,200/
&MESH ID='MESH7', IJK=200,10,200,XB=100,300,50,60,0,200/
&MESH ID='MESH8', IJK=200,10,200,XB=100,300,60,70,0,200/
&MESH ID='MESH9', IJK=200,10,200,XB=100,300,70,80,0,200/
```



```

&MESH ID='MESH10', IJK=200,10,200,XB=100,300,80,90,0,200/
&MESH ID='MESH11', IJK=200,10,200,XB=100,300,90,100,0,200/
&MESH ID='MESH12', IJK=200,10,200,XB=100,300,100,110,0,200/
&MESH ID='MESH13', IJK=200,10,200,XB=100,300,110,120,0,200/
&MESH ID='MESH14', IJK=200,10,200,XB=100,300,120,130,0,200/
&MESH ID='MESH15', IJK=200,10,200,XB=100,300,130,140,0,200/
&MESH ID='MESH16', IJK=200,10,200,XB=100,300,140,150,0,200/
&MESH ID='MESH17', IJK=200,10,200,XB=100,300,150,160,0,200/
&MESH ID='MESH18', IJK=200,10,200,XB=100,300,160,170,0,200/
&MESH ID='MESH19', IJK=200,10,200,XB=100,300,170,180,0,200/
&MESH ID='MESH20', IJK=200,10,200,XB=100,300,180,190,0,200/
&MESH ID='MESH21', IJK=200,10,200,XB=100,300,190,200,0,200/
&MESH ID='MESH22', IJK=125,50,100,XB=300,550,0,100,0,200/
&MESH ID='MESH23', IJK=125,50,100,XB=300,550,100,200,0,200/
&MESH ID='MESH24', IJK=100,100,50,XB=-200,0,0,200,0,100/
&MESH ID='MESH25', IJK=100,100,50,XB=-200,0,0,200,100,200/

```

An example of the meshes can be seen in Figure 17. In this picture the wind inflow entries from right to the left.

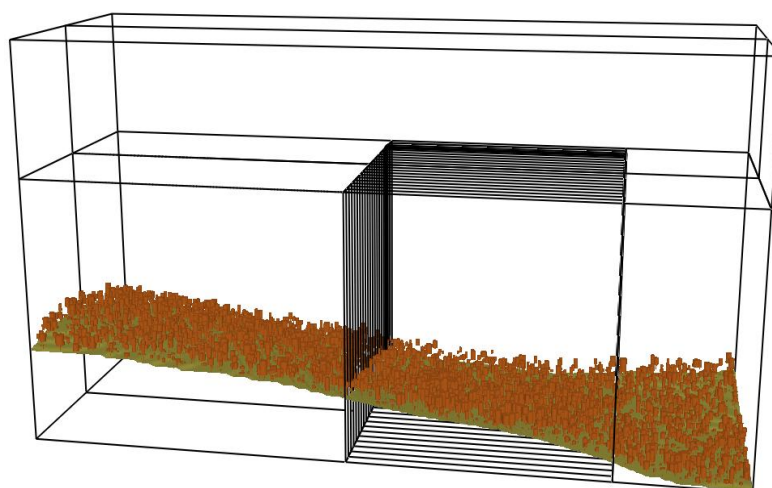


Figure 17: Study area with the meshes created. The Figure above, represents a test of the forest we were creating. It is possible to see that the topography has been extracted correctly and all the trees with their coordinates and data too.

At this point, the model is already built and with Smokeview it is possible to visualize it. The topography, trees and meshes are shown as in Figure 17.

The following step was to create the ignition. In order to do that the next parameters were wrote in the input file:

```

-Ignitor fire
&SURF ID='IGN FIRE', HRRPUA=500.,RAMP_Q='RAMPFIRE' /
&RAMP ID='RAMPFIRE',T=0.0,F=0.0 /
&RAMP ID='RAMPFIRE',T=310.0,F=0.0 /

```

```
&RAMP ID='RAMPFIRE',T=326.0,F=0.5 /
&RAMP ID='RAMPFIRE',T=332.0,F=1.0 /
&RAMP ID='RAMPFIRE',T=348.0,F=1.0 /
&RAMP ID='RAMPFIRE',T=359.0,F=0.5 /
&RAMP ID='RAMPFIRE',T=360.0,F=0.0 /
&VENT XB=150,155,40,160,0,0, SURF_ID='IGN FIRE'/
```

These lines define the location of the fire line and the time the fire will start burning. However, in order to have fire in the simulation, there is still another procedure to do: Draw the fire line in the topography that has already been created. To do so, an script similar to the one used to build the elevation is written in R studio:

```
memory.limit(size=15500)
options(scipen=999)
setwd('C:/Users/zieg9479/Documents/Olga')
warning(lapply(c('rgl','raster'), require, character.only = TRUE))

DEM <- raster("dem.bip")
DEM.df <- as.data.frame(DEM,xy=T)
DEM.df$x <- DEM.df$x-min(DEM.df$x)+1
DEM.df$y <- DEM.df$y-min(DEM.df$y)+1

DEM.df$SurfID <- 'surface'
DEM.df$text <- paste('&OBST XB=',DEM.df$x-1,',',DEM.df$x+1,',',DEM.df$y-
1,',',DEM.df$y+1,',',min(round(DEM.df$dem,0)),',',round(DEM.df$dem,0)),
SURF_ID='','',DEM.df$StandID,'" /",sep=")

fireline=DEM.df[c(DEM.df$x>=3&DEM.df$x<=5 & DEM.df$y>=2
& DEM.df$y<=8),] #Extract the fireline
fireline$text=paste('&VENT XB=',fireline$x-1,',',fireline$x+1,',',fireline$y-
1,',',fireline$y+1,',',round(fireline$dem,0)),',',round(fireline$dem,0),"", SURF_ID='IGN FIRE'
/","sep=")

write.table(fireline$text,paste('Fireline.csv',sep="),row.names=F)
```

As for the elevation procedure, after writing this script, an excel file is created in the directory indicated. The new Excel file contains the Vents that will define the fire line:

```
Fireline
&VENT XB=50,51,53,54,5,5, SURF_ID='IGN FIRE' /
&VENT XB=51,52,53,54,5,5, SURF_ID='IGN FIRE' /
&VENT XB=52,53,53,54,5,5, SURF_ID='IGN FIRE' /
&VENT XB=53,54,53,54,5,5, SURF_ID='IGN FIRE' /
&VENT XB=54,55,53,54,5,5, SURF_ID='IGN FIRE' /
&VENT XB=55,56,53,54,5,5, SURF_ID='IGN FIRE' /
&VENT XB=56,57,53,54,5,5, SURF_ID='IGN FIRE' /
&VENT XB=57,58,53,54,5,5, SURF_ID='IGN FIRE' /
&VENT XB=58,59,53,54,5,5, SURF_ID='IGN FIRE' /
etc.
```

After that, the ground vegetation was defined. From the vegetation description of the study zone, a SH1 fuel model from Scott&Burgan was chosen and distributed around the overall domain with the following characteristics:

```
- Ground VEG For Shrubs fuel class based on Scott & Burgan SH1
&SURF ID = 'surface1'
  VEGETATION = .TRUE.
  VEG_DRAG_CONSTANT = 0.25
  VEG_MOISTURE = 0.06
  VEG_SV= 5493
  VEG_CHAR_FRACTION = 0.265
  VEG_LOAD = 0.44
  VEG_HEIGHT = 0.30
  VEG_DENSITY= 510
  FIRELINE_MLR_MAX = 0.2
  RGB = 122,117,48 /
```

Before starting the simulations, the desired outputs had to be specified in the input file.

Output data to be viewed by Smokeview:

- Inflow

```
&SURF ID='INFLOW',VEL=-10.0, RAMP_V='RAMPVEL', PROFILE='ATMOSPHERIC',
ZO=10.,PLE=0.143 /
&RAMP ID='RAMPVEL',T=0.0,F=0.0 /
&RAMP ID='RAMPVEL',T=1.0,F=0.1 /
&RAMP ID='RAMPVEL',T=2.0,F=0.2 /
&RAMP ID='RAMPVEL',T=3.0,F=0.3 /
&RAMP ID='RAMPVEL',T=4.0,F=0.4 /
&RAMP ID='RAMPVEL',T=5.0,F=0.5 /
&RAMP ID='RAMPVEL',T=6.0,F=0.6 /
&RAMP ID='RAMPVEL',T=7.0,F=0.7 /
&RAMP ID='RAMPVEL',T=8.0,F=0.8 /
&RAMP ID='RAMPVEL',T=9.0,F=0.9 /
&RAMP ID='RAMPVEL',T=10.0,F=1.0 /
```

- Domain-Boundary conditions

```
&VENT MB = XMIN, SURF_ID = 'INFLOW' /
&VENT MB = XMAX, SURF_ID = 'OPEN' /
&VENT MB = YMIN, SURF_ID = 'MIRROR' /
&VENT MB = YMAX, SURF_ID = 'MIRROR' /
&VENT MB = ZMAX, SURF_ID = 'MIRROR' /
```

In this lines we specified the characteristics of the wind flow. The wind velocity (VEL=-10 in this example) is calculated in m/s and at 10 meters above the ground.

In this study case, 8 simulations with different conditions were carried out:

- Q1 pre treatment normal conditions
- Q1 pre treatment high conditions
- Q2 pre treatment normal conditions
- Q2 pre treatment high conditions
- Q1 post treatment normal conditions
- Q1 post treatment high conditions
- Q2 post treatment normal conditions
- Q2 post treatment high conditions

Where:

Q1 is the plot with a thinning of 30% of the trees.

Q2 is the plot with a thinning of 50% of the trees.

Normal conditions present wind velocities of 3.3 m/s.

High conditions present wind velocities of 7 m/s.

Other outputs that had to be specified were the slice files and boundary files. In this study case we created slice files in order to see how the wind and its different directions (u , v , w) change. The complete outputs wrote in the input files can be seen in Annex V and Annex VI.

Apart from these outputs that can be viewed in Smokeview, WFDS creates an excel file for every single tree of the study plot. These excel files contain values such as moisture, temperature, mass consumption, percentage of char... (A complete Excel File can be seen in Annex IV). This data allows to calculate outputs such as crown fire, overall mass consumption, rate of spread... All these results can be seen in the Results chapter. For this study case, 812 excel files were generated for the pre-treatment scenarios and 274 for the post-treatment scenarios.

This procedure was done for all simulations.

Once everything is set, to run a simulation the first step was to access remotely the Linux cluster. To do that it was necessary to download PuTTY (S.Tatham, 1999). PuTTY is a free and open-source terminal emulator, serial console and network file transfer application. It supports several network protocols, including SCO, SSH, Telnet, rlogin, and raw socket connection. It can also connect to a serial port.

This Linux cluster consists of 5 nodes. Four of the nodes are used for computations and the fifth is used as shared storage. The shared storage node is called Prometheus and can be mapped across platforms through the warner college of natural resources. The other four nodes are called loki, vulcan, kali and osiris. Each of these nodes has 64 AMD processors (2.2-2.6 GHZ) with 256 gb of RAM and about 1 TB of local storage space. In total the cluster has 256 processors and 1024 gb of ram. The one used for our simulations was vulcan.

Once PuTTY was downloaded and installed, we logged into the cluster with the host name: "vulcan.warnercnr.colostate.edu" and the personal ID and password. Once logged, all jobs were performed in the scratch folder. To get to scratch we typed the following command line: "cd / scratch". Once in the scratch folder, we had to access to the folder where all WFDS simulations are performed by typing: "cd / wfds_runs". Then, we created a new file structure by typing: "mkdir dirname" where dirname was the name given to the directory. In this case: "cd / olgatest".

To move data within the Linux cluster, we downloaded Bitvise SSH (Figure 188). The SSH protocol is used to connect remotely and safely to computers in a network. Thanks to this protocol we can connect and control a computer and transfer files safely and encoded. To establish these connections it is necessary a client and a server. Bitvise SSH is a free client and SSH server for Windows.

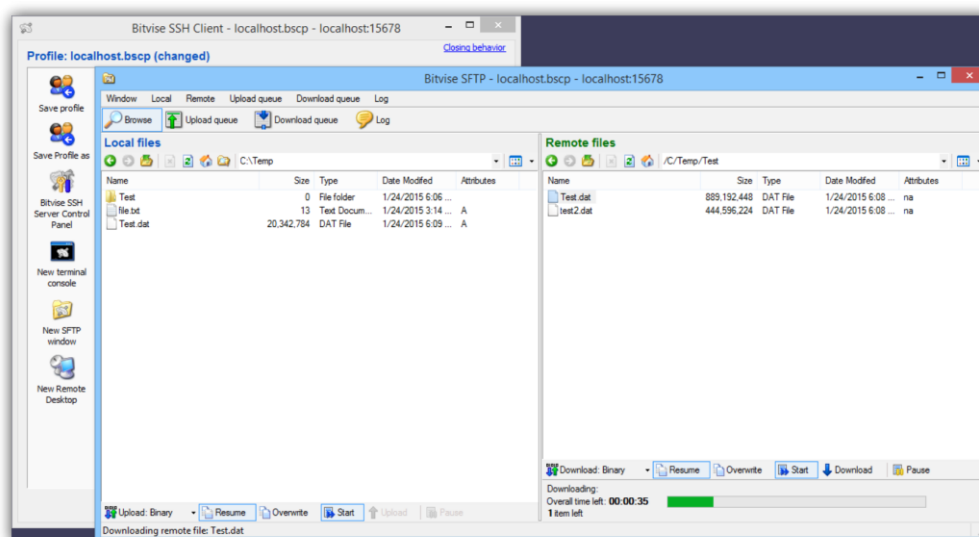


Figure 18: Bitvise SSH visualization.

Once logged in the cluster and connected to Bitvise, we were able to load the input file in a ".txt" format in the new directory created called "olgatest". Once the file was saved, we needed to type in PuTTY:

```
vulcan ~ % cd /scratch/
vulcan ~ % cd / scratch/wfds_runs
vulcan ~ % cd / scratch/wfds_runs/olgatest
vulcan ~ % cd / scratch/wfds_runs/olgatest/ls
vulcan /scratch/wfds_runs/olgatest % mpirun -np 24 /scratch/program-
source/FDS/FDS6/bin/WFDS6_Source/FDS_Compilation/fds_mpi_intel_linux_64
<WFDS input file>
```

"mpirun" is the command to initialize mpi -np states that are wanted to call a certain number of processors (in this case 24), then it was needed to type the full path to the executable followed by a space and the input file name. "ls" is the command to see which files are in that folder.

At this point, the scenarios in Smokeview looked like Figure 19 and was ready to run.

All the input files used in Topography simulations can be found in Annex V and The input files for Flat terrain simulations can be seen in Annex VI.

For Flat terrain simulations, some changes were made

Changes:

- No topography thus no obstructions.
- No vents.
- Bigger boundary area (750 x 200 x 200).
- Different meshes.

An area of 200 meters on the X axis, 200 meters on the Y axis and 200 meters on the Z axis was added.

On Topography simulations, the wind was entered with an atmospheric profile (vertical) but with no turbulence. To simulate the turbulent winds associated with an interior forest rather than an edge forest, in these simulations we added the extra length to the X direction. In general, it takes 5 to 20 tree heights to develop the turbulent fields associated with an interior forest. To cover that area, two coarse meshes were located in that new area as seen in Figure 19.

A comparison within Topography simulations and Flat terrain simulations and the different changes made can be seen in Figure 19.

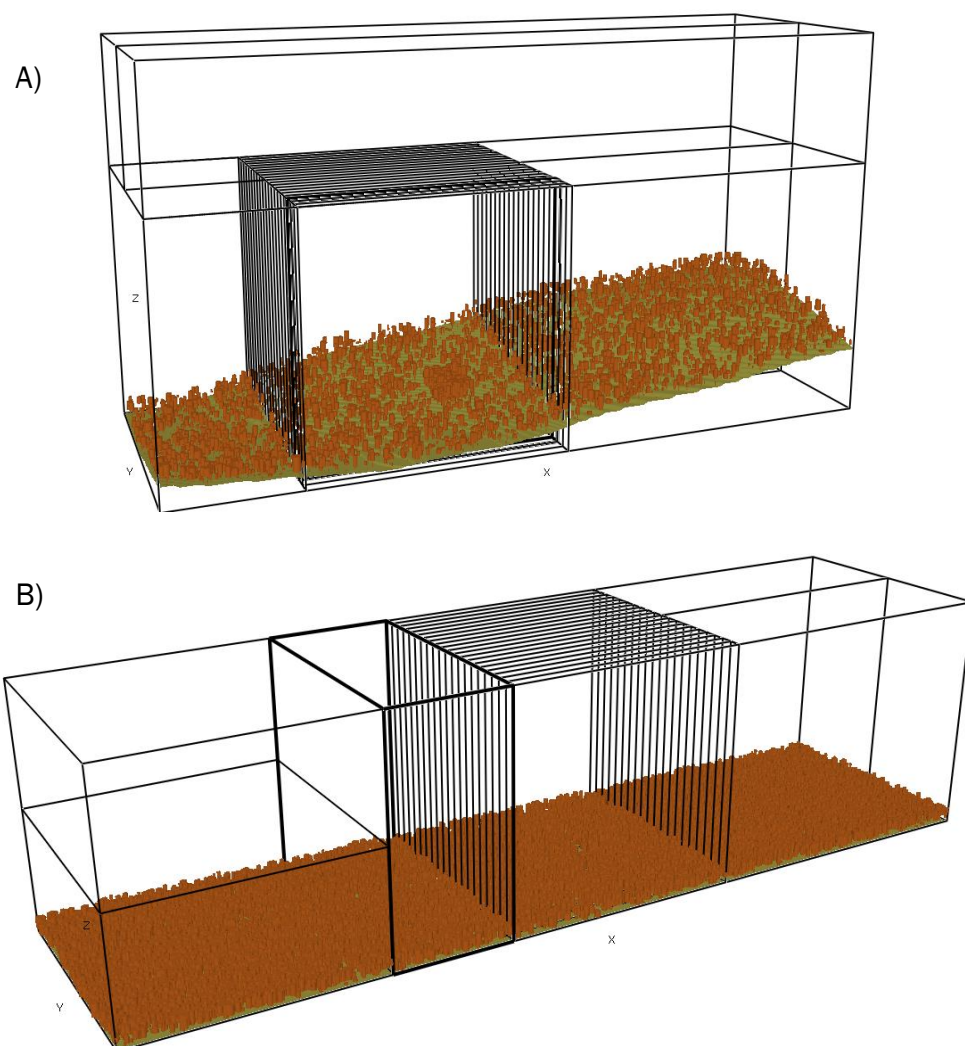


Figure 19: Topography simulations scenario (A) and Flat terrain simulations scenario (B).

4. Results

In order to be able to work with the output data that WFDS give us, it is necessary to process all the data with Rstudio or Matlab. This procedure was done in Chad Hoffman's lab. It is important to take into account, that for every single tree of the study area, WFDS generates an excel file. In this study case, 165GB of output data were generated.

Topography simulations

For the Topography simulations, when almost all simulations were finished, we found some problems. The first and biggest problem was: too large Rates of Spread, as shown in Table 6:

Table 6: Rates of Spread obtained from Topography simulations.

Plot	Status	Weather	Consumption	ROS (m/s)
Q1	pre treatment	normal	86%	2.02
Q1	pre treatment	high		1.66
Q1	post treatment	normal	6%	1.46
Q1	post treatment	high	82%	3
Q2	pre treatment	normal	67%	2.06
Q2	pre treatment	high	11%	2.75
Q2	post treatment	normal	24%	1.31
Q2	post treatment	high	10%	197

We noticed that the topography was having an extreme effect on fire behavior. What was happening was that the wind-fire got diverted around the hill towards the flat area along the bottom of the simulation. While this is a real effect that can be seen in actual fires, it results in part of the area of interest burning as a head fire, part as a flank fire (Figure 20), and in some instances the whole plot was not burning, thus obscuring the potential effects of treatment.

At this point, we took the decision of removing the topography and re-do all the simulations on flat ground so we could attempt to isolate the effect of treatments.

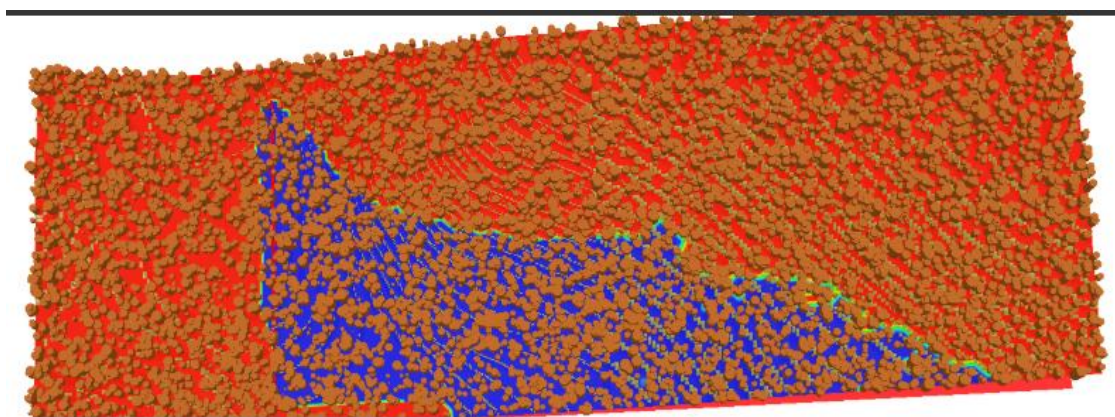


Figure 20: Visualization of fire spread in Topography simulations.

Flat terrain simulations

The results obtained from the simulations with flat terrain, and the differences before and after the treatments are shown below (Table 7 and Table 8):

Table 7: Flat terrain simulations results

	PLOT	STATUS	INITIAL WIND SPEED CONDITION	ROS [m/s]	CFA	MEAN STREAMWISE [m/s]	MEAN TURBULENT KINETIC ENERGY [m ² /s ²]
FLAT TERRAIN	Q1	PRE	LOW	0.42	0%	0.14	0.05
	Q1	POST	LOW	0.53	2%	0.20	0.06
	Q1	PRE	HIGH	0.92	83%	0.42	0.19
	Q1	POST	HIGH	0.71	19%	0.61	0.23
	Q2	PRE	LOW	0.53	4%	0.11	0.05
	Q2	POST	LOW	0.62	1%	0.34	0.07
	Q2	PRE	HIGH	0.78	42%	0.44	0.20
	Q2	POST	HIGH	0.54	10%	0.67	0.24

Table 8: Differences of the results obtained before and after the treatments.

	<i>Differences after the treatments</i>			
	RATE OF SPREAD	CANOPY CONSUMPTION	MEAN STREAMWISE	MEAN TURBULENT KINETIC ENERGY
Q1 LOW	0.11	0.02	0.06	0.01
Q1 HIGH	-0.21	-64%	0.19	0.04
Q2 LOW	0.09	0.03	0.23	0.02
Q2 HIGH	-0.24	-32%	0.23	0.04

Crown fire activity

The likelihood of crown fires was calculated as the amount of canopy fuel consumed after the fire. First, it was calculated the total initial amount of canopy fuel by summing the dry weights of individual trees at time=0. After the simulation, it was calculated the post-fire amount of canopy fuel by summing the dry weights of individual trees at the end of the simulation. By subtracting the final to the initial, the total amount of canopy fuel, and so the crown fire activity was obtained. The percentage of canopy fuel amount was calculated by subtracting the initial to the final and divided by the initial (Figure 21). In order to consider CFA, we determined that it was necessary more than 5% of canopy consumption. Less than 5% of canopy consumption can be due to the radiation effect of the surface fire and not necessarily crown fire activity.

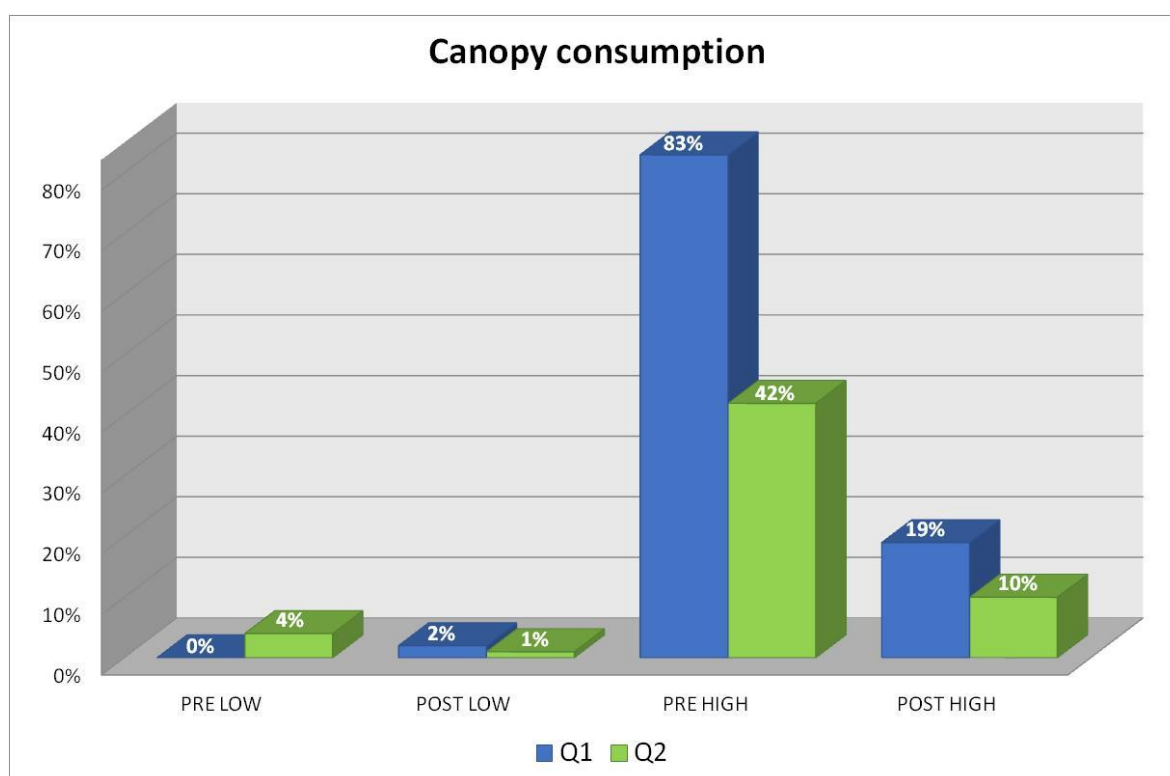


Figure 21: Canopy consumption results.

Before the treatments and with low wind speed conditions, plot Q1 presents no canopy consumption and Q2 presents 4% of canopy consumption, whereas for high wind conditions, Q1 reaches a 83% of canopy fuel consumption and Q2 presents a 42%. After the treatments were applied, for low wind speed conditions, plot Q1 presents a 2% of canopy consumption and plot Q2 a 1%. For high wind speed conditions, Q1 presents a much lower value than before the treatments with 19% of canopy consumption as well as Q2 with a 10% of canopy consumption.

In Figure 22 it is possible to observe the fuel amount before and after the fire.

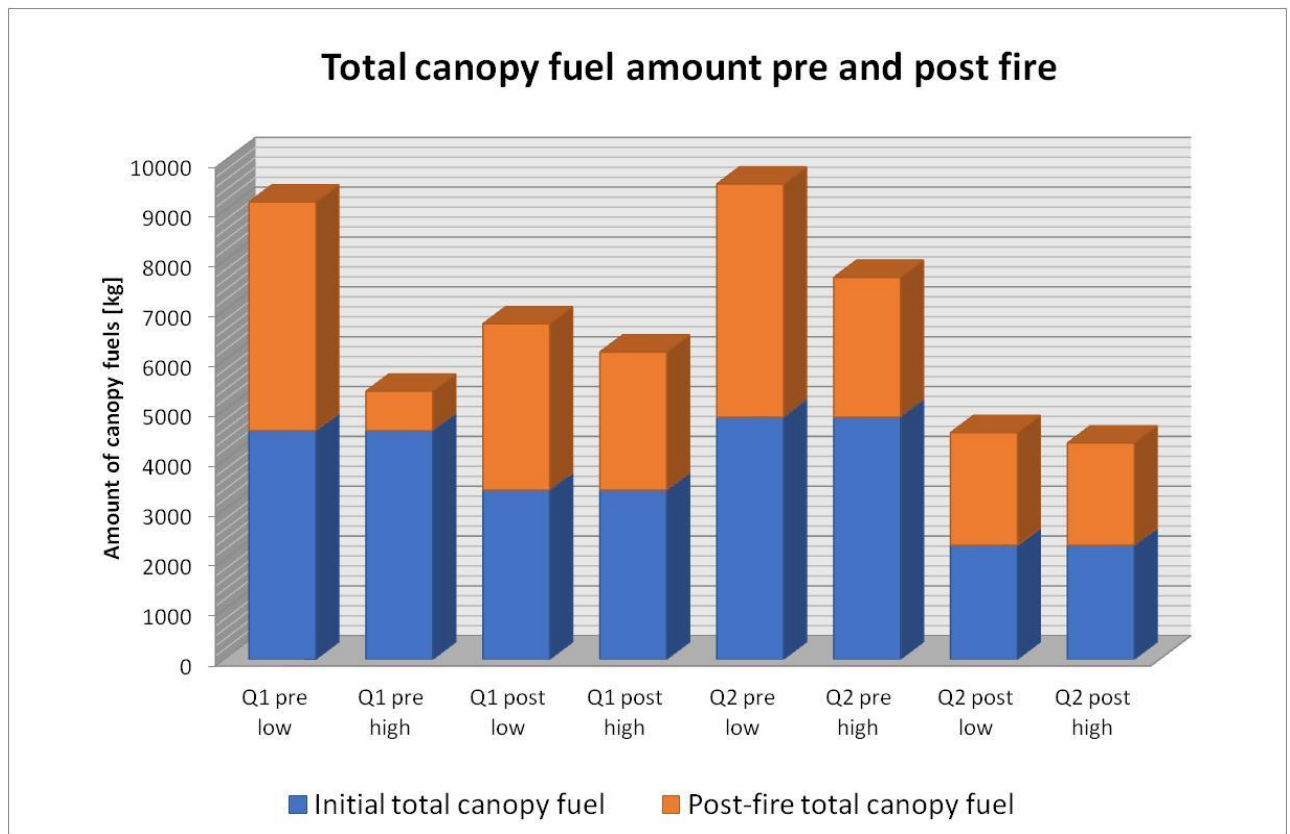


Figure 22: Total canopy fuel amount pre and post fire.

In Figure 23, it is possible to see the CFA with initial high wind speed conditions in both Q1 and Q2 plots, before and after the treatments.

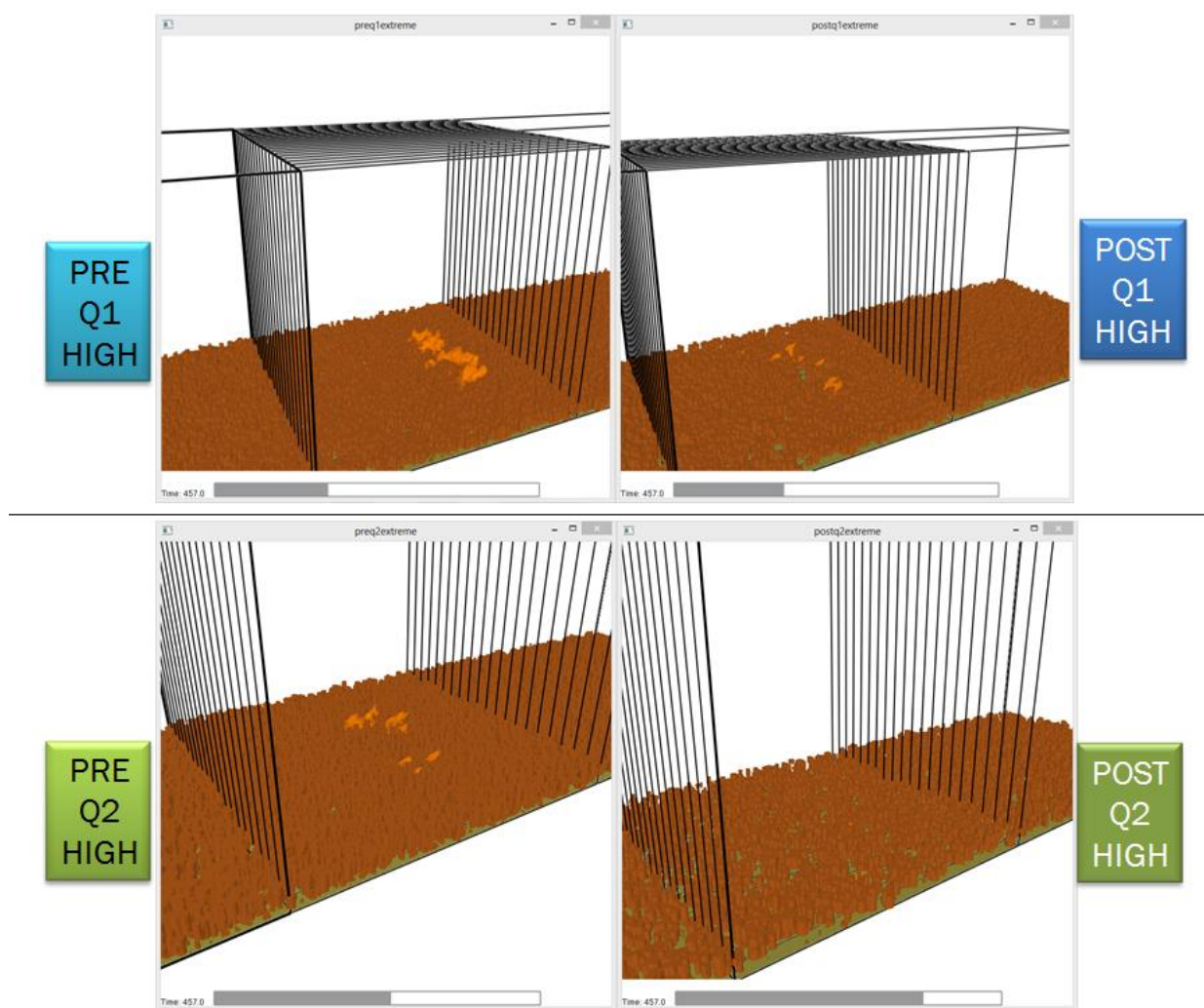


Figure 23: Smokeview visualization of the Crown Fire Activity in Q1 and Q2, before and after the treatments, with initial high wind speed conditions.

Rate of Spread

Another value calculated was the Rate of Spread. In order to do that, the time steps during which each boundary cell noted a decrease in fuel load were noted (this is the time of arrival). Then, the x locations of boundary cells were regressed against the time of arrival. The ordinary least squares (OLS) fitted slope is the average rate of spread.

In Table 9, it is possible to see some of the outputs calculated in relation to the Rate of Spread:

Table 9: Rate of Spread outputs.

Plot	Status	Wind	Mean ROS	Root mean square error of streamwise spread rate	Mean direction of the ROS
Q1	Pre	Lo	0.42	0.54	0.27
Q2	Pre	Lo	0.53	1.68	-2.07
Q1	Post	Lo	0.53	1.31	1.21
Q2	Post	Hi	0.54	1.92	-3.52
Q2	Post	Lo	0.62	1.23	-1.67
Q1	Post	Hi	0.71	1.79	2.54
Q2	Pre	Hi	0.78	1.22	1.65
Q1	Pre	Hi	0.92	1.83	-4.23

The Root mean square error of streamwise spread rate (RMSE) describes the spatiotemporal variability of the rate of spread. The mean direction of the rate of spread was calculated by determining the rate of spread from each location to its adjacent cells. Using vector algebra, the rate of spread-weighted direction of the fire in each boundary cell was determined. This is the average value of all cells' directions where 0 is precisely streamwise, negative values indicate fire turns to its left, and positive values indicate the fire is turning to its right.

Other values obtained from the simulations regarding rate of spread can be seen in Table 10:

Table 10: Other values obtained from ROS.

Plot	Status	Wind	Mean direction of the ROS	Standard deviation of the mean ROS direction	Sinosity [%]
Q1	Pre	Hi	-4.23	16.04	1.08
Q2	Post	Hi	-3.52	19.27	1.04
Q2	Pre	Lo	-2.07	18.44	1.04
Q2	Post	Lo	-1.67	16.18	1.05
Q1	Pre	Lo	0.27	19.83	1.02
Q1	Post	Lo	1.21	18.33	1.06
Q2	Pre	Hi	1.65	13.79	1.06
Q1	Post	Hi	2.54	13.93	1.05

In Figure 24 it is possible to observe the mean ROS. With low wind speed conditions, the ROS increases after the treatments for both Q1 and Q2, whereas for high wind speed conditions, the ROS decreases after the treatments for Q1 and Q2.

With high wind speed conditions, Q2 and so, thinning 50%, presents lower values of ROS than Q1 thus thinning 30%. In low wind speed conditions, Q1 presents lower values of ROS than Q2.

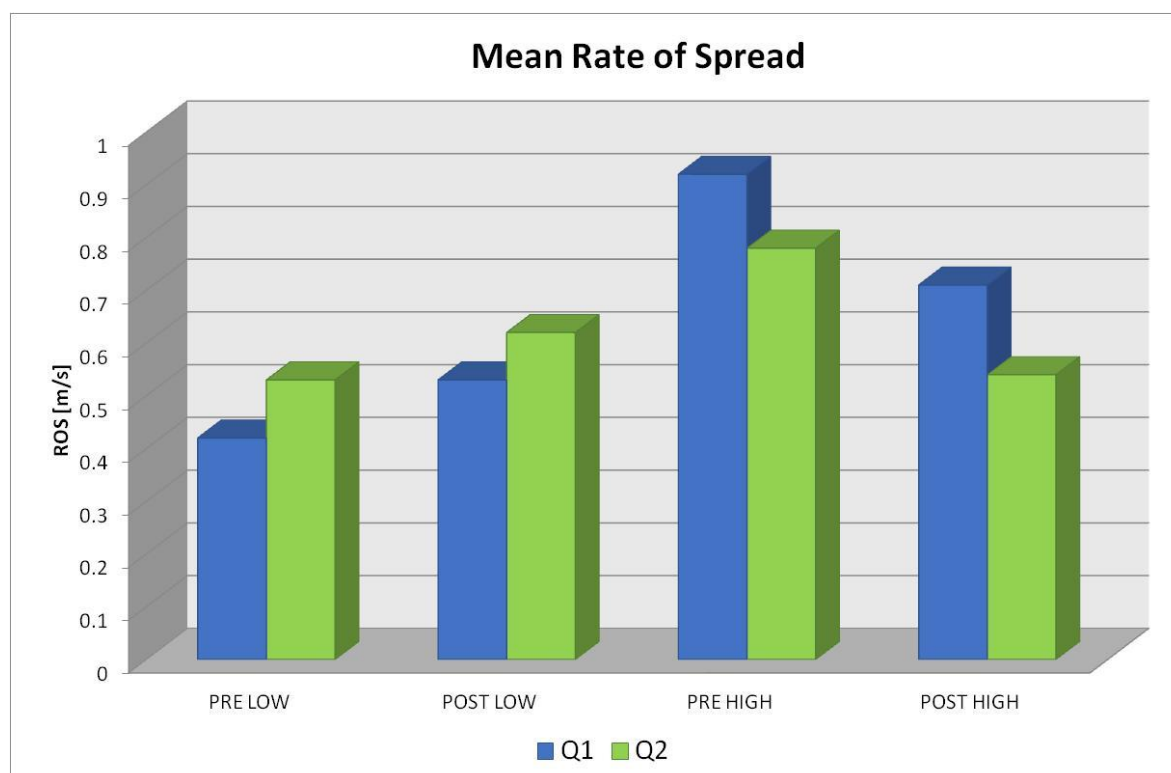


Figure 24: Mean Rate of Spread results.

Wind speed profiles

The mean streamwise (u , which is measured in the X axis) can be seen in Figure 25. Taking into account our study plot's structure, we can observe that the streamwise decreases within the stand and increases on the top of the canopy.

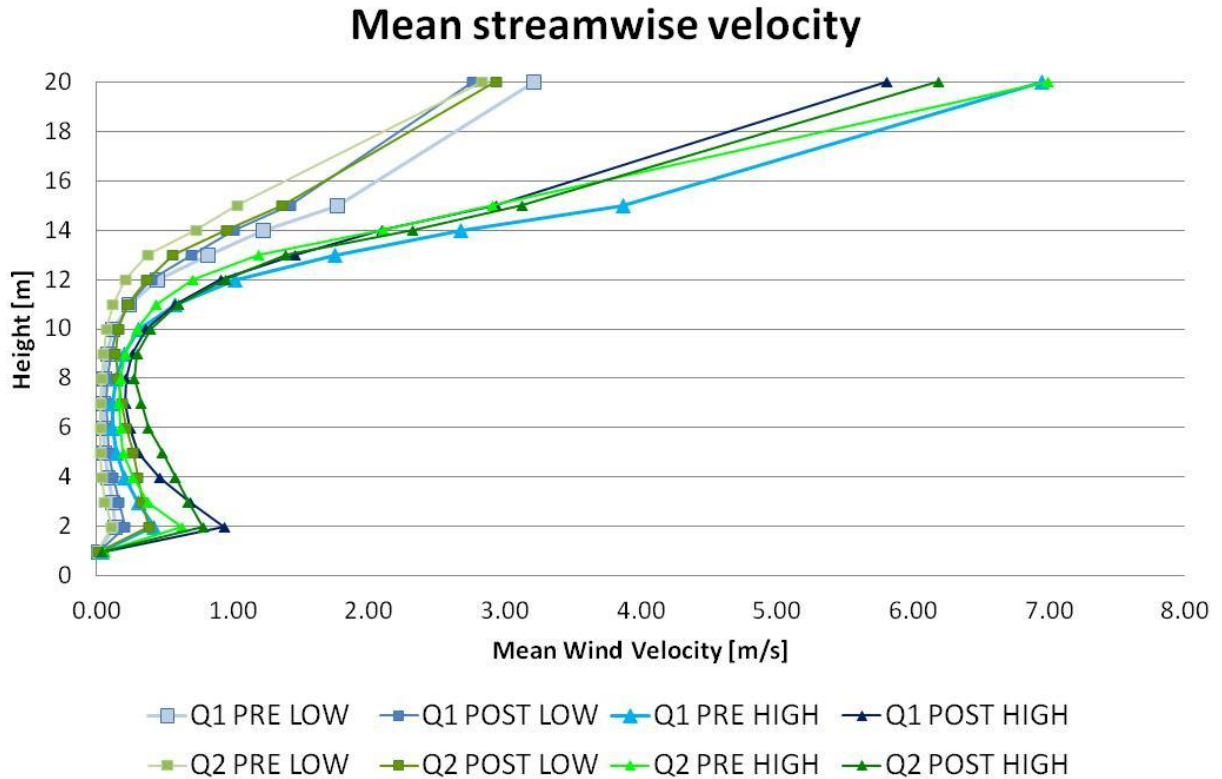


Figure 25: Mean streamwise wind velocity profile.

With low wind speed conditions, plot Q2 presents higher streamwise values than Q1 within the canopy. With high wind speed conditions, plot Q1 presents higher streamwise values below the canopy, but once within the canopy, this value decreases and Q2 streamwise values are higher than those in Q1. All this facts are easier to see in Figure 26, where high and low wind speed conditions are in separated graphics.

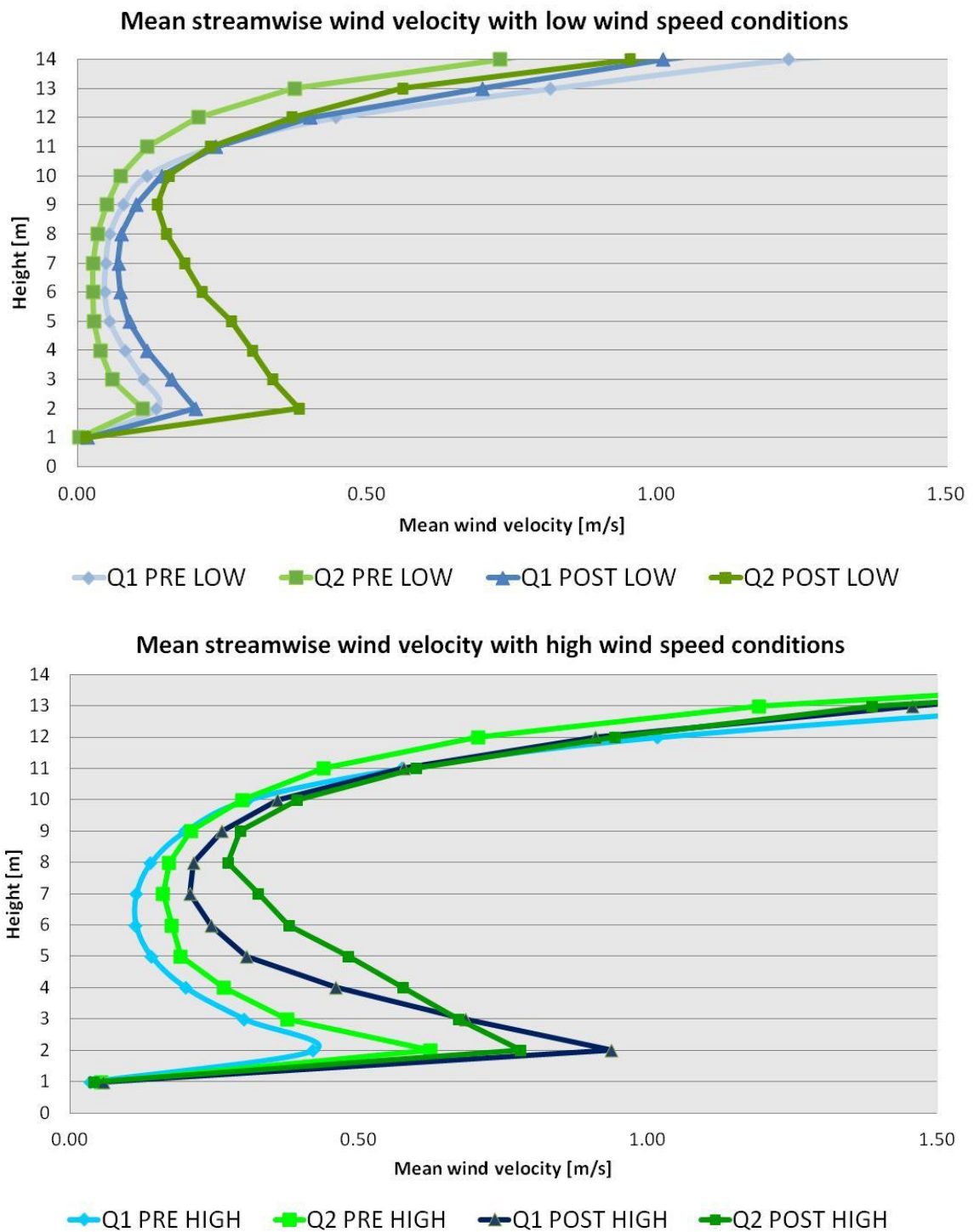


Figure 26: Mean streamwise wind velocity with high and low wind speed conditions respectively.

Both graphics conclude that pre-treatment status present lower values of mean streamwise wind velocity than post-treatment status.

In Figure 27, we can observe a graphic with the mean crosswind velocity (v , which is measured in the Y axis). Both Q1 and Q2, present the same mean crosswind velocities before the treatments with low wind speed conditions. The same happens with high wind speed conditions. However, those values change after the application of the treatments; with high wind speed conditions, Q1 presents a change in the wind direction once this one is within the canopy whereas Q2 presents a steadier wind direction. Q2 present higher velocities of the mean crosswind within the canopy than Q1.

With low wind speed conditions, the same fact happens and the only change is that once the wind exits from within the canopy in Q2, this changes drastically its direction and reaches the highest mean crosswind velocity.

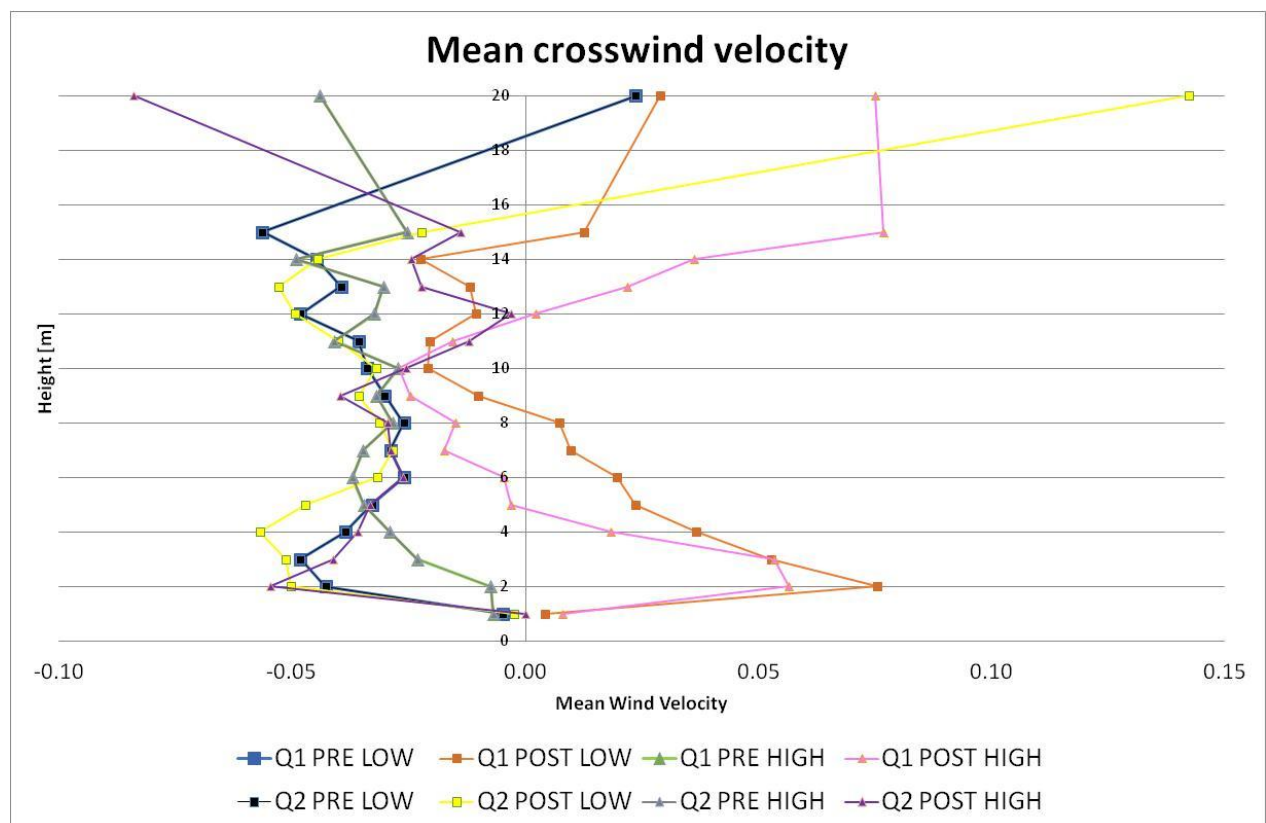


Figure 27: Mean crosswind velocity.

The mean vertical wind (w , which is measured in the Z axis) velocity can be seen in Figure 28. Q1 before the treatment, presents a similar mean vertical velocity for both low and high wind speed conditions. The vertical wind goes down while it is within the canopy, near the top of the canopy ascends (more wind high wind speed conditions) and out of the canopy descends again. Q2 before treatments present more variability with high wind speed conditions than with low ones. With low wind speed conditions, the wind velocity increases slowly while within the canopy and once on the top of the canopy it increases faster. With high wind speed conditions, the wind starts going down and once within the canopy, it changes its direction, starts going up and increases its velocity. Once out of the canopy it changes again and starts going down.

Regarding the post treatments scenarios, for plot Q1, both low and high wind speed conditions present a similar mean vertical wind velocity pattern, the only change is that, as expected, with high wind speed conditions, the wind velocities are higher. This pattern presents an upward and an increase of the wind velocity. A similar pattern is repeated in Q2 wind low wind speed conditions. However, in this scenario, once the wind is within the canopy the mean wind velocity remains steady until it reaches the top of the canopy when the mean wind velocity increases again. The last and most different pattern is the one that presents Q2 after the treatment and with high wind speed conditions. This pattern shows a starting upwards wind within the canopy and once on the top it changes to downward winds.

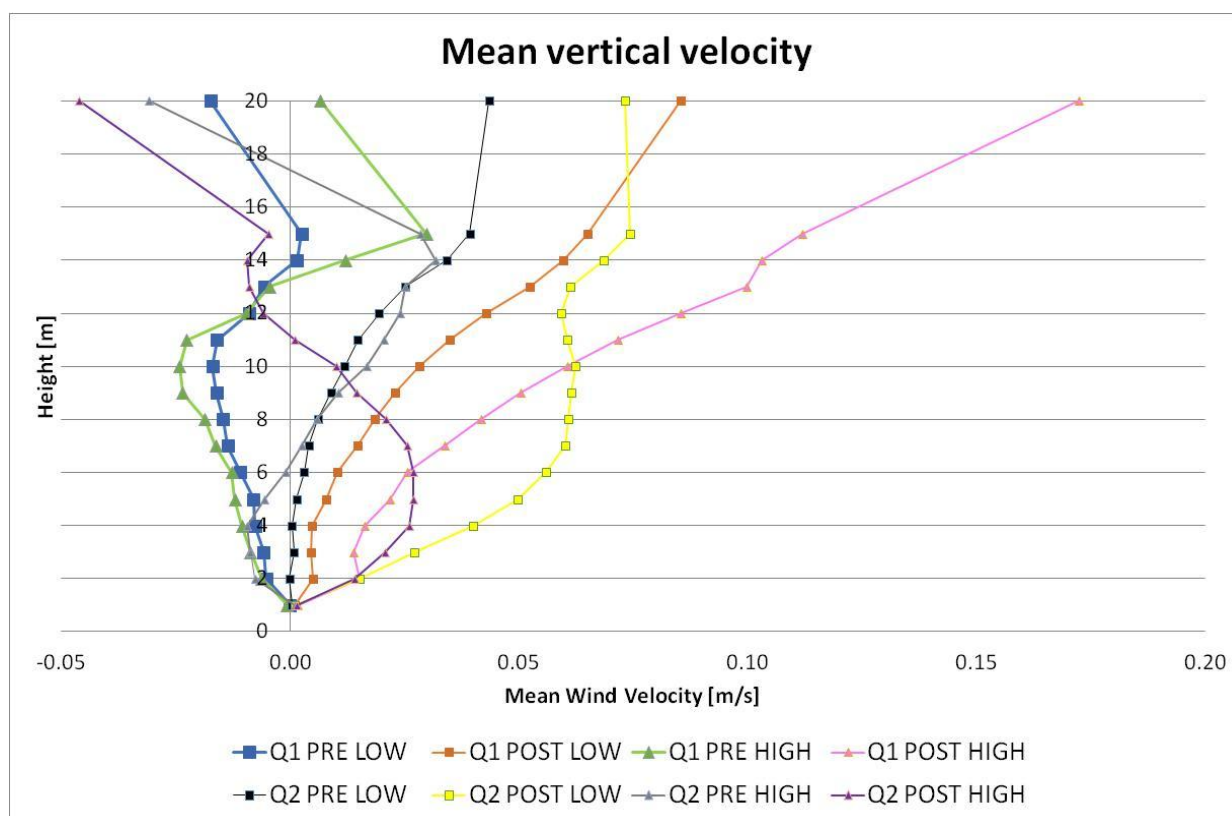


Figure 28: Mean vertical velocity.

The mean vertical velocity represents the upwards and downwards direction of the winds, producing turbulence. To measure the amount of turbulence produced by the interaction between the winds and the stand structure, it has been calculated the Turbulent Kinetic energy, which is the mean kinetic energy per unit mass associated with eddies in a turbulent flow.

This parameter can be visualized in Figure 29. It is possible to observe that as higher the wind speed conditions, higher are the values of the turbulent kinetic energy. It is also possible to see that this value, no matter if it is on low or high wind speed conditions, increases within the canopy and augments the most on the top of the canopy. Once out of the canopy it decreases drastically.

With high wind speed conditions, we can see that there is more turbulence on the top of the canopy before the treatments were applied than after the treatments. This difference is higher on Q2 than on Q1.

With low wind speed conditions, Q2 before and after the treatments present a similar pattern but the values after the treatment are slightly higher. On Q1, the scenario before the treatments presents a small increase on turbulent kinetic energy values in relation with the after-treatment scenario.

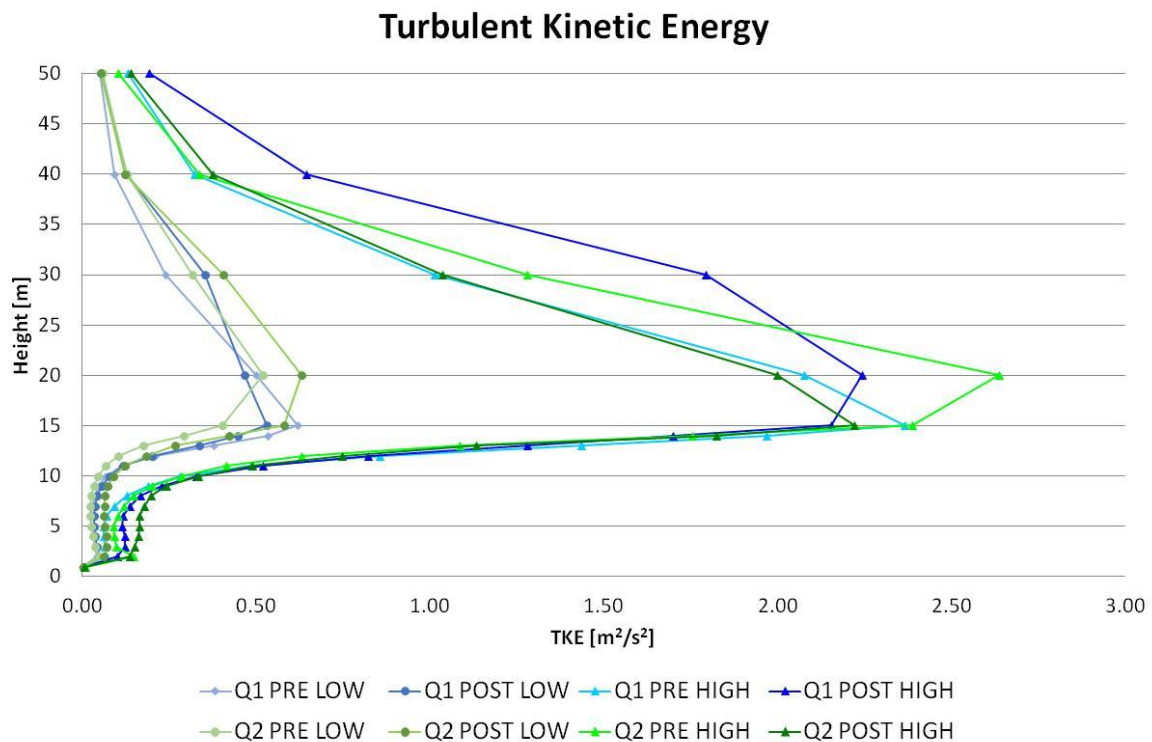


Figure 29: Turbulent Kinetic Energy.

In order to reinforce the wind output data obtained, in the next pages some Smokeview screenshots are shown.

Figure 30 and Figure 31 are Smokeview screenshots of slices files parallels to the floor and at 8 meters high, comparing streamwise velocities of Q1 before and after the treatment for low and high wind speed conditions respectively. Both demonstrate how winds velocities are higher after the treatments.

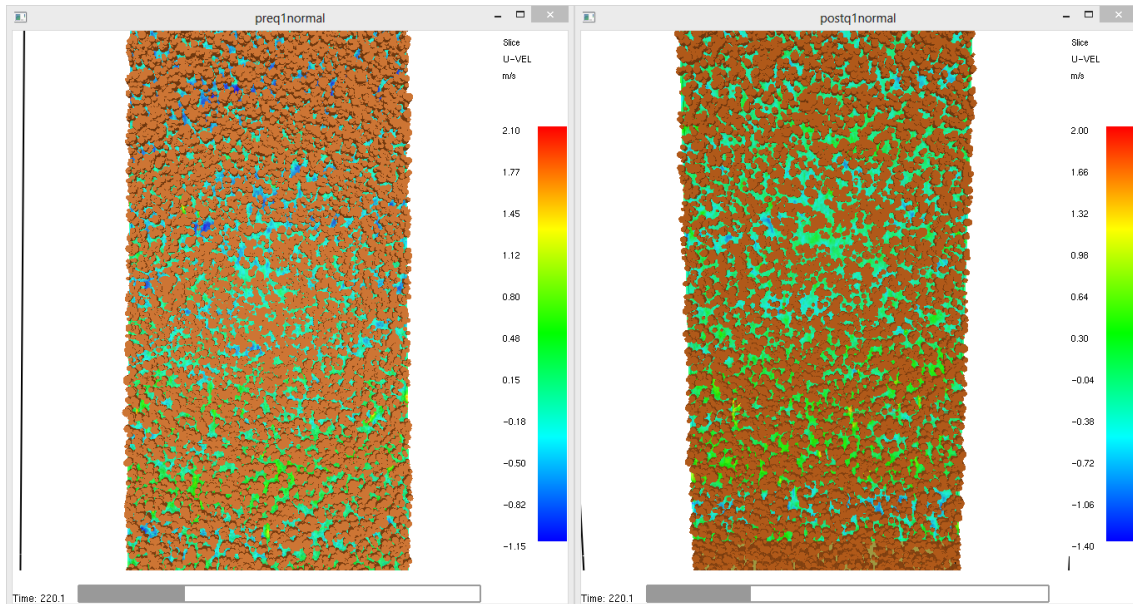


Figure 30: Smokeview visualization of streamwise velocities of pre Q1 and post Q1 with low wind speed conditions at 8 meters high.

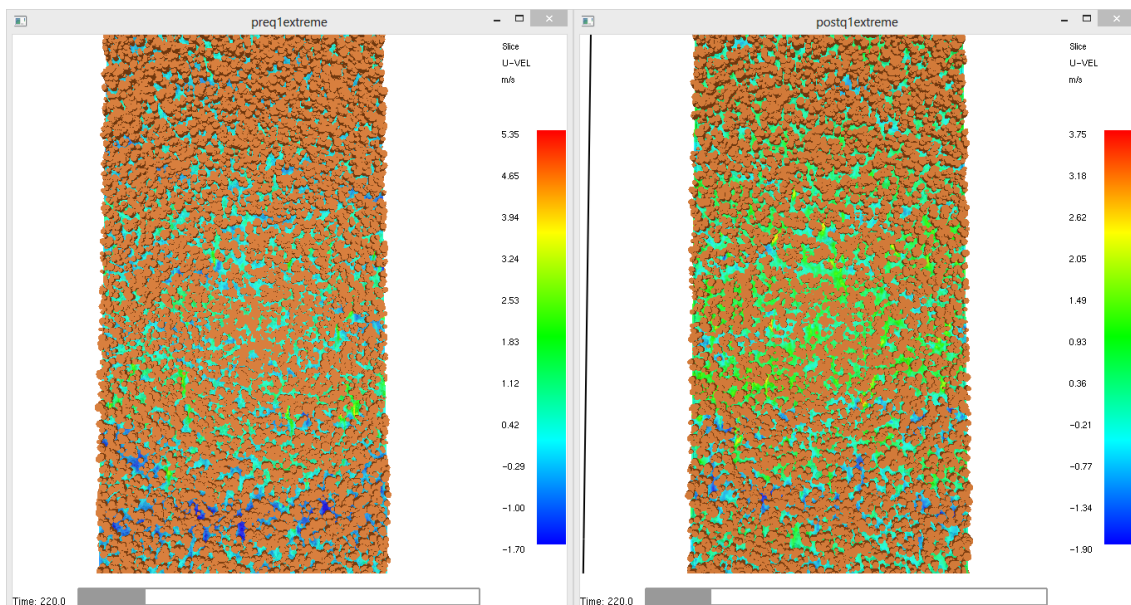


Figure 31: Smokeview visualization of streamwise velocities of pre Q1 and post Q1 with high wind speed conditions at 8 meters high.

Figure 32 shows the same case as the previous one explained, but the slice file is not located within the canopy, at 8 meters high, but on the top of the canopy at 15 meters high. It is possible to see how after the treatments some corridors of higher streamwise velocities are created.

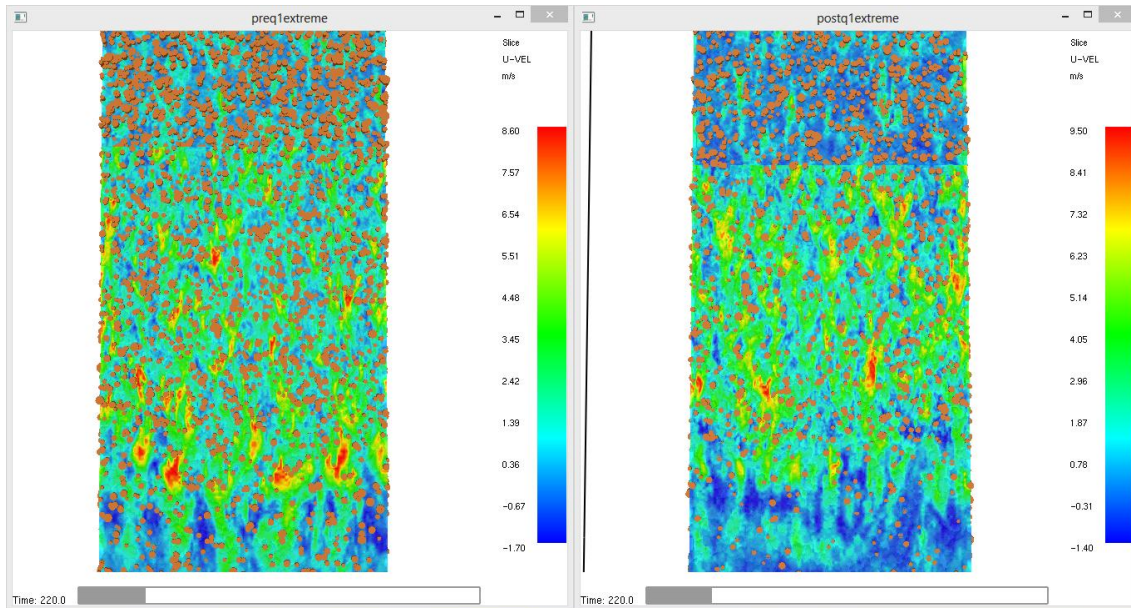


Figure 32: Smokeview visualization of streamwise velocities of pre Q1 and post Q1 with high wind speed conditions at 15 meters high.

Figure 33 shows Q1 before and after treatments, with high wind speed conditions, and with active fire. It is possible to see how, with the presence of fire, streamwise velocities are higher in pre treatment conditions due to the higher amount of fuel.

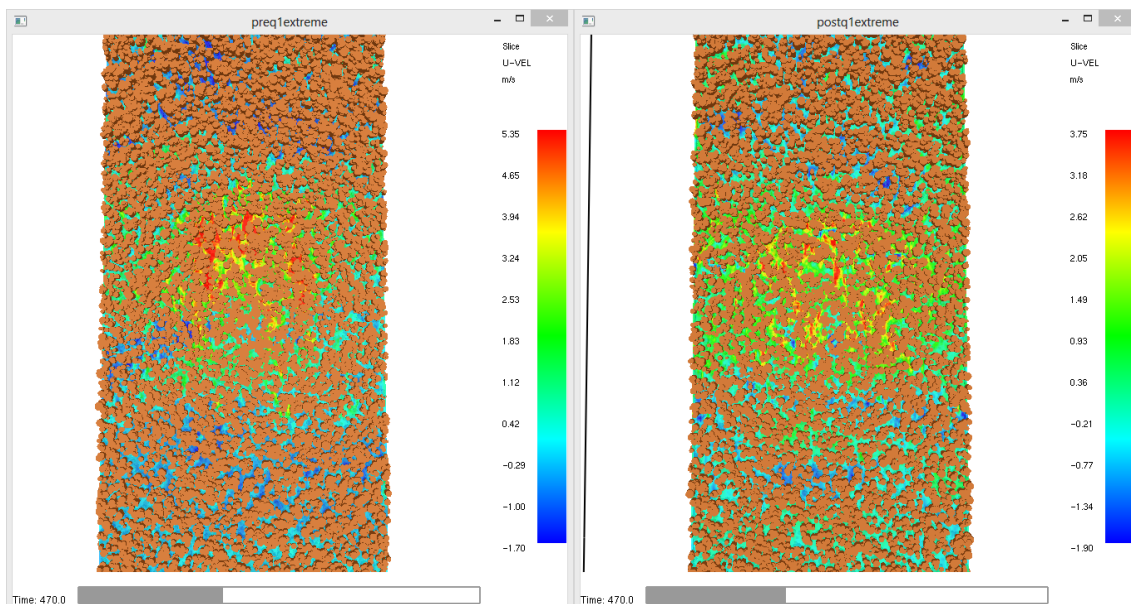


Figure 33: Smokeview visualization of streamwise velocities of pre Q1 and post Q1 with high wind speed conditions at 8 meters high and with active fire.

Figure 34 and Figure 35 show slices files parallels to the floor and at 8 meters high, comparing streamwise velocities of Q2 before and after the treatment for low and high wind speed condition respectively. Again, both demonstrate how winds velocities are higher after the treatments.

The smokeview visualizations of Q2 show an error with the slice files of some meshes of the study plot. Because of this, there is a part of the study plot that does not present results.

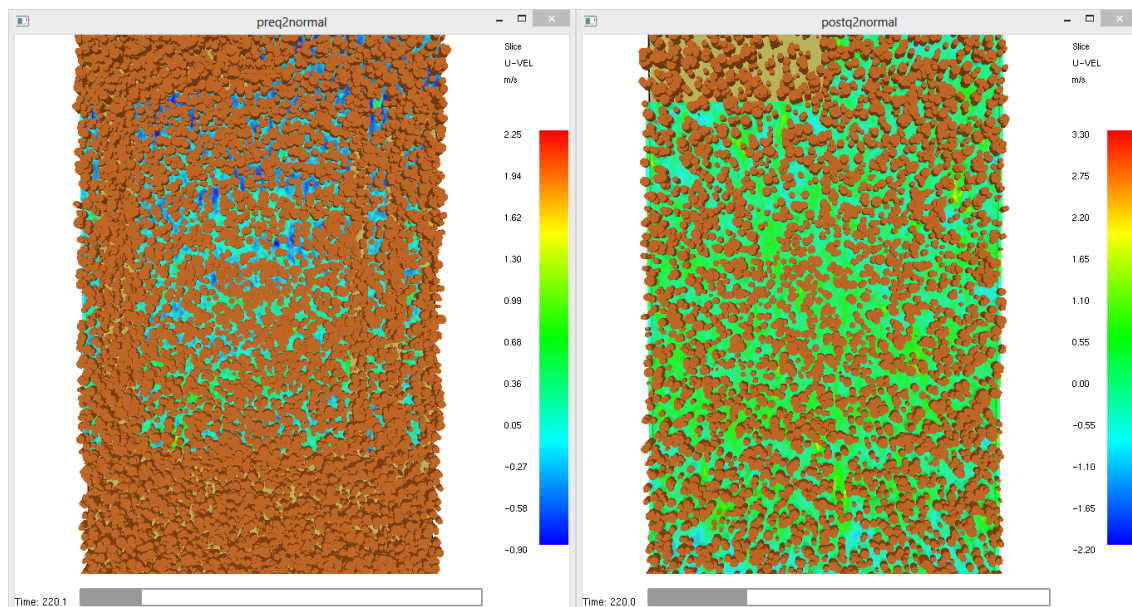


Figure 34: Smokeview visualization of streamwise velocities of pre Q2 and post Q2 with low wind speed conditions at 8 meters high.

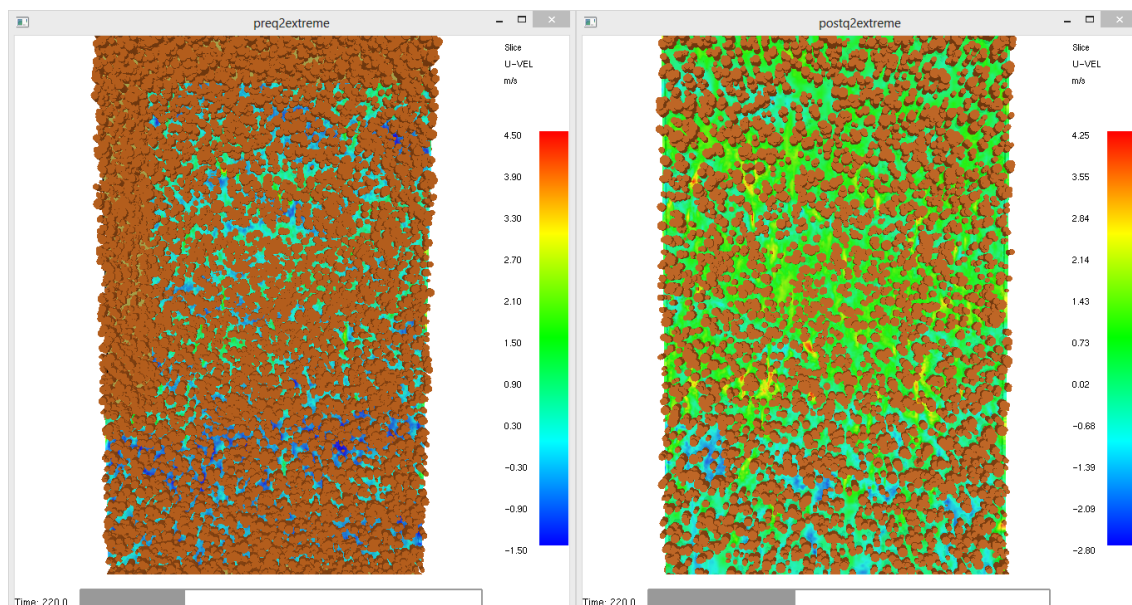


Figure 35: Smokeview visualization of streamwise velocities of pre Q2 and post Q2 with high wind speed conditions at 8 meters high.

Figure 36 shows the same case as the previous one explained, but again, the slice file is not located within the canopy, at 8 meters high, but on the top of the canopy at 15 meters high. It is possible to see how after the treatments some corridors of higher streamwise velocities are created and it is more noticeable than in plot Q1.

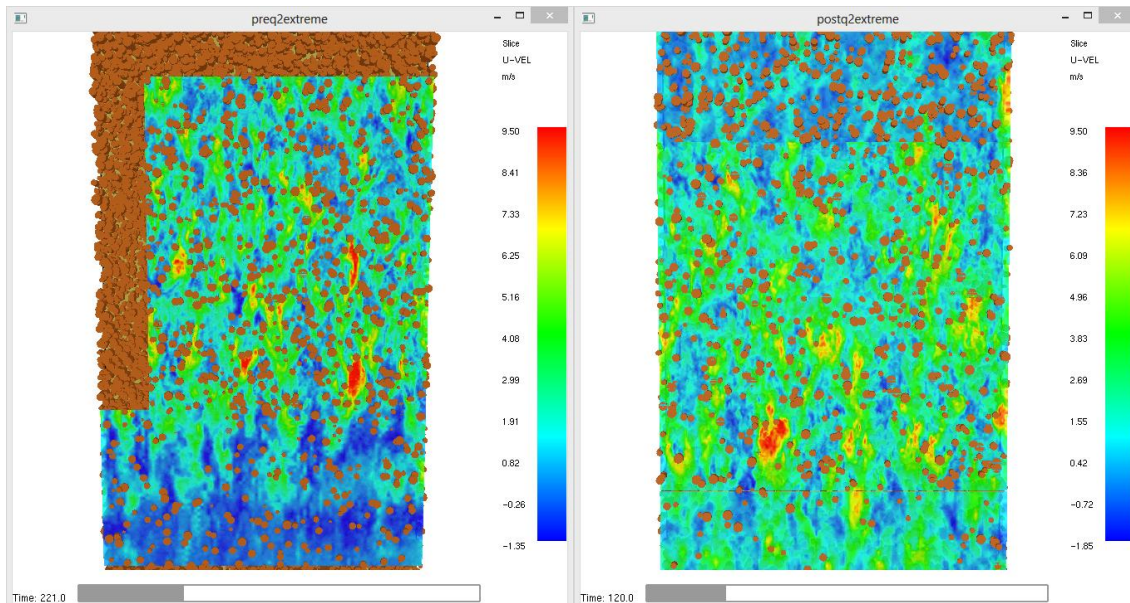


Figure 36: Smokeview visualization of streamwise velocities of pre Q2 and post Q2 with high wind speed conditions at 15 meters high.

Figure 37 shows Q2 before and after treatments under high wind speed conditions and with active fire. Again it is possible to see that with the presence of active fire, streamwise velocities are higher before treatments.

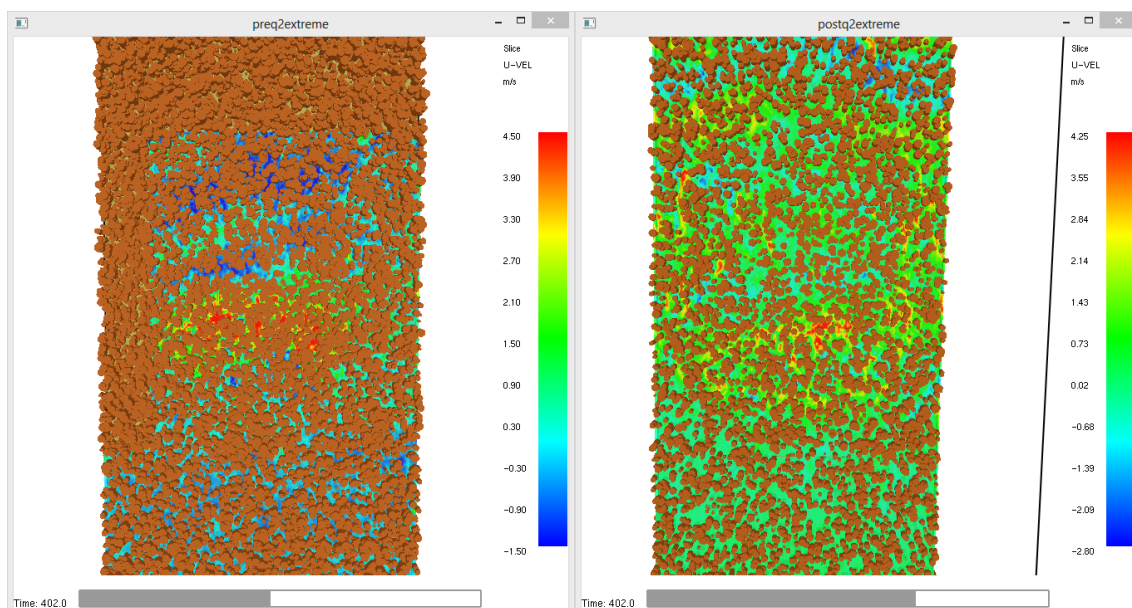


Figure 37: Smokeview visualization of streamwise velocities of pre Q2 and post Q2 with high wind speed conditions at 8 meters high and with active fire.

Figure 38 compares both Q1 and Q2 after treatments with high wind speed conditions and shows a slice file at 8 meters high that represents the streamwise velocity. It is noticeable that streamwise velocities are higher in Q2 than in Q1.

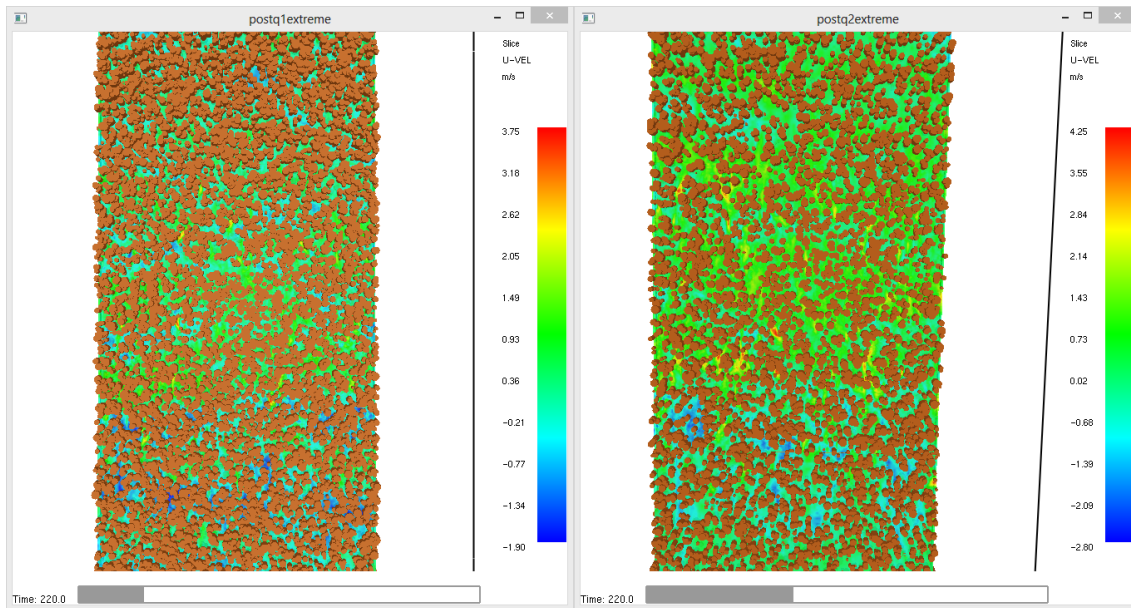


Figure 38: Smokeview visualization of streamwise velocities at Q1 and Q2 after treatments with high wind speed conditions at 8 meters high.

Figure 39 presents Q1 and Q2 after treatments under high wind speed conditions and with active fire. It is possible to see that with the presence of active fire, streamwise velocities are higher in Q1.

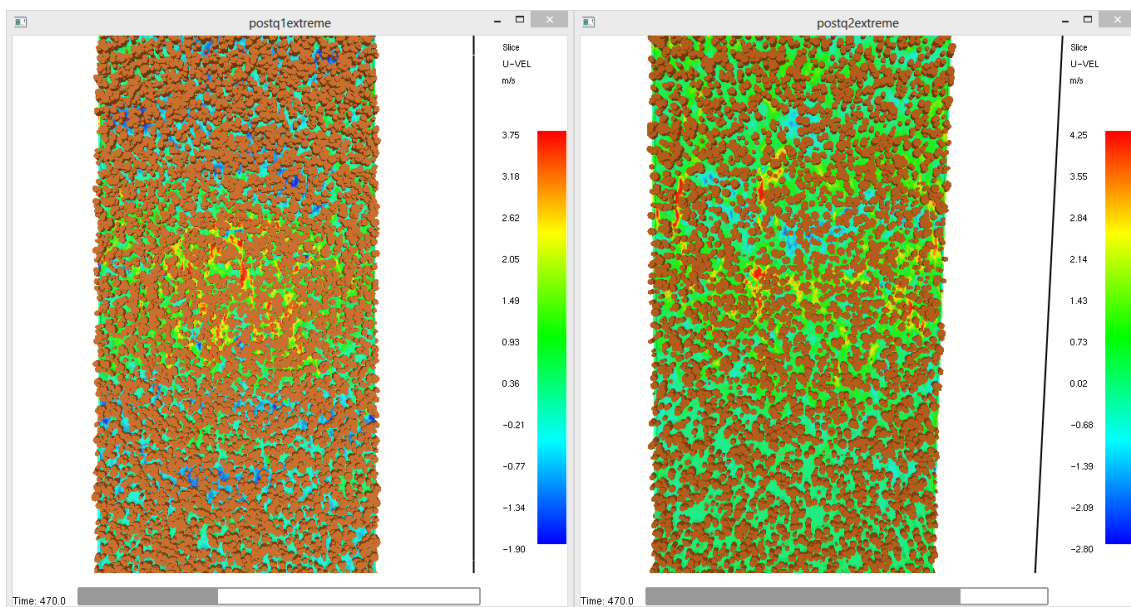


Figure 39 Smokeview visualization of streamwise velocities of Q1 and Q2 after treatments with high wind speed conditions at 8 meters high and with active fire.

Figure 40 compares Q1 and Q2 after treatments and with low wind speed conditions. Again, Q2 presents higher streamwise velocities than Q1.

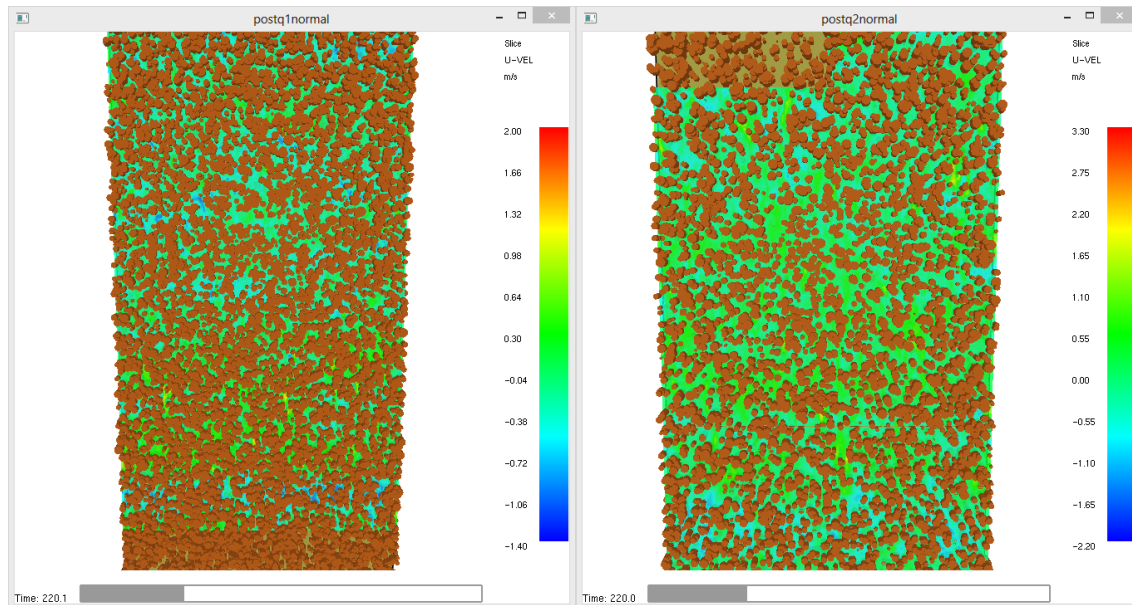


Figure 40: Smokeview visualization of streamwise velocities at Q1 and Q2 after treatments with low wind speed conditions at 8 meters high.

The same comparison is done in Figure 41 but with active fire.

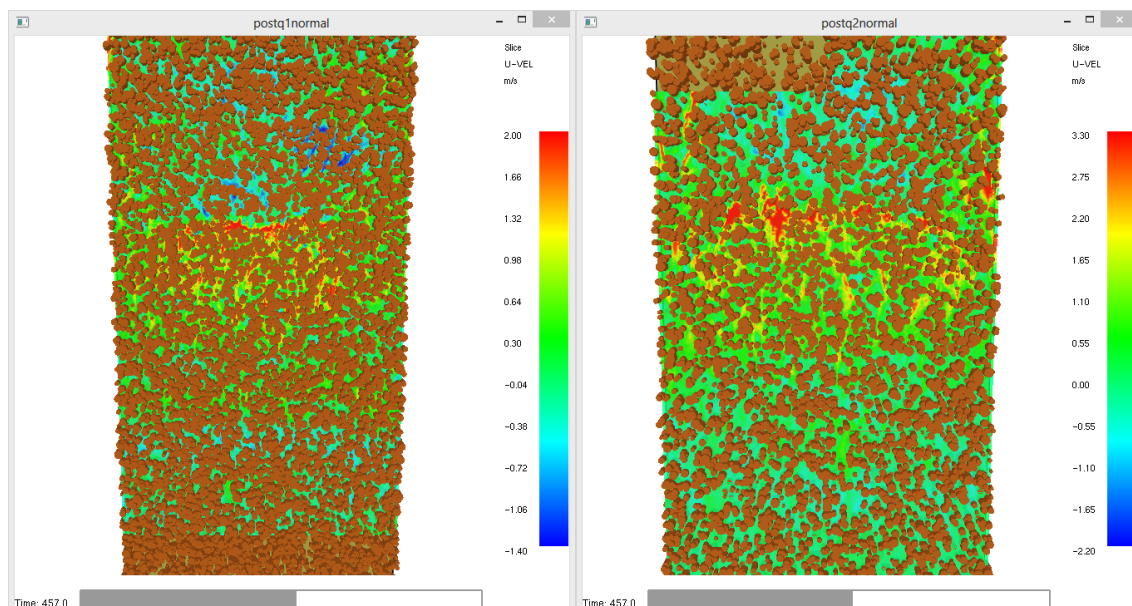


Figure 41: Smokeview visualization of streamwise velocities of Q1 and Q2 after treatments with low wind speed conditions at 8 meters high and with active fire.

5. Discussion and conclusions

When analyzing the effectiveness and the effects of vegetation treatments on fire behavior, it is important to take into account that vegetation, atmosphere and fire are closely tied to the structure of the forest, which controls both the fire and the wind penetration. The fact that opening up or reducing the density of the woodlands increases mean wind speed and changes the wind profile shape is consistent with observations and simulation results in previous works. The scale and magnitude of canopy heterogeneities affect the turbulence and mixing in the canopy, and momentum exchange between the winds above the vegetation and those within the canopy (Dupont and Brunet, 2006).

Concerning Crown fire activity, with low wind speed conditions, there is less than a 5% of canopy consumption and so it is considered that there is no CFA. With high wind speed conditions, there is an important amount of canopy consumption that is drastically reduced with both treatments. However, thinning 30% of the BA presents a higher reduction of the CFA than thinning 50% of the BA.

Regarding the Rate of Spread, low wind speed conditions present lower values than high wind speed conditions. This is not only because of the wind velocity but also because of the CFA. Low wind speed conditions don't present canopy consumption and so CFA, which results in a lower ROS than high wind speed conditions which do present CFA. With high wind speed conditions, the ROS decreases after the treatments with an insignificant difference between Q1 and Q2 (0.24 and 0.21 respectively). The reduction of the amount of fuel and the decrease of the CFA is translated in a lower ROS. For low wind speed conditions, there is an increase of the ROS after the treatment. This fact is due to opening the forest structure thus increasing the wind speed within the canopy.

The wind outputs obtained show how all wind speed decrease within the canopy. All post-treatment conditions present higher values of the mean streamwise wind velocity than pre-treatment conditions as a result of the thinning and the suppression of obstacles for the streamwise. The treatment that applies a thinning of the 50% of the BA presents higher wind speeds than the treatment that applies a thinning of the 30% of the BA. In relation to the turbulent kinetic energy, this presents higher values with thinning 50% of the basal area than with thinning 30% of the basal area.

In conclusion, the heterogeneity within the canopy structure affects the wind speed profiles, the turbulence and the mixing between the winds above the

vegetation and those within the canopy. This result in higher wind speeds after treatments than before treatment. Nevertheless, reduction of fuel vegetation also results in a decrease of the crown fires and on the ROS for high wind conditions. Thinning 30% of the BA, is the most efficient treatment because counteracts the effect of opening the forest structure and so increasing the wind speeds; and reducing vegetation thus decreasing the crown fire activity and the rate of spread.

Finally, WFDS is not a good fire simulator to be used for suppression activities because it takes time to build up the scenario but it is an excellent fire simulator for testing prevention managements as well as prescribed fires.

6. Acknowledgements

First of all, I want to express my gratitude to Dr. Domingo Molina for encourage me to live this experience and give me the opportunity to do my Master thesis at Colorado State University. Also thank you for your advises and corrections.

I would like to express my gratitude to Dr. Chad Hoffman for teaching me so many new concepts and open to me a new and unknown area of forest fires science.

I thank profusely Justin Ziegler for all his help at any time and for any question I had.

I sincerely thank the Colorado State University Office of International Programs for helping me with all the bureaucratic process and for their programs and activities to help and include International students.

I also thank Maria Fernandez-Gimenez and Gloria Edwards from Colorado State University for being close people and for offering me their help.

I also want to express my gratitude to Dr. Michele Salis for helping me and advising me.

I would like to thank to Míriam Piqué and Eduard Busquets from CTFC for providing me the forest inventories.

I also want to thank Mike Caggiano for giving me the opportunity to be part of an amazing experience as the New Mexico TREX was. And thanks to all the fantastic colleagues that I met there such as Lydia Zowada, Jose Luis Duce, Erin Banwell, Jeremy Baily, Don Kearney, David Lasky, etc. Thank you for all the knowledge and hope that you all gave me.

I thank profusely to Gilberto Solano, Javier Bernal and Almudena Martinez for their constant help and support and for making so easy being an International student.

I am extremely thankful to Judy and Bruce Warren, for all their time spent on me and for making me feel closer to the American society.

And last but not least, thanks to my family and friends who supported me during the whole experience.

7. References

- Bova, Anthony S., William E. Mell, and Chad M. Hoffman. "A comparison of level set and marker methods for the simulation of wildland fire front propagation." *International Journal of Wildland Fire* 25.2 (2015): 229-241.
- Costa-Alcubierre, Pau, et al. Prevention of Large Wildfires using the Fire Types Concept. Generalitat de Catalunya, 2011.
- Castellnou, Marc, M. Miralles, and M. Piqué. "Tipificación de los incendios forestales de Cataluña. Elaboración del mapa de incendios de diseño como herramienta para la gestión forestal." *Congreso Forestal Español*. 2009.
- Dupont, Sylvain, and Yves Brunet. "Simulation of turbulent flow in an urban forested park damaged by a windstorm." *Boundary-Layer Meteorology* 120.1 (2006): 133-161.
- Finney, Mark A. "FARSITE: Fire Area Simulator-model development and evaluation." Res. Pap. RMRS-RP-4, Revised 2004. Ogden, UT: US Department of Agriculture, Forest Service, Rocky Mountain Research Station. 47 p. 4 (1998).
- Finney, Mark A. FARSITE: Fire Area Simulator-Model Development and Evaluation, United States Department of Agriculture Forest Service Rocky Mountain Research Station Research Paper. RMRS-RP-4 Revised March 1998, revised February, 2004.
- Linn, Rodman R., et al. "Modeling wind fields and fire propagation following bark beetle outbreaks in spatially-heterogeneous pinyon-juniper woodland fuel complexes." *Agricultural and Forest Meteorology* 173 (2013): 139-153.
- Mell, William, et al. "A physics-based approach to modelling grassland fires." *International Journal of Wildland Fire* 16.1 (2007): 1-22.
- Mell, William, et al. "Numerical simulation and experiments of burning douglas fir trees." *Combustion and Flame* 156.10 (2009): 2023-2041.
- Parsons, Russell A., William Mell, and Peter McCauley. "Modeling the spatial distribution of forest crown biomass and effects on fire behavior with FUEL3D and WFDS." In: Viegas, DX, ed. *Proceedings of the VI International Conference on Forest Fire Research; 15-18 November*

2010; Coimbra, Portugal. Coimbra, Portugal: University of Coimbra. 15 p.. 2010.

Rehm, Ronald G., and Howard R. Baum. "The equations of motion for thermally driven, buoyant flows." *Journal of Research of the NBS* 83.297-308 (1978): 2.

Rehm, Ronald G., and Randall J. McDermott. *Fire-front propagation using the level set method*. US Department of Commerce, National Institute of Standards and Technology, 2009.

Sethian JA (1992) 'Level set methods and fast-marching methods', 2nd edn.(Cambridge University Press: Cambridge, UK).

Smagorinsky, Joseph. "General circulation experiments with the primitive equations: I. The basic experiment." *Monthly weather review* 91.3 (1963): 99-164.

Ziegler, Justin Paul, et al. "Spatially explicit measurements of forest structure and fire behavior following restoration treatments in dry forests." *Forest Ecology and Management* 386 (2017): 1-12.

8. Annexes

Annex I

Maps of the Study Zone:

- Topography.
- Aspect.
- Boundary Area of plot Q1.
- Boundary Area of plot Q2.

Annex II

Calculation of tree coordinates.

The first step was to calculate the X and Y coordinates by using trigonometry:

Angle and distance to X and Y	
0 to 45°	$X = \sin(\text{angle}) * \text{distance}$
	$Y = \cos(\text{angle}) * \text{distance}$
45 to 90°	$X = \cos(90 - \text{angle}) * \text{distance}$
	$Y = \sin(90 - \text{angle}) * \text{distance}$
90 to 135°	$X = \cos(\text{angle} - 90) * \text{distance}$
	$Y = \sin(\text{angle} - 90) * \text{distance}$
135 to 180°	$X = \sin(180 - \text{angle}) * \text{distance}$
	$Y = \cos(180 - \text{angle}) * \text{distance}$
180 to 225°	$X = \sin(\text{angle} - 180) * \text{distance}$
	$Y = \cos(\text{angle} - 180) * \text{distance}$
225 to 270°	$X = \cos(270 - \text{angle}) * \text{distance}$
	$Y = \sin(270 - \text{angle}) * \text{distance}$
270 to 315°	$X = \cos(\text{angle} - 270) * \text{distance}$
	$Y = \sin(\text{angle} - 270) * \text{distance}$
315 to 360°	$X = \sin(360 - \text{angle}) * \text{distance}$
	$Y = \cos(360 - \text{angle}) * \text{distance}$

After that, the location of the central point of the plot was calculated by loading this point in ArcGis. That step gave us the ETRS89 UTM coordinates of the central point. By summing the values obtained by trigonometry to the UTM coordinates of the central point, we obtained the UTM coordinates of all the trees. The next step, was to build the boundary area and define the corner that will be our 0,0 (X,Y) in WFDS. By extracting the UTM coordinates of this corner to the UTM coordinates of all the trees, we obtained the X and Y coordinates ready to work in WFDS.

To obtain the Z values, the altitude of each point was calculated in ArcGIS and then, the minimum value obtained was extracted to the Z values of all the trees.

Annex III

Forest inventories of the study plots.

Plot Q1: 385 trees

SURF_ID	Tree height [m]	CBH [m]	CW [m]	X	Y	Z	DBH [m]	shape
TREE	11.20	8.0	3.03	252	96	23	0.10	CYLINDER
TREE	9.00	3.8	2.68	251	94	23	0.08	CYLINDER
TREE	12.20	5.3	2.35	250	95	23	0.11	CYLINDER
TREE	12.40	6.4	6.05	248	96	22	0.23	CYLINDER
TREE	7.00	4.5	3.13	246	95	22	0.07	CYLINDER
TREE	5.90	3.0	2.20	250	97	23	0.05	CYLINDER
TREE	2.70	1.2	0.90	244	95	22	0.04	CYLINDER
TREE	11.00	7.7	3.50	242	96	22	0.09	CYLINDER
TREE	2.00	1.1	1.00	243	96	22	0.04	CYLINDER
TREE	13.60	6.3	3.38	241	96	21	0.17	CYLINDER
TREE	11.10	6.8	1.88	242	97	22	0.08	CYLINDER
TREE	3.10	2.2	1.75	241	97	21	0.05	CYLINDER
TREE	8.50	4.2	3.23	241	97	21	0.08	CYLINDER
TREE	11.50	7.1	3.03	242	94	21	0.09	CYLINDER
TREE	2.90	1.4	0.70	242	93	21	0.05	CYLINDER
TREE	6.00	4.2	1.70	241	94	21	0.07	CYLINDER
TREE	3.50	1.5	0.70	240	95	21	0.05	CYLINDER
TREE	11.80	5.0	3.90	240	95	21	0.10	CYLINDER
TREE	14.30	8.6	3.05	239	95	21	0.14	CYLINDER
TREE	10.90	6.2	2.85	237	95	21	0.10	CYLINDER
TREE	12.30	8.3	2.95	237	95	21	0.12	CYLINDER
TREE	12.00	9.2	1.98	237	95	21	0.11	CYLINDER
TREE	5.60	2.4	0.63	237	96	21	0.06	CYLINDER
TREE	15.70	5.7	3.03	234	96	20	0.18	CYLINDER
TREE	12.10	9.4	2.23	236	98	21	0.14	CYLINDER
TREE	11.30	5.5	2.80	233	96	20	0.10	CYLINDER
TREE	10.40	7.5	2.78	232	96	20	0.08	CYLINDER
TREE	3.60	2.1	0.80	231	97	20	0.05	CYLINDER
TREE	3.20	1.7	0.50	232	97	20	0.05	CYLINDER
TREE	10.50	8.6	2.53	230	97	20	0.11	CYLINDER
TREE	8.40	7.7	3.15	230	97	20	0.10	CYLINDER
TREE	8.50	6.4	2.68	228	95	19	0.09	CYLINDER
TREE	15.00	9.8	3.60	241	101	22	0.15	CYLINDER
TREE	6.80	3.2	1.70	232	99	21	0.06	CYLINDER
TREE	3.80	2.7	1.25	236	101	21	0.05	CYLINDER
TREE	5.20	3.9	3.45	230	104	21	0.08	CYLINDER
TREE	12.90	8.3	2.15	226	96	19	0.14	CYLINDER
TREE	8.00	6.3	2.70	225	95	19	0.09	CYLINDER

TREE	10.10	4.4	4.43	227	96	19	0.12	CYLINDER
TREE	3.30	2.4	3.15	226	93	19	0.06	CYLINDER
TREE	3.70	2.9	1.54	225	94	19	0.05	CYLINDER
TREE	7.00	5.4	3.18	225	93	19	0.07	CYLINDER
TREE	13.20	8.4	3.05	227	93	19	0.11	CYLINDER
TREE	12.60	9.0	3.33	227	93	19	0.09	CYLINDER
TREE	9.80	6.1	2.25	230	97	20	0.11	CYLINDER
TREE	13.40	3.8	3.25	232	96	20	0.14	CYLINDER
TREE	15.80	4.8	2.70	232	96	20	0.15	CYLINDER
TREE	5.60	3.4	1.65	229	92	19	0.06	CYLINDER
TREE	4.80	2.9	1.60	229	92	19	0.05	CYLINDER
TREE	10.50	7.0	2.85	231	93	19	0.10	CYLINDER
TREE	11.00	5.4	2.25	232	94	20	0.10	CYLINDER
TREE	11.10	8.6	2.50	233	95	20	0.10	CYLINDER
TREE	11.90	8.0	1.70	235	96	20	0.11	CYLINDER
TREE	2.40	1.7	0.60	235	96	20	0.04	CYLINDER
TREE	4.20	2.6	1.10	233	93	20	0.06	CYLINDER
TREE	5.60	4.2	1.93	235	94	20	0.05	CYLINDER
TREE	11.20	4.9	1.55	235	94	20	0.11	CYLINDER
TREE	1.90	0.5	0.70	235	94	20	0.03	CYLINDER
TREE	9.50	4.6	3.25	235	93	20	0.10	CYLINDER
TREE	8.30	5.3	2.45	236	93	20	0.08	CYLINDER
TREE	11.50	4.7	4.58	238	93	20	0.15	CYLINDER
TREE	3.00	1.5	0.80	238	94	21	0.04	CYLINDER
TREE	3.50	1.3	0.87	239	93	20	0.05	CYLINDER
TREE	3.20	1.2	0.78	239	93	21	0.05	CYLINDER
TREE	7.10	4.6	2.35	239	93	21	0.07	CYLINDER
TREE	12.00	5.1	4.05	244	94	21	0.17	CYLINDER
TREE	10.60	8.0	3.75	244	94	21	0.11	CYLINDER
TREE	10.50	7.0	3.53	245	95	22	0.13	CYLINDER
TREE	11.00	6.6	3.20	253	92	23	0.13	CYLINDER
TREE	12.60	6.4	3.25	252	92	22	0.13	CYLINDER
TREE	9.90	5.2	3.90	253	90	22	0.11	CYLINDER
TREE	12.30	4.2	5.75	253	90	22	0.20	CYLINDER
TREE	10.10	4.4	4.53	248	89	21	0.15	CYLINDER
TREE	12.60	3.0	4.40	247	89	21	0.17	CYLINDER
TREE	9.60	6.4	3.58	247	88	21	0.10	CYLINDER
TREE	6.40	4.7	5.20	247	88	21	0.07	CYLINDER
TREE	4.50	3.8	3.05	247	88	21	0.06	CYLINDER
TREE	5.50	4.5	2.05	246	88	21	0.09	CYLINDER
TREE	8.00	4.1	2.38	246	88	21	0.10	CYLINDER
TREE	4.60	2.4	3.75	242	87	20	0.06	CYLINDER
TREE	14.50	3.7	6.10	240	89	20	0.19	CYLINDER
TREE	3.10	1.7	1.30	240	91	20	0.04	CYLINDER
TREE	13.30	7.0	4.98	242	92	21	0.18	CYLINDER

TREE	6.20	4.5	3.73	239	92	20	0.08	CYLINDER
TREE	11.80	10.2	1.70	239	92	20	0.11	CYLINDER
TREE	7.00	5.0	1.68	239	91	20	0.05	CYLINDER
TREE	3.10	1.9	1.65	239	91	20	0.04	CYLINDER
TREE	10.40	7.0	2.98	239	91	20	0.09	CYLINDER
TREE	4.40	1.8	1.23	239	90	20	0.05	CYLINDER
TREE	7.90	4.4	2.95	239	90	20	0.07	CYLINDER
TREE	13.40	6.7	2.75	238	91	20	0.12	CYLINDER
TREE	13.40	9.9	2.65	237	91	20	0.07	CYLINDER
TREE	7.50	6.0	2.38	237	91	20	0.06	CYLINDER
TREE	3.70	2.7	1.75	236	90	20	0.06	CYLINDER
TREE	3.10	2.2	0.80	236	91	20	0.05	CYLINDER
TREE	14.40	7.0	3.75	235	91	20	0.16	CYLINDER
TREE	8.90	6.8	2.93	234	91	19	0.08	CYLINDER
TREE	8.90	6.8	2.93	234	90	19	0.08	CYLINDER
TREE	6.90	4.9	1.45	233	90	19	0.05	CYLINDER
TREE	9.90	7.6	2.20	232	90	19	0.09	CYLINDER
TREE	12.90	8.4	2.00	233	91	19	0.12	CYLINDER
TREE	2.70	1.7	1.20	231	90	19	0.04	CYLINDER
TREE	8.60	7.0	2.13	230	90	19	0.08	CYLINDER
TREE	9.00	6.2	1.75	229	89	18	0.09	CYLINDER
TREE	7.10	5.7	1.65	228	92	19	0.07	CYLINDER
TREE	11.30	7.3	3.60	228	90	18	0.14	CYLINDER
TREE	7.50	6.2	2.70	227	92	19	0.08	CYLINDER
TREE	7.60	5.7	2.55	227	91	19	0.09	CYLINDER
TREE	7.20	6.3	1.58	228	89	18	0.06	CYLINDER
TREE	5.80	3.6	2.35	227	89	18	0.06	CYLINDER
TREE	6.20	4.9	2.15	226	90	18	0.07	CYLINDER
TREE	3.50	2.9	3.10	224	90	18	0.06	CYLINDER
TREE	6.00	4.3	2.60	225	90	18	0.08	CYLINDER
TREE	9.70	5.7	2.18	225	90	18	0.09	CYLINDER
TREE	4.50	3.8	2.20	225	87	17	0.06	CYLINDER
TREE	7.50	4.7	1.73	225	85	17	0.10	CYLINDER
TREE	8.00	5.5	0.00	223	83	17	0.09	CYLINDER
TREE	7.50	5.6	2.60	228	88	18	0.11	CYLINDER
TREE	12.00	4.3	4.10	228	88	18	0.15	CYLINDER
TREE	10.00	4.0	3.48	229	88	18	0.08	CYLINDER
TREE	10.50	7.5	2.40	230	87	18	0.10	CYLINDER
TREE	12.40	7.5	2.60	231	86	18	0.11	CYLINDER
TREE	9.00	5.2	2.10	231	87	18	0.08	CYLINDER
TREE	12.60	3.9	2.48	233	87	19	0.13	CYLINDER
TREE	9.60	6.1	3.65	233	86	18	0.10	CYLINDER
TREE	5.30	4.4	2.60	234	87	19	0.06	CYLINDER
TREE	12.40	4.2	3.33	234	86	19	0.15	CYLINDER
TREE	13.90	3.2	3.25	234	88	19	0.13	CYLINDER

TREE	4.00	1.7	0.80	235	88	19	0.04	CYLINDER
TREE	8.20	4.3	2.95	236	88	19	0.09	CYLINDER
TREE	4.00	1.6	0.80	237	88	19	0.04	CYLINDER
TREE	9.30	5.1	2.38	237	88	19	0.09	CYLINDER
TREE	14.80	5.0	4.80	237	87	19	0.24	CYLINDER
TREE	2.30	0.7	0.50	239	85	19	0.04	CYLINDER
TREE	8.10	5.3	2.30	240	86	19	0.07	CYLINDER
TREE	13.90	10.3	2.15	240	87	20	0.13	CYLINDER
TREE	14.40	8.4	3.75	243	86	20	0.16	CYLINDER
TREE	11.90	5.2	5.15	244	86	20	0.23	CYLINDER
TREE	5.80	2.5	3.20	244	86	20	0.05	CYLINDER
TREE	2.00	0.4	0.30	245	86	20	0.03	CYLINDER
TREE	6.20	3.9	2.05	245	86	20	0.06	CYLINDER
TREE	6.20	3.9	2.05	247	86	21	0.06	CYLINDER
TREE	12.90	6.5	4.05	251	85	21	0.18	CYLINDER
TREE	9.20	6.6	1.80	254	85	22	0.08	CYLINDER
TREE	13.80	2.8	3.25	254	82	21	0.14	CYLINDER
TREE	2.50	0.8	0.60	252	82	21	0.04	CYLINDER
TREE	13.50	7.0	2.75	253	81	21	0.17	CYLINDER
TREE	9.40	6.8	2.50	253	79	20	0.11	CYLINDER
TREE	12.60	7.1	3.70	248	80	20	0.14	CYLINDER
TREE	12.50	7.0	2.90	248	80	20	0.13	CYLINDER
TREE	5.80	2.6	1.40	248	80	20	0.08	CYLINDER
TREE	13.60	7.4	2.75	247	80	20	0.13	CYLINDER
TREE	12.10	5.8	3.50	247	80	20	0.16	CYLINDER
TREE	4.10	2.2	1.10	247	79	19	0.05	CYLINDER
TREE	3.80	1.9	1.60	247	79	19	0.05	CYLINDER
TREE	5.60	3.2	1.73	246	79	19	0.06	CYLINDER
TREE	11.90	6.0	2.80	247	82	20	0.11	CYLINDER
TREE	14.10	10.5	2.45	246	84	20	0.15	CYLINDER
TREE	3.60	2.4	1.40	246	82	20	0.05	CYLINDER
TREE	12.50	9.0	3.30	244	79	19	0.14	CYLINDER
TREE	11.70	8.3	3.23	244	79	19	0.14	CYLINDER
TREE	10.90	8.3	2.68	244	82	20	0.09	CYLINDER
TREE	13.20	4.8	3.35	244	83	20	0.15	CYLINDER
TREE	1.80	0.5	0.30	244	82	19	0.04	CYLINDER
TREE	10.70	3.9	3.50	244	82	19	0.11	CYLINDER
TREE	8.20	5.7	2.75	244	81	19	0.11	CYLINDER
TREE	15.00	7.5	3.45	243	82	19	0.19	CYLINDER
TREE	9.50	4.0	3.55	244	79	19	0.09	CYLINDER
TREE	6.00	2.2	3.03	242	83	19	0.06	CYLINDER
TREE	5.60	3.8	2.55	241	83	19	0.06	CYLINDER
TREE	3.60	2.0	2.48	242	82	19	0.05	CYLINDER
TREE	8.00	4.6	3.05	241	83	19	0.10	CYLINDER
TREE	15.40	6.6	4.60	241	84	19	0.17	CYLINDER

TREE	6.60	5.5	3.20	240	83	19	0.09	CYLINDER
TREE	13.00	5.0	2.80	239	83	19	0.15	CYLINDER
TREE	5.20	3.7	1.97	239	83	19	0.06	CYLINDER
TREE	11.70	7.1	3.95	237	84	19	0.18	CYLINDER
TREE	8.10	6.6	3.35	237	84	19	0.12	CYLINDER
TREE	5.20	3.1	2.95	237	84	19	0.07	CYLINDER
TREE	2.00	1.1	0.90	236	83	19	0.04	CYLINDER
TREE	3.20	1.2	0.70	234	81	18	0.05	CYLINDER
TREE	5.20	3.7	1.98	234	80	18	0.06	CYLINDER
TREE	4.50	3.5	2.80	233	81	18	0.06	CYLINDER
TREE	14.90	8.1	3.65	234	81	18	0.16	CYLINDER
TREE	10.00	6.1	3.95	233	81	18	0.14	CYLINDER
TREE	9.00	6.4	2.05	232	81	18	0.10	CYLINDER
TREE	5.80	2.7	1.70	233	82	18	0.06	CYLINDER
TREE	10.80	7.3	1.83	231	81	17	0.09	CYLINDER
TREE	9.30	7.5	1.55	230	82	17	0.07	CYLINDER
TREE	13.60	6.9	3.25	229	82	17	0.17	CYLINDER
TREE	8.80	5.2	1.85	230	84	18	0.07	CYLINDER
TREE	11.50	7.0	2.90	229	84	18	0.12	CYLINDER
TREE	8.50	5.0	1.70	227	84	17	0.08	CYLINDER
TREE	9.70	7.2	2.25	227	84	17	0.11	CYLINDER
TREE	4.00	2.1	1.40	226	83	17	0.05	CYLINDER
TREE	7.10	4.8	1.55	224	84	17	0.07	CYLINDER
TREE	6.00	4.7	2.60	224	83	17	0.07	CYLINDER
TREE	15.70	7.7	2.45	225	84	17	0.15	CYLINDER
TREE	14.20	8.0	4.23	224	82	17	0.19	CYLINDER
TREE	11.80	6.3	3.10	227	80	17	0.14	CYLINDER
TREE	14.90	7.2	2.60	228	80	17	0.13	CYLINDER
TREE	6.00	4.0	2.25	228	78	17	0.06	CYLINDER
TREE	12.80	6.2	2.55	228	79	17	0.12	CYLINDER
TREE	7.50	3.4	3.70	228	80	17	0.09	CYLINDER
TREE	5.80	4.2	2.35	227	79	17	0.07	CYLINDER
TREE	10.80	7.9	2.95	227	79	17	0.08	CYLINDER
TREE	12.60	5.8	3.90	227	78	16	0.17	CYLINDER
TREE	7.00	5.0	2.65	229	94	19	0.09	CYLINDER
TREE	10.80	6.1	2.43	228	94	19	0.09	CYLINDER
TREE	6.30	2.9	3.63	229	94	19	0.08	CYLINDER
TREE	10.50	5.4	3.83	230	94	20	0.10	CYLINDER
TREE	8.90	4.8	2.48	232	94	20	0.08	CYLINDER
TREE	4.50	2.6	2.93	228	96	19	0.08	CYLINDER
TREE	10.40	5.9	3.00	228	97	20	0.13	CYLINDER
TREE	9.90	6.8	3.45	229	96	20	0.11	CYLINDER
TREE	7.30	4.7	2.95	228	97	20	0.07	CYLINDER
TREE	2.70	1.8	1.60	229	96	20	0.04	CYLINDER
TREE	11.30	6.1	4.98	230	96	20	0.14	CYLINDER

TREE	6.10	2.7	2.85	234	97	20	0.08	CYLINDER
TREE	8.00	4.7	3.75	232	98	20	0.12	CYLINDER
TREE	3.40	2.1	2.00	234	100	21	0.04	CYLINDER
TREE	8.50	3.5	3.18	234	100	21	0.10	CYLINDER
TREE	10.80	3.1	4.15	235	101	21	0.14	CYLINDER
TREE	2.80	1.5	3.30	234	103	21	0.08	CYLINDER
TREE	1.70	0.4	0.60	235	102	21	0.04	CYLINDER
TREE	1.60	0.3	0.50	234	103	22	0.03	CYLINDER
TREE	4.90	2.2	2.75	236	102	22	0.08	CYLINDER
TREE	5.70	2.9	2.60	240	103	22	0.10	CYLINDER
TREE	4.10	1.7	3.35	241	104	23	0.08	CYLINDER
TREE	3.10	1.5	1.20	241	104	23	0.05	CYLINDER
TREE	6.90	2.1	3.80	241	104	23	0.13	CYLINDER
TREE	5.50	2.6	2.70	241	105	23	0.09	CYLINDER
TREE	4.60	2.1	1.85	242	105	23	0.08	CYLINDER
TREE	2.00	0.7	0.50	244	105	23	0.03	CYLINDER
TREE	7.50	3.6	3.15	244	105	23	0.14	CYLINDER
TREE	4.60	2.2	2.85	245	104	23	0.10	CYLINDER
TREE	4.80	2.4	2.55	244	103	23	0.11	CYLINDER
TREE	5.20	2.8	2.40	244	103	23	0.08	CYLINDER
TREE	4.00	2.3	1.20	245	102	23	0.05	CYLINDER
TREE	3.50	1.7	0.90	245	103	23	0.05	CYLINDER
TREE	3.60	1.4	2.25	243	100	22	0.09	CYLINDER
TREE	4.80	3.0	3.35	245	100	23	0.08	CYLINDER
TREE	10.50	3.0	3.50	245	101	23	0.14	CYLINDER
TREE	6.90	2.9	3.75	245	100	23	0.13	CYLINDER
TREE	10.80	3.7	4.50	247	104	24	0.17	CYLINDER
TREE	2.10	1.8	2.20	247	105	24	0.06	CYLINDER
TREE	3.90	1.7	2.30	247	105	24	0.07	CYLINDER
TREE	2.70	1.6	3.20	246	106	24	0.06	CYLINDER
TREE	3.60	1.5	1.70	248	106	24	0.05	CYLINDER
TREE	3.90	1.5	0.80	253	103	24	0.05	CYLINDER
TREE	7.80	2.9	3.75	253	104	24	0.10	CYLINDER
TREE	8.00	4.4	3.50	253	104	24	0.09	CYLINDER
TREE	13.00	6.2	3.30	254	103	25	0.14	CYLINDER
TREE	9.20	2.9	3.80	255	104	25	0.15	CYLINDER
TREE	14.10	6.3	4.30	255	103	25	0.17	CYLINDER
TREE	12.20	4.6	4.95	255	106	25	0.15	CYLINDER
TREE	11.50	4.4	3.90	256	108	25	0.15	CYLINDER
TREE	10.40	7.3	2.15	255	108	25	0.10	CYLINDER
TREE	10.40	6.6	2.10	254	106	25	0.11	CYLINDER
TREE	11.40	4.2	2.73	255	109	26	0.12	CYLINDER
TREE	5.90	4.1	2.25	254	109	25	0.06	CYLINDER
TREE	8.40	6.2	3.70	253	109	25	0.12	CYLINDER
TREE	12.00	4.1	4.05	253	108	25	0.15	CYLINDER

TREE	12.60	7.2	3.50	253	107	25	0.11	CYLINDER
TREE	8.40	4.1	3.65	253	109	25	0.10	CYLINDER
TREE	11.00	6.0	2.40	253	109	25	0.10	CYLINDER
TREE	12.50	2.3	3.45	252	109	25	0.14	CYLINDER
TREE	4.70	2.5	3.65	251	107	25	0.10	CYLINDER
TREE	3.50	2.5	2.25	247	108	24	0.09	CYLINDER
TREE	3.50	2.4	2.30	245	109	24	0.06	CYLINDER
TREE	7.30	4.8	2.50	245	109	24	0.10	CYLINDER
TREE	5.60	3.7	2.85	244	109	24	0.09	CYLINDER
TREE	11.10	5.5	3.80	244	110	24	0.12	CYLINDER
TREE	7.80	5.3	3.40	244	110	24	0.09	CYLINDER
TREE	10.90	4.8	3.80	243	110	24	0.14	CYLINDER
TREE	8.10	4.8	3.15	244	106	24	0.10	CYLINDER
TREE	3.90	1.7	2.50	243	107	23	0.08	CYLINDER
TREE	2.40	1.4	2.65	242	107	23	0.06	CYLINDER
TREE	3.00	2.1	2.30	239	108	23	0.07	CYLINDER
TREE	4.20	1.7	4.18	239	107	23	0.13	CYLINDER
TREE	4.70	2.1	4.15	238	107	23	0.06	CYLINDER
TREE	4.90	2.7	3.25	238	106	22	0.05	CYLINDER
TREE	7.60	4.1	2.45	236	106	22	0.09	CYLINDER
TREE	3.60	2.0	2.95	237	106	22	0.07	CYLINDER
TREE	5.70	3.2	2.75	237	107	23	0.09	CYLINDER
TREE	10.10	2.1	6.95	237	107	23	0.17	CYLINDER
TREE	3.90	1.8	1.30	238	108	23	0.04	CYLINDER
TREE	3.80	1.9	2.45	238	108	23	0.06	CYLINDER
TREE	2.40	1.9	2.00	235	104	22	0.05	CYLINDER
TREE	12.80	7.2	3.60	227	97	20	0.11	CYLINDER
TREE	5.00	3.0	2.45	232	103	21	0.08	CYLINDER
TREE	7.80	3.6	5.20	232	104	21	0.10	CYLINDER
TREE	13.10	4.9	4.70	232	105	22	0.19	CYLINDER
TREE	11.80	6.0	4.95	230	104	21	0.15	CYLINDER
TREE	9.70	3.6	3.05	226	96	19	0.14	CYLINDER
TREE	8.40	5.8	2.50	226	95	19	0.10	CYLINDER
TREE	4.20	1.9	1.87	227	105	21	0.05	CYLINDER
TREE	6.10	3.7	1.75	226	108	21	0.06	CYLINDER
TREE	8.90	4.8	3.35	226	109	22	0.10	CYLINDER
TREE	8.60	3.7	3.40	225	110	22	0.12	CYLINDER
TREE	6.80	2.5	4.03	226	110	22	0.11	CYLINDER
TREE	3.00	1.4	1.10	226	110	22	0.04	CYLINDER
TREE	2.70	0.9	1.30	229	112	22	0.04	CYLINDER
TREE	6.80	2.3	5.55	229	111	22	0.12	CYLINDER
TREE	6.90	1.6	4.70	230	112	23	0.11	CYLINDER
TREE	4.20	1.6	3.68	230	112	23	0.07	CYLINDER
TREE	4.10	2.3	3.50	229	112	23	0.07	CYLINDER
TREE	3.60	2.7	4.35	229	112	23	0.07	CYLINDER

TREE	2.90	1.7	0.80	227	114	23	0.04	CYLINDER
TREE	12.90	5.4	3.90	227	115	23	0.12	CYLINDER
TREE	13.50	6.9	3.70	228	115	23	0.20	CYLINDER
TREE	13.80	5.6	3.20	229	116	23	0.16	CYLINDER
TREE	7.10	5.5	1.90	230	116	23	0.09	CYLINDER
TREE	9.80	6.0	2.68	230	116	23	0.13	CYLINDER
TREE	13.20	7.3	2.80	231	112	23	0.12	CYLINDER
TREE	3.40	1.7	1.10	230	112	23	0.05	CYLINDER
TREE	2.50	1.4	1.10	231	112	23	0.04	CYLINDER
TREE	10.00	5.1	3.28	232	112	23	0.09	CYLINDER
TREE	9.40	5.7	1.58	232	110	22	0.11	CYLINDER
TREE	6.70	3.9	2.45	232	110	22	0.10	CYLINDER
TREE	7.30	5.5	1.93	233	111	23	0.10	CYLINDER
TREE	10.20	6.4	3.23	235	112	23	0.14	CYLINDER
TREE	7.30	5.4	1.40	235	112	23	0.07	CYLINDER
TREE	11.00	5.3	2.60	235	111	23	0.11	CYLINDER
TREE	12.00	6.3	3.45	235	110	23	0.15	CYLINDER
TREE	10.80	7.3	2.70	236	110	23	0.11	CYLINDER
TREE	7.60	5.4	1.40	237	111	23	0.08	CYLINDER
TREE	12.10	6.5	5.00	236	112	23	0.17	CYLINDER
TREE	7.80	4.0	3.60	237	111	23	0.07	CYLINDER
TREE	12.50	4.3	3.35	237	111	23	0.14	CYLINDER
TREE	10.20	5.4	4.65	240	113	24	0.13	CYLINDER
TREE	11.10	6.5	5.25	243	114	25	0.18	CYLINDER
TREE	9.70	6.9	2.60	242	112	24	0.10	CYLINDER
TREE	2.20	1.2	3.15	245	114	25	0.08	CYLINDER
TREE	4.00	2.8	1.73	246	112	25	0.05	CYLINDER
TREE	4.20	2.9	1.80	246	112	25	0.05	CYLINDER
TREE	11.50	4.8	3.10	245	111	24	0.12	CYLINDER
TREE	6.10	2.3	1.95	249	112	25	0.06	CYLINDER
TREE	2.80	1.8	1.30	250	113	26	0.04	CYLINDER
TREE	13.70	5.1	5.00	251	114	26	0.20	CYLINDER
TREE	10.40	4.9	4.35	251	114	26	0.19	CYLINDER
TREE	12.10	3.9	5.60	253	113	26	0.17	CYLINDER
TREE	9.10	5.9	4.30	251	115	26	0.14	CYLINDER
TREE	12.50	2.9	4.98	254	119	27	0.13	CYLINDER
TREE	12.90	3.7	4.10	254	119	27	0.15	CYLINDER
TREE	7.00	3.2	2.30	254	118	27	0.08	CYLINDER
TREE	15.00	8.6	4.15	255	118	27	0.17	CYLINDER
TREE	11.20	5.7	3.55	256	117	27	0.13	CYLINDER
TREE	15.40	7.2	5.03	255	117	27	0.21	CYLINDER
TREE	5.90	3.2	2.80	254	117	27	0.07	CYLINDER
TREE	5.50	4.1	2.65	254	118	27	0.06	CYLINDER
TREE	14.50	8.3	3.95	252	117	26	0.20	CYLINDER
TREE	6.20	3.2	2.60	250	116	26	0.07	CYLINDER

TREE	10.90	4.7	2.45	250	119	26	0.09	CYLINDER
TREE	7.10	3.3	2.35	248	117	26	0.08	CYLINDER
TREE	11.10	6.7	3.25	248	118	26	0.08	CYLINDER
TREE	3.90	2.5	2.90	247	116	26	0.06	CYLINDER
TREE	5.90	3.2	2.80	247	115	25	0.07	CYLINDER
TREE	2.00	0.7	0.30	247	114	25	0.04	CYLINDER
TREE	11.60	3.5	4.10	246	117	25	0.14	CYLINDER
TREE	7.60	5.6	2.45	241	117	25	0.08	CYLINDER
TREE	1.80	0.6	0.50	237	116	24	0.04	CYLINDER
TREE	10.30	7.3	2.30	238	115	24	0.07	CYLINDER
TREE	12.30	4.3	6.75	237	114	24	0.20	CYLINDER
TREE	12.40	4.7	4.40	236	115	24	0.22	CYLINDER
TREE	14.10	5.3	4.70	236	115	24	0.25	CYLINDER
TREE	5.40	4.1	2.63	234	114	23	0.06	CYLINDER
TREE	3.30	1.5	1.20	233	118	24	0.04	CYLINDER
TREE	12.50	6.6	3.30	232	118	24	0.13	CYLINDER
TREE	11.50	4.5	3.10	232	118	24	0.11	CYLINDER
TREE	9.40	5.6	2.65	230	118	24	0.09	CYLINDER
TREE	3.00	1.4	1.10	229	118	24	0.05	CYLINDER
TREE	11.30	7.8	2.70	229	119	24	0.08	CYLINDER
TREE	13.10	7.8	3.05	229	119	24	0.12	CYLINDER
TREE	9.20	7.6	2.90	230	119	24	0.10	CYLINDER
TREE	11.50	7.4	3.05	230	119	24	0.11	CYLINDER
TREE	11.70	4.0	2.50	230	119	24	0.10	CYLINDER
TREE	3.70	2.1	1.80	229	120	24	0.05	CYLINDER
TREE	6.50	2.7	1.95	228	119	24	0.05	CYLINDER
TREE	7.10	4.4	3.40	228	117	23	0.07	CYLINDER
TREE	9.90	8.4	2.10	228	119	24	0.08	CYLINDER
TREE	4.00	1.8	1.70	227	118	23	0.06	CYLINDER
TREE	9.60	5.6	2.28	227	117	23	0.08	CYLINDER
TREE	11.50	2.7	3.65	227	116	23	0.14	CYLINDER

Plot Q2: 427 trees

SURF_ID	Tree height [m]	CBH [m]	CW [m]	X	Y	Z	DBH [m]	shape
TREE	2.00	1.6	0.80	245	97	23	0.04	CYLINDER
TREE	8.00	3.3	3.05	242	97	23	0.08	CYLINDER
TREE	11.00	6.0	3.93	241	97	23	0.12	CYLINDER
TREE	3.00	2.1	1.05	240	97	23	0.04	CYLINDER
TREE	14.00	11.0	5.20	234	95	22	0.18	CYLINDER
TREE	4.50	2.0	1.13	243	97	23	0.05	CYLINDER
TREE	5.50	4.0	2.29	247	99	24	0.06	CYLINDER
TREE	12.25	4.3	5.00	244	98	24	0.17	CYLINDER
TREE	4.00	2.0	0.99	245	98	24	0.04	CYLINDER
TREE	11.25	4.5	4.65	243	99	24	0.16	CYLINDER
TREE	4.00	2.5	2.50	244	100	24	0.06	CYLINDER
TREE	7.00	5.1	2.55	240	98	23	0.04	CYLINDER
TREE	8.00	5.0	3.03	236	97	23	0.13	CYLINDER
TREE	4.50	3.0	2.35	236	97	23	0.07	CYLINDER
TREE	8.50	4.5	4.40	237	98	23	0.14	CYLINDER
TREE	3.00	1.3	0.65	236	98	23	0.04	CYLINDER
TREE	12.50	5.5	4.45	237	98	23	0.13	CYLINDER
TREE	14.00	3.0	5.83	239	99	23	0.19	CYLINDER
TREE	6.50	4.0	3.10	235	97	23	0.09	CYLINDER
TREE	9.00	3.5	2.23	232	96	22	0.07	CYLINDER
TREE	7.00	4.6	2.28	232	96	22	0.04	CYLINDER
TREE	8.50	6.0	3.78	239	99	23	0.08	CYLINDER
TREE	11.00	8.5	4.95	237	98	23	0.13	CYLINDER
TREE	6.25	3.3	2.75	239	100	23	0.06	CYLINDER
TREE	2.70	2.0	1.18	232	96	22	0.05	CYLINDER
TREE	9.50	6.0	2.45	232	96	22	0.08	CYLINDER
TREE	5.00	3.3	1.65	239	101	24	0.03	CYLINDER
TREE	3.00	1.9	0.95	238	100	23	0.04	CYLINDER
TREE	7.50	6.5	1.55	236	100	23	0.13	CYLINDER
TREE	13.50	7.5	4.03	234	98	23	0.15	CYLINDER
TREE	9.50	5.0	3.00	237	101	24	0.12	CYLINDER
TREE	4.50	3.5	3.67	224	98	21	0.07	CYLINDER
TREE	11.50	8.5	3.52	225	98	21	0.13	CYLINDER
TREE	5.50	2.5	2.40	225	98	21	0.06	CYLINDER
TREE	7.50	5.0	2.85	226	98	21	0.09	CYLINDER
TREE	5.00	4.5	2.30	225	98	21	0.07	CYLINDER
TREE	13.00	6.5	4.00	226	98	21	0.13	CYLINDER
TREE	7.10	5.5	3.20	225	98	21	0.07	CYLINDER
TREE	8.50	5.0	3.72	225	99	21	0.12	CYLINDER
TREE	13.00	6.5	4.50	223	101	22	0.18	CYLINDER
TREE	7.50	6.0	2.43	224	102	22	0.09	CYLINDER

TREE	4.00	1.8	0.90	224	102	22	0.05	CYLINDER
TREE	9.00	7.5	1.95	229	96	21	0.07	CYLINDER
TREE	5.00	3.2	1.60	229	96	21	0.03	CYLINDER
TREE	9.50	7.5	1.73	229	101	23	0.09	CYLINDER
TREE	7.50	3.5	1.85	227	96	21	0.10	CYLINDER
TREE	11.00	6.0	2.95	230	104	23	0.16	CYLINDER
TREE	9.50	6.5	2.10	231	99	22	0.08	CYLINDER
TREE	10.50	7.5	2.30	229	98	22	0.09	CYLINDER
TREE	8.50	6.0	2.43	221	103	22	0.09	CYLINDER
TREE	8.00	4.5	2.20	226	96	21	0.07	CYLINDER
TREE	4.00	3.8	1.75	227	103	23	0.05	CYLINDER
TREE	8.50	6.5	0.88	226	105	23	0.06	CYLINDER
TREE	5.50	2.0	2.05	220	106	22	0.10	CYLINDER
TREE	5.50	4.3	1.83	221	106	22	0.10	CYLINDER
TREE	12.75	4.5	3.45	227	102	22	0.13	CYLINDER
TREE	9.75	1.8	4.48	219	106	22	0.18	CYLINDER
TREE	8.00	3.2	1.60	227	101	22	0.04	CYLINDER
TREE	10.25	8.0	1.72	226	102	22	0.11	CYLINDER
TREE	9.50	6.0	1.93	226	103	22	0.09	CYLINDER
TREE	10.50	4.3	3.95	226	102	22	0.15	CYLINDER
TREE	5.50	2.7	3.52	226	102	22	0.09	CYLINDER
TREE	3.00	1.7	0.85	226	102	22	0.04	CYLINDER
TREE	4.00	1.7	0.85	230	97	22	0.05	CYLINDER
TREE	4.00	2.3	2.15	227	99	22	0.08	CYLINDER
TREE	9.50	2.5	4.05	227	99	22	0.13	CYLINDER
TREE	4.60	4.5	2.73	226	100	22	0.07	CYLINDER
TREE	5.00	2.5	1.23	226	100	22	0.04	CYLINDER
TREE	5.00	4.3	2.10	223	102	22	0.06	CYLINDER
TREE	10.00	5.5	0.98	224	100	22	0.06	CYLINDER
TREE	7.00	3.5	3.38	223	101	22	0.09	CYLINDER
TREE	5.00	2.4	1.18	223	100	22	0.04	CYLINDER
TREE	6.00	5.2	2.60	222	100	21	0.03	CYLINDER
TREE	8.00	7.0	2.30	221	101	21	0.06	CYLINDER
TREE	3.00	2.7	1.35	221	100	21	0.03	CYLINDER
TREE	5.00	4.0	2.75	218	101	21	0.09	CYLINDER
TREE	9.1	9.0	3.05	219	100	21	0.12	CYLINDER
TREE	5.50	3.0	2.50	220	99	21	0.09	CYLINDER
TREE	6.20	2.4	2.90	217	100	21	0.07	CYLINDER
TREE	8.00	6.5	2.20	219	99	21	0.13	CYLINDER
TREE	10.00	6.0	3.25	218	99	20	0.12	CYLINDER
TREE	8.6	8.5	6.13	220	98	21	0.21	CYLINDER
TREE	3.25	2.3	3.05	220	98	21	0.06	CYLINDER
TREE	7.40	2.0	2.90	217	98	20	0.06	CYLINDER
TREE	7.00	2.0	3.10	217	97	20	0.06	CYLINDER
TREE	10.00	7.0	2.55	217	97	20	0.12	CYLINDER

TREE	3.00	2.2	1.10	217	97	20	0.04	CYLINDER
TREE	10.50	7.5	2.55	216	97	20	0.12	CYLINDER
TREE	10.50	8.0	4.35	216	97	20	0.18	CYLINDER
TREE	9.50	7.5	2.40	216	96	20	0.16	CYLINDER
TREE	9.50	6.5	3.30	215	96	20	0.12	CYLINDER
TREE	8.00	6.5	2.93	215	95	20	0.15	CYLINDER
TREE	11.50	8.0	3.48	217	95	20	0.15	CYLINDER
TREE	11.00	6.0	3.85	223	95	21	0.13	CYLINDER
TREE	6.00	4.2	2.10	214	95	19	0.04	CYLINDER
TREE	6.00	2.9	1.45	214	95	19	0.04	CYLINDER
TREE	11.00	7.0	3.55	223	95	21	0.12	CYLINDER
TREE	8.00	4.0	3.10	213	95	19	0.12	CYLINDER
TREE	8.50	7.5	3.15	216	95	20	0.14	CYLINDER
TREE	17.00	6.5	3.65	220	95	20	0.19	CYLINDER
TREE	7.00	5.5	2.15	215	94	19	0.08	CYLINDER
TREE	7.50	1.9	1.90	216	94	19	0.09	CYLINDER
TREE	6.50	5.0	3.70	223	94	21	0.11	CYLINDER
TREE	7.00	5.0	3.60	214	94	19	0.10	CYLINDER
TREE	5.00	4.3	2.15	224	94	20	0.03	CYLINDER
TREE	13.50	6.0	3.48	225	94	21	0.18	CYLINDER
TREE	5.00	2.5	0.98	222	93	20	0.08	CYLINDER
TREE	5.50	4.0	2.29	222	94	20	0.06	CYLINDER
TREE	6.00	2.5	1.25	222	93	20	0.05	CYLINDER
TREE	13.50	8.0	3.35	223	91	20	0.12	CYLINDER
TREE	13.00	8.5	2.90	224	93	21	0.13	CYLINDER
TREE	7.4	7.3	3.15	225	93	21	0.06	CYLINDER
TREE	13.50	8.0	3.30	226	93	21	0.14	CYLINDER
TREE	5.00	2.5	3.45	219	91	19	0.09	CYLINDER
TREE	8.50	4.5	3.38	219	91	19	0.10	CYLINDER
TREE	4.30	3.5	2.60	219	90	19	0.06	CYLINDER
TREE	11.50	2.5	4.05	220	89	19	0.13	CYLINDER
TREE	15.50	4.0	1.80	226	92	21	0.05	CYLINDER
TREE	12.00	6.5	2.75	228	94	21	0.17	CYLINDER
TREE	9.50	6.5	3.10	219	88	19	0.11	CYLINDER
TREE	12.50	5.0	3.85	219	87	19	0.15	CYLINDER
TREE	13.50	6.0	3.89	227	93	21	0.14	CYLINDER
TREE	3.80	2.5	2.50	227	92	21	0.05	CYLINDER
TREE	4.50	2.8	1.38	225	90	20	0.06	CYLINDER
TREE	13.00	6.0	3.15	227	92	21	0.10	CYLINDER
TREE	13.50	5.5	3.75	228	93	21	0.13	CYLINDER
TREE	4.50	2.3	1.85	223	88	19	0.05	CYLINDER
TREE	10.50	8.5	3.15	225	88	20	0.17	CYLINDER
TREE	9.00	8.0	2.60	226	89	20	0.10	CYLINDER
TREE	10.50	8.5	2.60	227	89	20	0.12	CYLINDER
TREE	12.00	4.0	3.28	228	92	21	0.13	CYLINDER

TREE	8.00	6.0	2.45	227	89	20	0.07	CYLINDER
TREE	12.50	6.0	2.78	228	92	21	0.14	CYLINDER
TREE	5.50	2.5	2.05	226	86	19	0.08	CYLINDER
TREE	8.50	6.5	2.40	227	86	20	0.09	CYLINDER
TREE	9.00	6.5	3.50	228	88	20	0.12	CYLINDER
TREE	3.00	1.5	2.15	229	89	20	0.06	CYLINDER
TREE	9.00	6.5	4.50	229	88	20	0.14	CYLINDER
TREE	11.00	6.0	3.70	229	88	20	0.13	CYLINDER
TREE	3.50	3.0	2.15	230	88	20	0.05	CYLINDER
TREE	8.00	5.5	3.40	230	88	20	0.11	CYLINDER
TREE	7.50	5.5	2.30	231	88	20	0.07	CYLINDER
TREE	10.50	6.5	2.65	231	88	20	0.10	CYLINDER
TREE	8.50	7.0	2.50	232	85	20	0.10	CYLINDER
TREE	12.00	7.0	3.75	232	85	20	0.14	CYLINDER
TREE	3.70	1.6	1.65	230	93	21	0.06	CYLINDER
TREE	9.00	7.0	3.50	233	86	20	0.14	CYLINDER
TREE	7.00	3.4	1.70	232	88	20	0.04	CYLINDER
TREE	6.00	2.8	1.40	232	88	20	0.04	CYLINDER
TREE	8.00	5.9	2.95	232	89	20	0.04	CYLINDER
TREE	13.00	7.5	4.13	235	83	20	0.16	CYLINDER
TREE	5.00	2.5	1.68	232	89	20	0.05	CYLINDER
TREE	8.00	5.0	2.23	233	88	20	0.08	CYLINDER
TREE	15.25	5.0	3.98	233	88	20	0.22	CYLINDER
TREE	4.50	3.8	3.38	236	84	20	0.11	CYLINDER
TREE	3.00	2.2	1.10	235	86	20	0.04	CYLINDER
TREE	3.70	1.6	1.65	230	93	21	0.06	CYLINDER
TREE	11.00	6.5	3.35	230	93	21	0.15	CYLINDER
TREE	12.60	12.5	3.75	235	86	20	0.16	CYLINDER
TREE	11.75	4.5	4.30	238	83	20	0.18	CYLINDER
TREE	3.00	2.1	1.05	234	87	20	0.04	CYLINDER
TREE	9.00	5.8	2.50	238	84	20	0.16	CYLINDER
TREE	7.50	3.0	3.93	236	86	20	0.12	CYLINDER
TREE	13.00	3.0	5.55	237	85	20	0.20	CYLINDER
TREE	13.00	4.5	4.74	237	85	20	0.17	CYLINDER
TREE	4.00	2.8	1.40	236	86	20	0.03	CYLINDER
TREE	5.00	2.5	1.25	236	86	20	0.04	CYLINDER
TREE	10.00	4.5	1.80	238	85	20	0.15	CYLINDER
TREE	8.50	4.5	4.72	237	86	20	0.13	CYLINDER
TREE	7.00	3.9	1.95	237	86	20	0.03	CYLINDER
TREE	7.00	5.0	2.98	231	93	21	0.11	CYLINDER
TREE	12.00	8.5	2.80	237	87	20	0.11	CYLINDER
TREE	11.75	7.5	3.38	239	85	20	0.13	CYLINDER
TREE	2.00	1.2	0.60	237	87	21	0.05	CYLINDER
TREE	5.00	2.4	1.20	237	87	21	0.04	CYLINDER
TREE	7.00	4.0	2.50	231	93	21	0.09	CYLINDER

TREE	4.00	2.0	1.00	237	88	21	0.04	CYLINDER
TREE	11.75	3.8	3.35	240	85	21	0.12	CYLINDER
TREE	3.00	1.8	0.90	238	88	21	0.05	CYLINDER
TREE	10.50	6.0	2.00	239	87	21	0.09	CYLINDER
TREE	15.00	3.0	2.08	241	86	21	0.05	CYLINDER
TREE	4.00	2.5	3.65	240	87	21	0.06	CYLINDER
TREE	6.50	5.0	2.35	235	91	21	0.05	CYLINDER
TREE	10.00	8.0	2.75	232	93	21	0.15	CYLINDER
TREE	9.80	5.8	3.30	240	88	21	0.09	CYLINDER
TREE	6.00	4.0	1.84	238	89	21	0.08	CYLINDER
TREE	11.00	4.0	4.20	241	88	21	0.17	CYLINDER
TREE	11.00	7.5	2.08	238	89	21	0.10	CYLINDER
TREE	12.50	7.0	1.83	237	90	21	0.08	CYLINDER
TREE	5.00	4.5	2.05	235	91	21	0.05	CYLINDER
TREE	8.40	4.3	3.25	241	88	21	0.08	CYLINDER
TREE	12.50	8.5	1.86	238	90	21	0.11	CYLINDER
TREE	6.50	4.5	1.95	235	91	21	0.05	CYLINDER
TREE	5.00	2.5	3.10	233	93	21	0.07	CYLINDER
TREE	8.00	6.0	1.98	239	89	21	0.07	CYLINDER
TREE	9.00	5.0	2.85	236	91	21	0.08	CYLINDER
TREE	5.00	4.0	2.10	231	93	21	0.05	CYLINDER
TREE	7.00	5.3	2.65	241	89	21	0.04	CYLINDER
TREE	11.50	7.0	2.59	239	90	21	0.10	CYLINDER
TREE	13.00	6.0	3.08	238	90	21	0.13	CYLINDER
TREE	13.00	7.5	2.86	238	90	21	0.10	CYLINDER
TREE	5.50	2.5	2.50	233	93	21	0.07	CYLINDER
TREE	8.00	4.0	1.25	234	93	21	0.07	CYLINDER
TREE	6.00	4.0	1.95	234	93	21	0.06	CYLINDER
TREE	7.00	5.0	3.10	233	93	21	0.11	CYLINDER
TREE	4.00	2.1	1.05	244	90	22	0.05	CYLINDER
TREE	2.00	1.5	0.75	234	93	22	0.04	CYLINDER
TREE	7.00	5.0	2.28	235	93	22	0.08	CYLINDER
TREE	10.50	6.0	3.40	243	92	22	0.12	CYLINDER
TREE	10.50	5.0	3.80	242	92	22	0.09	CYLINDER
TREE	7.50	5.0	2.20	235	94	22	0.07	CYLINDER
TREE	10.00	7.5	3.20	243	93	22	0.17	CYLINDER
TREE	5.00	2.9	1.45	243	93	22	0.05	CYLINDER
TREE	3.00	1.4	0.70	242	93	22	0.04	CYLINDER
TREE	10.00	6.5	4.40	243	93	22	0.13	CYLINDER
TREE	7.00	5.5	2.76	236	94	22	0.04	CYLINDER
TREE	5.00	2.5	1.88	237	94	22	0.06	CYLINDER
TREE	6.00	2.2	1.10	242	95	23	0.04	CYLINDER
TREE	6.00	5.0	2.35	234	95	22	0.08	CYLINDER
TREE	9.00	8.0	2.15	234	95	22	0.11	CYLINDER
TREE	4.20	3.4	2.40	234	109	25	0.08	CYLINDER

TREE	13.80	7.5	5.35	238	105	24	0.23	CYLINDER
TREE	15.10	8.9	5.30	239	105	24	0.22	CYLINDER
TREE	5.90	2.6	2.00	240	105	25	0.07	CYLINDER
TREE	7.80	4.5	3.25	240	106	25	0.09	CYLINDER
TREE	3.20	2.2	1.80	240	106	25	0.04	CYLINDER
TREE	5.40	3.6	2.20	238	107	25	0.06	CYLINDER
TREE	6.70	3.9	2.95	242	106	25	0.07	CYLINDER
TREE	3.00	1.5	3.00	239	108	25	0.06	CYLINDER
TREE	5.10	3.4	1.60	242	106	25	0.05	CYLINDER
TREE	12.60	6.8	3.05	243	106	25	0.14	CYLINDER
TREE	5.70	4.8	3.50	243	106	25	0.07	CYLINDER
TREE	11.70	8.6	2.05	240	108	25	0.12	CYLINDER
TREE	8.50	4.9	2.40	237	109	25	0.08	CYLINDER
TREE	2.10	0.8	1.80	242	107	25	0.03	CYLINDER
TREE	4.70	2.8	1.80	245	105	25	0.06	CYLINDER
TREE	5.00	3.2	2.45	242	108	25	0.09	CYLINDER
TREE	11.20	5.0	3.60	242	108	25	0.13	CYLINDER
TREE	10.70	6.0	3.60	243	108	25	0.14	CYLINDER
TREE	14.10	9.2	4.05	244	108	26	0.17	CYLINDER
TREE	12.40	8.2	3.05	239	110	25	0.16	CYLINDER
TREE	3.70	2.5	1.70	240	110	25	0.05	CYLINDER
TREE	9.40	4.5	2.10	237	111	25	0.10	CYLINDER
TREE	7.50	5.2	3.90	241	109	26	0.08	CYLINDER
TREE	15.20	8.7	4.60	237	111	25	0.17	CYLINDER
TREE	12.30	8.1	3.45	243	110	26	0.13	CYLINDER
TREE	12.40	8.5	4.10	237	111	26	0.14	CYLINDER
TREE	1.20	0.4	0.80	240	111	26	0.04	CYLINDER
TREE	15.80	7.1	4.58	243	111	26	0.22	CYLINDER
TREE	6.70	3.7	3.65	243	110	26	0.10	CYLINDER
TREE	11.00	8.0	3.15	238	112	26	0.13	CYLINDER
TREE	15.70	9.1	3.10	242	111	26	0.18	CYLINDER
TREE	11.40	6.7	2.58	237	112	26	0.12	CYLINDER
TREE	16.00	2.6	5.60	242	112	26	0.25	CYLINDER
TREE	4.40	2.5	2.95	244	112	26	0.08	CYLINDER
TREE	1.80	1.1	1.30	245	112	26	0.03	CYLINDER
TREE	6.20	4.1	3.75	243	112	26	0.10	CYLINDER
TREE	10.50	3.8	5.85	244	113	27	0.20	CYLINDER
TREE	3.00	2.1	1.90	245	114	27	0.05	CYLINDER
TREE	2.70	2.1	1.90	241	113	26	0.05	CYLINDER
TREE	6.90	4.4	3.73	239	113	26	0.11	CYLINDER
TREE	6.10	6.0	3.30	238	113	26	0.17	CYLINDER
TREE	4.80	2.2	2.60	243	114	27	0.06	CYLINDER
TREE	7.00	4.7	2.35	242	114	27	0.09	CYLINDER
TREE	4.10	3.2	2.54	241	114	26	0.05	CYLINDER
TREE	5.30	4.1	1.30	240	114	26	0.04	CYLINDER

TREE	11.20	5.8	3.30	239	116	27	0.13	CYLINDER
TREE	6.80	4.5	4.25	239	116	27	0.09	CYLINDER
TREE	8.20	5.4	2.73	238	116	26	0.08	CYLINDER
TREE	12.20	4.7	5.40	247	120	28	0.16	CYLINDER
TREE	8.50	3.4	4.30	247	121	28	0.12	CYLINDER
TREE	11.90	6.3	3.40	238	116	27	0.18	CYLINDER
TREE	12.50	3.8	4.50	246	121	29	0.17	CYLINDER
TREE	6.20	3.3	3.28	234	115	26	0.10	CYLINDER
TREE	14.20	7.8	5.00	241	120	28	0.19	CYLINDER
TREE	9.40	7.1	3.65	234	115	26	0.15	CYLINDER
TREE	3.90	1.8	3.18	235	117	26	0.07	CYLINDER
TREE	13.20	7.0	4.50	237	120	27	0.14	CYLINDER
TREE	13.50	5.8	5.88	238	120	27	0.20	CYLINDER
TREE	1.30	0.4	0.40	235	117	26	0.03	CYLINDER
TREE	11.70	8.6	3.38	233	116	26	0.15	CYLINDER
TREE	10.50	8.5	3.40	232	115	25	0.12	CYLINDER
TREE	5.60	3.7	2.58	233	116	26	0.06	CYLINDER
TREE	7.30	4.1	2.80	232	114	25	0.09	CYLINDER
TREE	4.70	3.1	2.10	233	117	26	0.06	CYLINDER
TREE	8.20	3.6	1.93	233	116	26	0.08	CYLINDER
TREE	12.30	1.7	5.28	235	120	27	0.21	CYLINDER
TREE	8.00	7.0	3.93	232	115	26	0.11	CYLINDER
TREE	4.10	2.5	2.68	233	118	26	0.06	CYLINDER
TREE	14.00	2.5	4.05	232	117	26	0.19	CYLINDER
TREE	13.80	8.3	5.30	232	115	25	0.19	CYLINDER
TREE	6.10	1.9	3.20	232	117	26	0.09	CYLINDER
TREE	2.40	1.4	3.05	232	117	26	0.05	CYLINDER
TREE	11.10	7.8	3.85	231	116	25	0.10	CYLINDER
TREE	4.50	2.9	2.65	231	116	25	0.06	CYLINDER
TREE	14.60	8.7	3.40	231	115	25	0.16	CYLINDER
TREE	5.80	4.4	2.15	231	114	25	0.08	CYLINDER
TREE	3.10	1.7	2.63	229	122	26	0.06	CYLINDER
TREE	3.90	2.7	2.90	230	115	25	0.06	CYLINDER
TREE	2.40	1.5	1.60	226	125	26	0.04	CYLINDER
TREE	5.40	3.6	2.25	228	120	25	0.06	CYLINDER
TREE	3.70	2.4	1.80	226	123	26	0.06	CYLINDER
TREE	7.50	3.0	4.35	225	124	26	0.10	CYLINDER
TREE	5.30	4.6	4.40	226	123	26	0.09	CYLINDER
TREE	5.70	4.7	5.40	226	124	26	0.09	CYLINDER
TREE	8.60	6.5	3.48	226	122	26	0.12	CYLINDER
TREE	14.80	7.5	3.15	225	124	26	0.14	CYLINDER
TREE	15.10	5.6	4.65	228	118	25	0.19	CYLINDER
TREE	15.30	2.3	4.70	228	117	25	0.22	CYLINDER
TREE	5.60	3.1	2.80	225	123	26	0.07	CYLINDER
TREE	10.00	5.4	3.90	225	123	26	0.14	CYLINDER

TREE	5.80	4.5	4.40	225	122	25	0.12	CYLINDER
TREE	15.40	8.1	3.20	225	122	25	0.16	CYLINDER
TREE	1.70	0.7	1.10	222	125	25	0.03	CYLINDER
TREE	9.70	6.7	3.40	230	114	25	0.12	CYLINDER
TREE	3.90	2.3	2.10	221	125	25	0.05	CYLINDER
TREE	5.90	1.6	4.30	224	120	25	0.08	CYLINDER
TREE	12.10	8.2	2.33	222	122	25	0.09	CYLINDER
TREE	5.90	4.2	2.45	220	124	25	0.06	CYLINDER
TREE	4.10	2.1	1.45	219	125	25	0.05	CYLINDER
TREE	2.80	0.8	1.10	220	124	25	0.05	CYLINDER
TREE	13.80	7.3	4.00	224	120	25	0.12	CYLINDER
TREE	11.30	7.3	2.05	219	124	25	0.11	CYLINDER
TREE	12.00	7.4	3.25	230	113	25	0.13	CYLINDER
TREE	7.60	5.4	2.05	228	115	25	0.06	CYLINDER
TREE	9.30	5.9	1.95	219	125	25	0.07	CYLINDER
TREE	9.20	6.3	2.68	219	124	25	0.10	CYLINDER
TREE	3.10	2.0	1.95	219	124	25	0.04	CYLINDER
TREE	10.90	7.0	3.93	222	121	25	0.12	CYLINDER
TREE	3.80	2.2	1.33	223	120	25	0.05	CYLINDER
TREE	4.00	1.9	2.56	223	120	25	0.06	CYLINDER
TREE	2.90	1.1	1.40	220	123	25	0.06	CYLINDER
TREE	14.20	5.3	4.90	223	119	25	0.12	CYLINDER
TREE	10.10	7.5	2.65	220	122	25	0.12	CYLINDER
TREE	4.23	2.0	1.00	220	122	25	0.08	CYLINDER
TREE	2.60	1.5	1.00	220	122	24	0.05	CYLINDER
TREE	13.50	7.5	2.93	221	121	25	0.16	CYLINDER
TREE	3.45	2.3	1.64	222	120	25	0.04	CYLINDER
TREE	11.40	3.8	2.85	220	122	24	0.13	CYLINDER
TREE	6.60	4.1	3.70	220	121	24	0.07	CYLINDER
TREE	7.50	5.6	2.40	228	115	25	0.09	CYLINDER
TREE	4.20	3.5	2.15	220	121	24	0.05	CYLINDER
TREE	13.50	6.9	4.53	221	119	24	0.19	CYLINDER
TREE	15.40	8.6	3.23	227	115	25	0.16	CYLINDER
TREE	15.10	7.5	4.80	221	117	24	0.22	CYLINDER
TREE	13.60	7.3	3.25	223	116	24	0.13	CYLINDER
TREE	8.10	6.0	1.95	220	118	24	0.07	CYLINDER
TREE	13.10	7.2	2.63	217	119	23	0.10	CYLINDER
TREE	6.40	3.6	3.30	225	114	24	0.07	CYLINDER
TREE	12.10	7.9	2.55	225	115	24	0.10	CYLINDER
TREE	5.40	3.2	2.90	217	118	23	0.06	CYLINDER
TREE	5.10	2.1	2.20	220	116	24	0.06	CYLINDER
TREE	10.80	7.6	2.33	217	117	23	0.08	CYLINDER
TREE	10.60	7.7	2.25	222	115	24	0.14	CYLINDER
TREE	12.00	7.7	2.85	224	115	24	0.15	CYLINDER
TREE	13.30	6.0	3.90	218	116	23	0.19	CYLINDER

TREE	7.50	3.7	3.30	223	114	24	0.08	CYLINDER
TREE	4.50	2.8	2.67	219	115	23	0.04	CYLINDER
TREE	12.40	7.7	2.55	225	113	24	0.12	CYLINDER
TREE	13.60	9.6	3.30	221	114	23	0.14	CYLINDER
TREE	14.60	7.0	2.15	216	115	23	0.10	CYLINDER
TREE	13.30	11.3	1.95	221	114	23	0.10	CYLINDER
TREE	10.60	8.0	2.75	220	114	23	0.11	CYLINDER
TREE	12.00	8.1	2.38	219	114	23	0.10	CYLINDER
TREE	4.10	2.4	2.57	229	113	25	0.05	CYLINDER
TREE	12.40	8.7	2.85	224	113	24	0.11	CYLINDER
TREE	14.00	9.3	2.40	226	113	24	0.10	CYLINDER
TREE	7.80	6.4	2.70	217	114	23	0.11	CYLINDER
TREE	8.60	6.9	2.10	225	113	24	0.07	CYLINDER
TREE	10.40	3.3	3.80	216	113	22	0.14	CYLINDER
TREE	2.40	2.0	1.70	218	113	23	0.04	CYLINDER
TREE	12.40	8.5	4.93	218	112	23	0.18	CYLINDER
TREE	13.00	9.8	3.30	216	112	22	0.11	CYLINDER
TREE	12.40	8.9	2.45	220	112	23	0.13	CYLINDER
TREE	11.00	7.4	2.58	217	112	22	0.14	CYLINDER
TREE	12.80	7.9	3.00	219	112	23	0.17	CYLINDER
TREE	10.20	6.8	2.40	220	111	23	0.11	CYLINDER
TREE	2.80	2.1	1.98	219	111	23	0.04	CYLINDER
TREE	12.50	8.1	1.73	216	110	22	0.12	CYLINDER
TREE	12.70	9.5	2.45	220	111	23	0.12	CYLINDER
TREE	6.40	4.5	2.90	216	110	22	0.08	CYLINDER
TREE	4.60	3.9	2.25	216	110	22	0.07	CYLINDER
TREE	13.80	8.1	2.10	220	110	23	0.15	CYLINDER
TREE	10.50	4.4	2.65	220	110	22	0.11	CYLINDER
TREE	8.60	3.0	2.75	221	109	23	0.11	CYLINDER
TREE	3.70	2.5	2.57	222	105	22	0.05	CYLINDER
TREE	3.80	2.6	2.10	224	110	23	0.07	CYLINDER
TREE	2.70	1.8	1.10	224	110	23	0.04	CYLINDER
TREE	10.00	8.1	3.05	223	109	23	0.08	CYLINDER
TREE	6.10	4.5	2.43	223	109	23	0.07	CYLINDER
TREE	10.60	5.6	3.35	224	109	23	0.13	CYLINDER
TREE	5.90	4.7	2.78	224	110	23	0.06	CYLINDER
TREE	11.70	5.3	2.85	219	107	22	0.12	CYLINDER
TREE	3.50	2.8	1.97	219	106	22	0.04	CYLINDER
TREE	15.00	5.7	4.20	224	108	23	0.13	CYLINDER
TREE	15.40	9.8	2.35	223	108	23	0.13	CYLINDER
TREE	2.50	2.0	1.98	219	106	22	0.04	CYLINDER
TREE	2.50	2.0	1.88	220	105	22	0.04	CYLINDER
TREE	9.30	6.1	2.65	224	108	23	0.11	CYLINDER
TREE	13.10	8.9	3.45	224	107	23	0.17	CYLINDER
TREE	15.50	9.9	4.05	224	107	23	0.16	CYLINDER

TREE	10.60	8.0	3.20	225	108	23	0.11	CYLINDER
TREE	4.50	2.7	2.98	226	107	23	0.08	CYLINDER
TREE	4.50	3.0	2.70	227	108	23	0.06	CYLINDER
TREE	4.80	2.9	2.70	227	107	23	0.07	CYLINDER
TREE	5.10	3.2	2.50	227	107	23	0.06	CYLINDER
TREE	13.50	6.1	3.95	230	111	24	0.11	CYLINDER
TREE	13.90	7.7	2.65	227	105	23	0.14	CYLINDER
TREE	8.00	5.1	3.80	228	107	23	0.14	CYLINDER
TREE	3.80	2.4	1.50	230	108	24	0.07	CYLINDER
TREE	3.10	2.5	1.78	230	108	24	0.04	CYLINDER
TREE	14.80	7.1	3.55	231	111	25	0.15	CYLINDER
TREE	4.70	2.0	2.65	231	110	24	0.06	CYLINDER
TREE	2.10	0.7	1.10	231	109	24	0.03	CYLINDER
TREE	12.60	6.1	4.20	232	108	24	0.10	CYLINDER
TREE	11.80	6.1	2.35	234	103	23	0.12	CYLINDER
TREE	1.50	0.5	0.80	232	109	24	0.03	CYLINDER
TREE	12.60	8.2	4.00	232	108	24	0.18	CYLINDER
TREE	12.50	5.8	3.70	234	103	23	0.09	CYLINDER
TREE	14.00	8.6	2.55	234	103	23	0.15	CYLINDER
TREE	12.00	9.0	2.20	234	104	24	0.12	CYLINDER
TREE	3.40	3.0	1.87	234	105	24	0.05	CYLINDER
TREE	2.40	1.9	1.75	234	106	24	0.04	CYLINDER
TREE	14.40	7.5	3.45	233	108	24	0.17	CYLINDER
TREE	3.50	2.4	1.98	233	107	24	0.04	CYLINDER
TREE	7.20	5.0	2.60	231	111	25	0.07	CYLINDER
TREE	13.40	9.2	4.18	234	108	25	0.15	CYLINDER

Annex IV

Example of an Excel File output of one tree.

[s]	[C]	[C]	[kg]	[kg]	[kg]	[kg]	[kg]	[kW]	[kg]	[kW]	[kW]
Time	TreeAvg TempVe g	TreeAvg TempGa s	Total_Tr ee_Dry_ Mass	Total_Tr ee_Mois t_Mass	Total_Tr ee_Char _Mass	Total_Tr ee_Ash_ Mass	TreeAvg _int_div (qveg_c	TreeAvg _int_div (qveg_ra	Total Char Loss	Total CharOx HRR	
	1.1E+01	2.0E+01	2.9E+01	2.9E+01	0.0E+00	0.0E+00	7.3E-08	0.0E+00	0.0E+00	0.0E+00	
	1.8E+00	2.0E+01	2.9E+01	2.9E+01	0.0E+00	0.0E+00	1.4E-06	2.0E-07	0.0E+00	0.0E+00	
	3.5E+00	2.0E+01	2.9E+01	2.9E+01	0.0E+00	0.0E+00	2.1E-06	2.2E-07	0.0E+00	0.0E+00	
	5.1E+00	2.0E+01	2.9E+01	2.9E+01	0.0E+00	0.0E+00	2.5E-06	1.9E-07	0.0E+00	0.0E+00	
	6.8E+00	2.0E+01	2.9E+01	2.9E+01	0.0E+00	0.0E+00	2.8E-06	-4.7E-07	0.0E+00	0.0E+00	
	8.5E+00	2.0E+01	2.9E+01	2.9E+01	0.0E+00	0.0E+00	6.5E-06	-1.2E-05	0.0E+00	0.0E+00	
	1.0E+01	2.0E+01	2.9E+01	2.9E+01	0.0E+00	0.0E+00	7.8E-05	-1.7E-04	0.0E+00	0.0E+00	
	1.2E+01	2.0E+01	2.9E+01	2.9E+01	0.0E+00	0.0E+00	1.1E-03	-8.4E-04	0.0E+00	0.0E+00	
1.4E+01	2.0E+01	2.9E+01	2.9E+01	0.0E+00	0.0E+00	3.3E-03	-1.6E-03	0.0E+00	0.0E+00		
etc.	etc.	etc.	etc.	etc.	etc.	etc.	etc.	etc.	etc.		

Annex V

Simulation A Input files:

- Q1 pre treatment low conditions.
- Q2 pre treatment low conditions.
- Q1 pre treatment high conditions.
- Q2 pre treatment high conditions.
- Q1 post treatment low conditions.
- Q2 post treatment low conditions.
- Q1 post treatment high conditions.
- Q2 post treatment high conditions.

Annex VI

Simulation B Input files:

- Q1 pre treatment low conditions.
- Q2 pre treatment low conditions.
- Q1 pre treatment high conditions.
- Q2 pre treatment high conditions.
- Q1 post treatment low conditions.
- Q2 post treatment low conditions.
- Q1 post treatment high conditions.
- Q2 post treatment high conditions.

Annex VII

Scripts used to calculate Topography, Fireline, Canopy consumption and Rate of Spread:

```
#####Topography#####Fireline#####
```

```
memory.limit(size=15500)
options(scipen=999)
setwd('C:\\Users\\Olga\\Desktop\\TFM\\CTFC\\P_ROURE\\capes\\rastcopies')
warning(lapply(c('rgl','raster'), require, character.only = TRUE))

DEM <- raster("q1rastcopy.tif")
DEM.df <- round(as.data.frame(DEM,xy=T),0)
names(DEM.df)[3] <- 'Elev'

DEM.df$SurfID <- 'surface'
print(c(min(DEM.df$x),min(DEM.df$y),min(DEM.df$Elev)))
DEM.df$x <- DEM.df$x - min(DEM.df$x)
DEM.df$y <- DEM.df$y - min(DEM.df$y)
DEM.df$Elev <- DEM.df$Elev - min(DEM.df$Elev)

DEM.df$text <- paste('&OBST
XB=',DEM.df$x,',',DEM.df$x+1,',',DEM.df$y,',',DEM.df$y+1,',',min(round(DEM.df$Elev,0)),',',round(DEM.
df$Elev,0),', SURF_ID=', "",DEM.df$SurfID," /",sep=")

fireline=DEM.df[c(DEM.df$x>=3&DEM.df$x<=5 & DEM.df$y>=2 & DEM.df$y<=8),] #Extract the
fireline
fireline$text=paste('&VENT
XB=',fireline$x,',',fireline$x+1,',',fireline$y,',',fireline$y+1,',',round(fireline$Elev,0),',',round(fireline$Elev,
0),", SURF_ID='IGN FIRE' /",sep=")

write.table(DEM.df$text,paste('Elevation.csv',sep=""),row.names=F)
write.table(fireline$text,paste('Fireline.csv',sep=""),row.names=F)
```



```
#####Canopy consumption#####

library(data.table)
root='Z:\\Research\\Hoffman\\olga\\'

subdir = c('q2prehi')

for (j in subdir){
  setwd(paste(root,j,'\\tree',sep=""))

  TreeList=data.table(ID=NA,StartFuel=0,EndFuel=0)
  files=list.files(pattern = ".csv$")
  TreeList=TreeList[rep(seq_len(length(files))),]

  for (i in 1:length(files)) {
    TreeFile=read.csv(files[i],header=T,skip=1)
    TreeList$ID[i]=as.numeric(gsub("TREE", "",
    strsplit(files[i],("_"))[[1]][grep("TREE",strsplit(files[i],("_"))[[1]])])
    TreeList$StartFuel[i]=max(TreeFile$Total_Tree_Dry_Mass)
    TreeList$EndFuel[i]=min(TreeFile$Total_Tree_Dry_Mass)
  }
  #TreeList$Thinning=strsplit(j,"tree")[[1]][1]

  setwd(root)
  write.table(TreeList,paste(root,'TreeConsumption.csv',sep=""),row.names=F,append=T,sep=',',col.names=
  !file.exists(paste(root,'HeilTreeConsumption.csv',sep=")))

  TreeSummary <- data.frame(Sim = j, StartFuel = sum(TreeList$StartFuel), EndFuel =
  sum(TreeList$EndFuel))
  TreeSummary$Consumption <- (TreeSummary$StartFuel - TreeSummary$EndFuel) /
  TreeSummary$StartFuel
  write.table(TreeSummary,paste(root,'TreeConsumptionSummary.csv',sep=""),row.names=F,append=T,s
  ep=',',col.names=!file.exists(paste(root,'HeilTreeConsumption.csv',sep=")))
```

```
####Rate of Spread####
```

```
library(reshape)
setwd('Z:\\Research\\Hoffman\\People\\Justin_Z\\RAwork\\CuttingEfficiency\\TOA')
my.max <- function(x) ifelse( !all(is.na(x)), max(x, na.rm=T), NA)
```

```
files <- list.files(pattern = "\\\\.csv$")
```

```
for ( j in 36:length(files)){
  TOAi = read.csv(files[j],header=F)
  TOAi = TOAi-min(TOAi,na.rm=T)
```

```
TOAilist=TOAi[,1:148]
TOAilist=melt(TOAilist)
```

```
TOAilist$x = rep(1:201,148)
TOAilist$y = sort(rep(1:148,201))
ROSI = lm(x~value,data=TOAilist)
LM_ROS = coef(ROSI)[2]
RSS <- c(crossprod(ROSI$residuals))
MSE <- RSS / length(ROSI$residuals)
RMSE <- sqrt(MSE)
```

```
### forward ROS###
```

```
ROS <- TOAi
ROS[ROS>0]=NA
```

```
for (i in 6:dim(TOAi)[1]){
  ROS[i,] = TOAi[i,]-TOAi[i-5,]
}
ROS=5/ROS[6:200,1:148]
```

```
#ROS[ROS<0,]=NA
ROSlist=na.omit(melt(ROS))
meanROS = mean(ROSlist$value)
sdROS = sd(ROSlist$value)
```

```
### Vector ROS###
```

```
dist=
rbind(c(2.82842712474619,2.64575131106459,2.44948974278318,2.23606797749979,4,2.2
3606797749979,2.44948974278318,2.64575131106459,2.82842712474619),
c(2.64575131106459,2.44948974278318,2.23606797749979,2,3,2,2.23606797749979,2.449
48974278318,2.64575131106459),
c(2.44948974278318,2.23606797749979,2,1.73205080756888,2,1.73205080756888,2,2.236
06797749979,2.44948974278318),
c(2.23606797749979,2,1.73205080756888,1.4142135623731,1,1.4142135623731,1.732050
80756888,2,2.23606797749979),
c(4,3,2,1,0,1,2,3,4),
c(2.23606797749979,2,1.73205080756888,1.4142135623731,1,1.4142135623731,1.732050
80756888,2,2.23606797749979),
c(2.44948974278318,2.23606797749979,2,1.73205080756888,2,1.73205080756888,2,2.236
06797749979,2.44948974278318),
c(2.64575131106459,2.44948974278318,2.23606797749979,2,3,2,2.23606797749979,2.449
48974278318,2.64575131106459),
c(2.82842712474619,2.64575131106459,2.44948974278318,2.23606797749979,4,2.236067
97749979,2.44948974278318,2.64575131106459,2.82842712474619))
```

```
angles=
```

```

rbind(c(135,143.130102354156,153.434948822922,165.963756532074,180,194.0362434679
26,206.565051177078,216.869897645844,225),
c(126.869897645844,135,146.30993247402,161.565051177078,180,198.434948822922,213
.69006752598,225,233.130102354156),
c(116.565051177078,123.69006752598,135,153.434948822922,180,206.565051177078,225
,236.30993247402,243.434948822922),
c(104.036243467926,108.434948822922,116.565051177078,135,180,225,243.43494882292
2,251.565051177078,255.963756532074),
c(90,90,90,90,0,270,270,270,270),
c(75.9637565320735,71.565051177078,63.434948822922,45,0,315,296.565051177078,288.
434948822922,284.036243467926),
c(63.434948822922,56.3099324740202,45,26.565051177078,0,333.434948822922,315,303.
69006752598,296.565051177078),
c(53.130102354156,45,33.6900675259798,18.434948822922,0,341.565051177078,326.309
93247402,315,306.869897645844),
c(45,36.869897645844,26.565051177078,14.0362434679265,0,345.963756532074,333.434
948822922,323.130102354156,315))

```

```

deg2rad <- function(deg) {(deg * pi) / (180)}
rad2deg <- function(rad) {(rad * 180) / (pi)}

```

```

cosrad <- cos(deg2rad(angles))
sinrad <- sin(deg2rad(angles))

```

```

dist = dist[4:6,4:6]
angles = angles[4:6,4:6]
cosrad = cosrad[4:6,4:6]
sinrad = sinrad[4:6,4:6]
Vectors=TOAi; Vectors[Vectors>0]=NA;
for (m in 3:(dim(TOAi)[1]-3)) {
  for (n in 3:(dim(TOAi)[2]-3)) {
    cells = TOAi[(m-1):(m+1),(n-1):(n+1)]
    toadiffcells= cells-cells[2,2]
    toadiffcells=matrix(as.matrix(toadiffcells,nrow=3,ncol=3),nrow=3,ncol=3)
    roscells= dist/toadiffcells
    roscells[roscells<=0]=NA
    roscells[is.infinite(roscells)] <- NA
    x = cosrad*roscells
    y = sinrad*roscells

```

```

xsum = sum(x[is.finite(x)])
ysum = sum(y[is.finite(y)])
vectorangle = rad2deg(atan(ysum/xsum))

```

```

#if (vectorangle<=0 & is.finite(vectorangle)) {vectorangle=vectorangle+360}
Vectors[m,n]=round(vectorangle,1);
}
}
Vectors = melt(as.data.frame(Vectors))
Vectors = Vectors[complete.cases(Vectors),]

```

```

###Sinuosity###

```

```

TOAiSin = TOAilist$TOAilist$value==min(TOAilist$value[TOAilist$x==180]),]
gplot <- ggplot(TOAiSin,aes(y,x))+geom_point()+ stat_smooth(span = .08,se=F,fullrange=T,)
loessfit <- data.frame(x=ggplot_build(gplot)$data[[2]]$x,
y=ggplot_build(gplot)$data[[2]]$y)
loessfit$dist <- NA

```

```

    for (i in 2:length(loessfit$dist)){
      loessfit$dist[i] <- sqrt((loessfit$x[i]-loessfit$x[i-1])^2+(loessfit$y[i]-loessfit$y[i-1])^2)
    }

sinuosity =      sum(na.omit(loessfit$dist))/      sqrt((loessfit$x[1]-
loessfit$x[length(loessfit$x)]^2+(loessfit$y[1]-loessfit$y[length(loessfit$y)]^2)

name = strsplit(files[j],"_")[[1]][1]
ROSSummary = data.frame(sim =
name,meanROS=meanROS,sdROS=sdROS,meanDir=mean(Vectors$value,na.rm=T),sdDir=sd(Vectors
$value,na.rm=T),LM_ROS=LM_ROS,RMSE=RMSE,sinuosity= sinuosity)
write.table(ROSSummary,'ROSSummary.csv',row.names=F,col.names=T,sep=',',append=T)

```